3. DESIGN AND CONSTRUCTION OF A MOTORCYCLE WITH VARIABLE BRAKE CONTROL GRADIENTS

3.1 INTRODUCTION

The study of three production motorcycles in Chapter 2 showed fairly wide variations in the 'feel' properties of the brakes, both between front and rear, and between machines. Overall, there was a three-fold variation in the force/deceleration control gradient, and a two-fold variation in the displacement/deceleration gradient.

Because the response of the braking system to control inputs is so rapid, the response time of the system is not a variable of importance. The major control variables appear to be the force and displacement gradients, although which of these is of more fundamental concern to the rider is not known. A secondary characteristic of importance is the level of brake force hysteresis, which causes a lack of precision in the force control of deceleration.

In order to make a comprehensive study of the effects on braking performance of the displacement and force gradients, and their distribution between front and rear, a motorcycle with variable brake control gradients (VBCG) was required. This Chapter describes the design and construction of a VBCG system.

3.2 VBCG SYSTEM DESIGN

3.2.1 Definition of VBCG System Performance Specifications

The brake system control gradients should be capable of variation over a wide range in order to completely explore their influence on deceleration performance. The upper and lower values should be outside the range normally found on conventional motorcycles.

The upper limit of the force/deceleration gradient for the front and rear brake controls is determined by the strength capabilities of the motorcycle rider population. Considerable data exist relating to limb strength, but are not specific to motorcycle brake controls. Zellner (1980) has summarized the available data. The fifth percentile force capability of males studied was approximately 400 N, for both hand and foot strengths. With this information, it was decided to design for an upper limit of hand force of 360 N to lock the front wheel when only the front brake was used, and 360 N foot force to lock the rear wheel when only the rear brake was applied. The lower limits of force/deceleration gradient were subjectively determined in order to produce a 'feather touch' deceleration response, without being so light as to make the motorcycle totally uncontrollable. On this basis (and with some experimentation) 90 N was selected as the minimum force requirement to lock the wheel, for both the hand and foot controls. The VBCG system should be able to produce selected force gradients within these upper and lower limits.

The maximum displacement/deceleration gradient for the hand control was determined by the geometric constraint of the hand lever meeting the handle-bar grip. The starting point was the non-applied rest position of a typical motorcycle hand brake lever. These conditions then defined a maximum lever displacement of 50 mm, measured 115 mm from the lever fulcrum in order to lock the front wheel (when applied alone). The 115 mm distance corresponds to the usual position of the third finger when the hand is operating the lever. A lever movement of 7.5 mm (again measured 115 mm from the lever fulcrum) causing locking of the front wheel in the absence of rear wheel braking was selected to represent the minimum displacement/deceleration gradient. This value was expected to yield a brake system that would be effectively force controlled, with the operator not being able to detect any significant lever movement.

The maximum displacement/deceleration gradient for the foot lever was chosen to correspond to 60mm of pedal displacement to lock the rear wheel. This is consistent with the displacement limit of the ball of the foot with its arch resting on a peg, as is found with a motorcycle rear brake control. The minimum displacement/deceleration gradient was 6mm, selected to simulate a force controlled brake where the rider is not aware of any significant pedal movement.

Thus the VBCG performance specifications were determined, and are summarized in Table 3.1.

3.2.2 Realization Of Performance Specifications

Table 3.2 summarizes the brake system parameters which influence the force gradient and displacement gradient. It can be seen that only two of the parameters influence force gradient independently of displacement gradient. Thus, obtaining the required gradients by alteration of the parameters in Table 3.2 would appear impractical.

In order to provide the wide range of control gradients desired, a servo-system was considered. One of its main features should be the ability to quickly change the control settings, to expedite data collection in multi-candidate experiments.

Upon consideration of the relative advantages of electrical, mechanical, pneumatic and hydraulic servo systems, an air-assisted hydraulic brake was conceived. A schematic layout of this system is given in Figure 3.1.

The VBCG system retains the standard motorcycle hydraulic master cylinder/wheel cylinder brake system. However, for the new system the master cylinder is actuated by an air-controlled diaphragm cylinder. This is a single-acting, spring-return type. The air pressure controller supplied variable pressure to the

TABLE 3.1

VBCG PERFORMANCE SPECIFICATION

Wheel	Force Required To Lock Wheel		Displacement Required To Lock Wheel	
	Max. (N)	Min. (N)	Max. (mm)	Min. (mm)
Front	360	90	50	7.5
Rear	360	90	60	6

TABLE 3.2

BRAKE DESIGN PARAMETERS WHICH INFLUENCE CONTROL GRADIENTS

Parameter	Force Gradient ($N\ s^2/m$)	Displacement Gradient ($mm\ s^2/m$)
Ratio $\frac{\text{Master cylinder area}}{\text{Wheel cylinder area}}$	*	*
Mechanical advantage of mastercylinder piston actuating lever	*	*
Effective disc radius, r_d	*	
Pad/disc friction coefficient,	*	
Pad stiffness	*	*
Brakeline stiffness	*	*

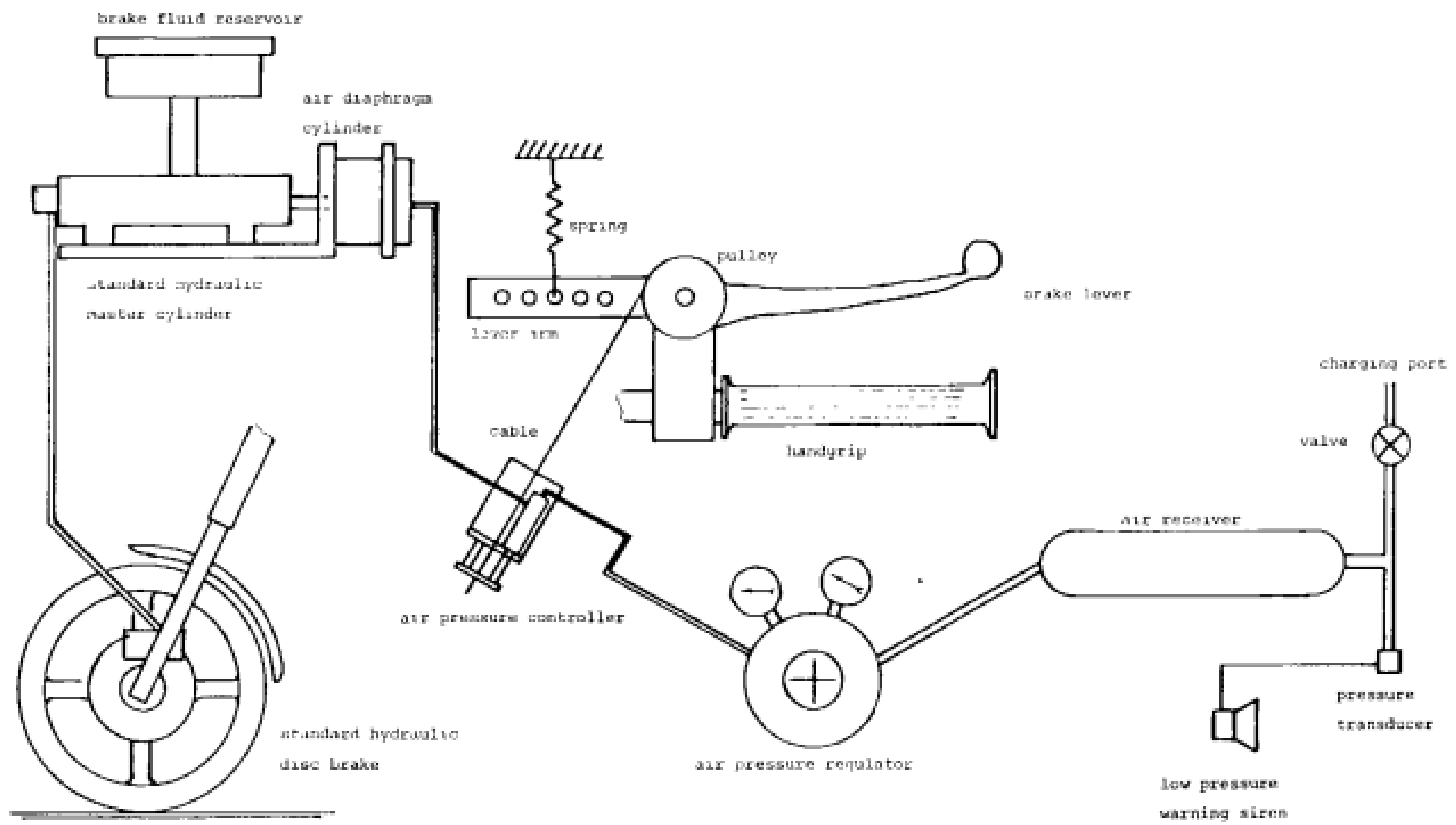

Figure 3.1 Schematic layout of VBGC system.

diaphragm cylinder in response to brake lever position. The diameter of the pulley connecting the pressure controller plunger to the brake lever, via the cable, determines the overall brake system displacement gradient. Very little force is required to depress the pressure controller plunger. Variation of force gradient is obtained with the spring and lever arm. The holes along the lever arm change the mechanical advantage of the brake lever acting on it, and hence change the force gradient of the system. The pressure controller and diaphragm cylinder are designed to have a maximum working pressure of 690 kPa. The air supply for the system was stored in a one litre stainless steel pressure vessel, initially charged to 14 MPa. This was reduced to the required 690 kPa working pressure with a welding-type oxygen regulator. A pressure transducer connected to the reservoir gave an electrical signal which was used to monitor its pressure, and to trigger a low pressure warning siren. A duplicate servo brake system was manufactured for the rear brake.

The details of the VBCG hardware design have been included as Appendix D.

3.3 CALIBRATION OF VBCG SYSTEM

3.3.1 Experimental Procedure

The displacement modulation testing described in Section 2.5.3 was used to determine the displacement gradient and the force gradient for each front and rear brake configuration. The data for the VBCG motorcycle was collected with the lightweight data acquisition system. The motorcycle speed used for testing was approximately 60 km/h, and all tests were conducted on the flat, smooth, hot mix bitumen surface at Monegeetta (described in Section 2.4). These data also permitted assessment of force and displacement hysteresis levels.

3.3.2 Analysis and Interpretation of Data

The data was digitized and stored on a PDP 11/03 computer with an analogue to digital converter facility. The sampling rate was 102.4 Hz.

A computer program was written which corrected the deceleration trace for motorcycle pitch effects, as described in Appendix A. Figures 3.2 and 3.3 contain sample plots of lever force versus displacement, and deceleration versus lever displacement and force, for the front and rear brakes respectively. These plots may be compared with the corresponding ones for the production motorcycles tested in Figures 2.5, 2.6, 2.14, 2.25, 2.26 and 2.31. It can be seen that the brake 'stiffness' presented by the VBCG system to the rider is more nearly constant than for the production machines. As with the production motorcycles, modulation of deceleration by lever displacement involves much less hysteresis than does control by lever force. The force hysteresis for the VBCG system is due in part to the pressure controller characteristics, and increases in magnitude as the modulation frequency increases. The level of hysteresis, although somewhat higher than on the production machines, appears to be within the range measured by Zellner and Klaber (1981) on standard motorcycles.

The slope of the displacement-deceleration graph during brake application represents the displacement gradient for that configuration. The force gradient is related to the displacement gradient by the force-displacement stiffness. The slope of the force-deceleration graph may be used alternatively. A computer program was written to extract the force, displacement and deceleration data during the brake application phase. Using linear regression analysis, straight lines were fitted to the deceleration-displacement, deceleration-force and displacement-force relationships. The slopes of these lines yielded the

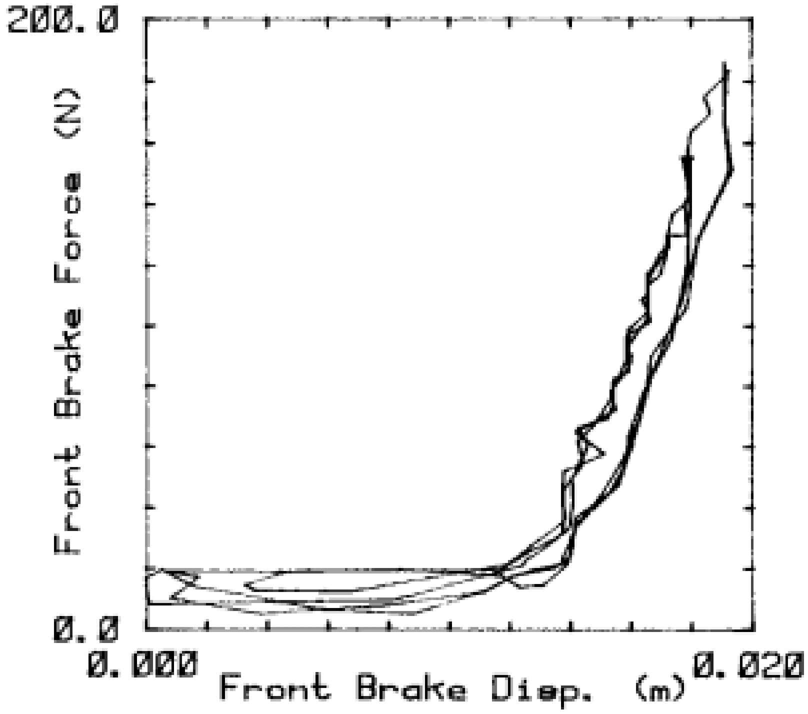

(a)

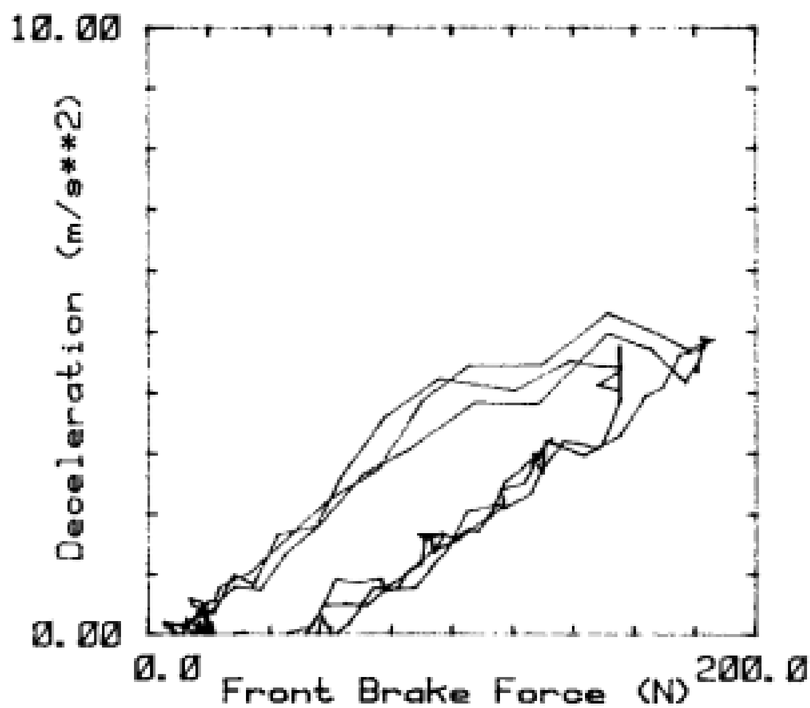

(b)

Figure 3.2 VBCG front brake force/displacement/deceleration characteristics.

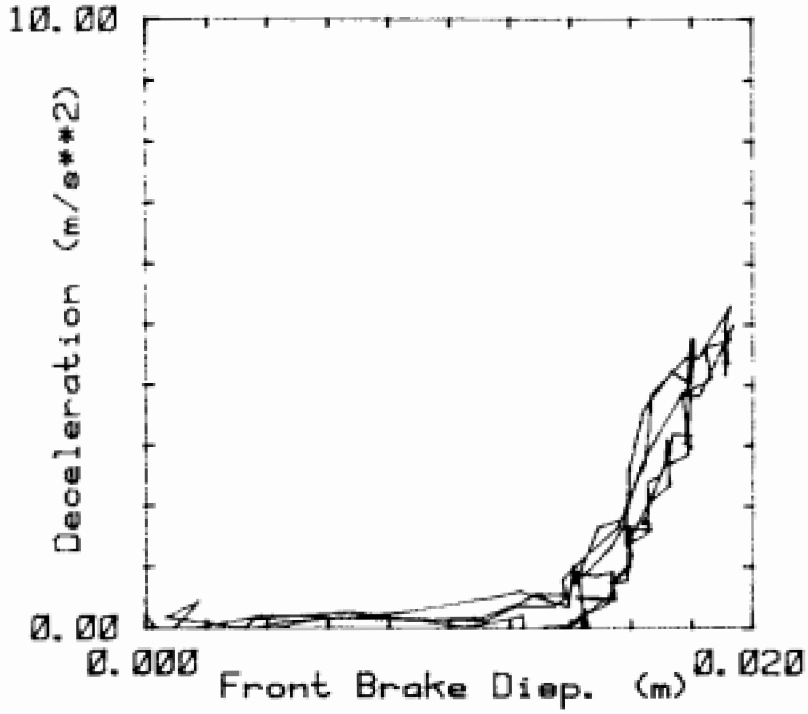

(c)

Figure 3.2 (cont.)

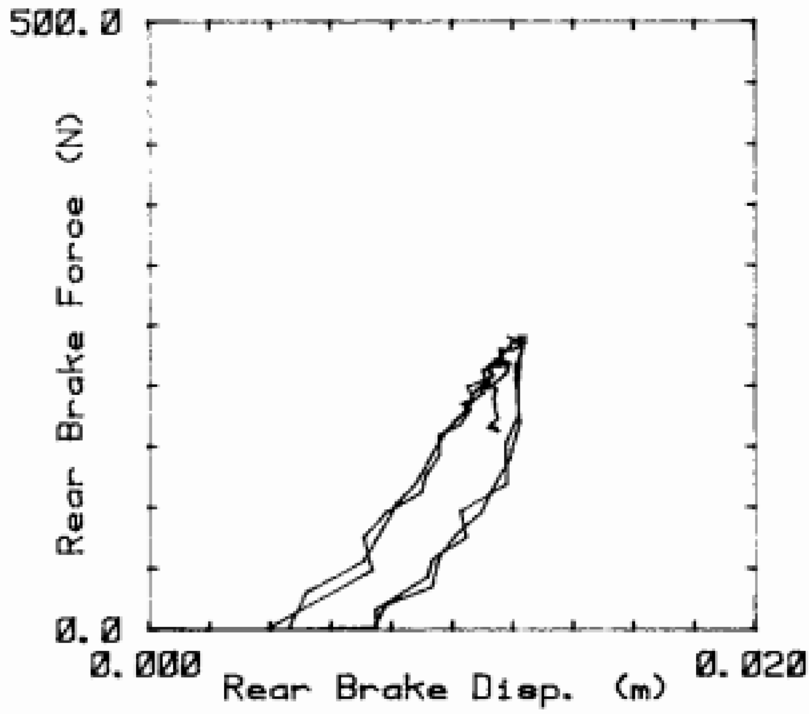

(a)

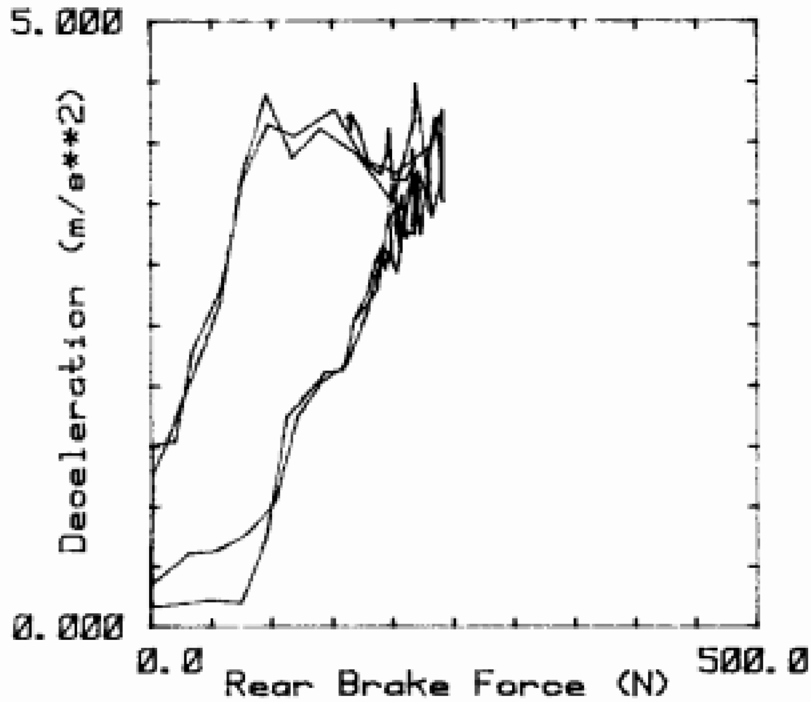

(b)

Figure 3.3 VBCG rear brake force/displacement/deceleration characteristics.

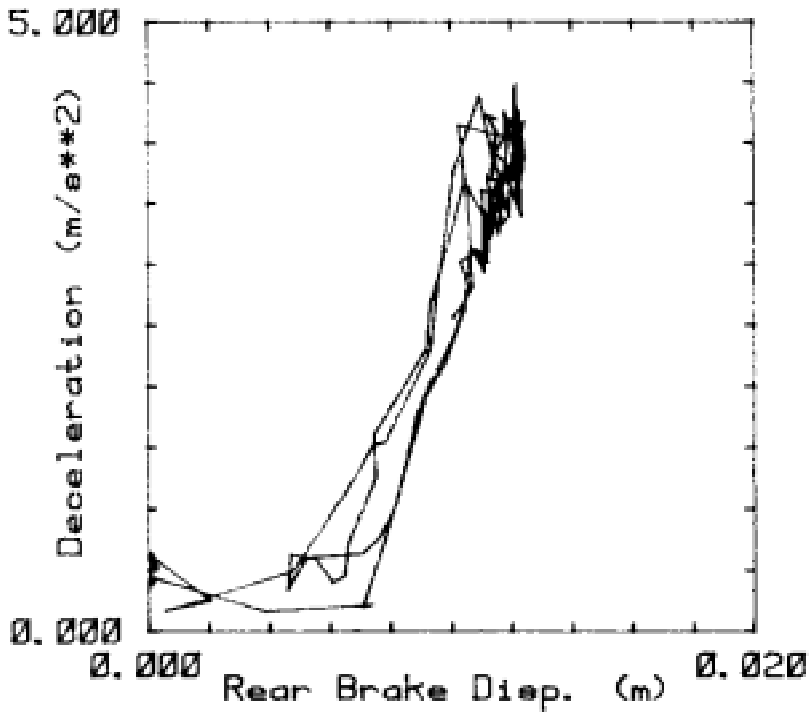

(c)

Figure 3.3 (cont.)

displacement gradient, force gradient and brake stiffness for each configuration.

3.3.3 Calibration Results

Calibration of the VBCG motorcycle was performed in order to quantify the front and rear brake displacement and force gradients which had been estimated in the design phase. The usable range of these four variables which could be obtained are shown in Table 3.3.

Also shown in this tabulation are the range of gradients measured in the Chapter 2 study of three production motorcycles, and the range of gradients estimated from Figures 3 and 8 of the paper by Zellner and Klaber (1981). The latter estimates are, at best, approximate, particularly for the displacement gradients, because the point at which the lever displacements were measured is not mentioned. The five machines in Zellner and Klaber's study were all of 1000 ml capacity or larger.

The comparisons in Table 3.3 show that the control gradients on the production motorcycles generally lie within the range of values attainable with the VBCG system.

After subjectively evaluating the VBCG motorcycle, test riders reported that it performed in a similar manner to a normal motorcycle, indicating that the servo-assisted system response was adequate. Some riders commented on the force hysteresis with the rear brake (which for some configurations was as high as 200N). Any future system design should aim to reduce this to a lower level. Ball bearing fulcrum pins should be satisfactory. Another comment related to the noisiness of the air discharge when the brakes were released. This initially caused some riders concern because it was such an unexpected aspect of the response of a motorcycle. However the riders quickly became accustomed to this system idiosyncrasy.

TABLE 3.3.

COMPARISON OF CONTROL GRADIENTS OBTAINABLE WITH VBCG SYSTEM WITH MEASUREMENTS ON PRODUCTION MOTORCYCLES.

Control Gradient	VBCG Motorcycle	Production Motorcycles: Present Study*	Production Motorcycles: Zelner & Klaber**
Front Displacement (mm per m/s^2)	1.0 - 5.7	2.5 - 2.6	2.0 - 8.5
Front Force (N per m/s^2)	17.5 - 76.7	16.8 - 36.5	14.6 - 36.3
Rear Displacement (mm per m/s^2)	1.6 - 12.9	2.0 - 4.4	2.8 - 4.2
Rear Force (N per m/s^2)	25.8 - 84.6	25.5 - 48.9	60.0 - 91.4

* 3 motorcycles: 250, 400, 750 ml (see Chapter 2).

** 5 motorcycles: four 1000 ml, one 1300 ml (estimates of gradients by present authors from data of Zelner and Klaber (1981).

4. INVESTIGATION INTO ERGONOMIC ASPECTS OF MOTORCYCLE DECELERATION CONTROL

4.1 INTRODUCTION

Chapter 2 established that rider-motorcycle brake control parameters vary widely from machine to machine and from front to rear for a particular motorcycle. The literature review (see Juniper and Good, 1983) highlighted braking deficiencies in motorcycle accidents.

The VBCG motorcycle was developed to enable investigation into ergonomic aspects of motorcycle braking controls. This system is capable of independently varying the displacement/deceleration and force/deceleration gradients over wide ranges, for both the front and rear brakes. Details of its design and construction have been described in Chapter 3 and Appendix D.

This chapter describes a 'pilot' study of brake control parameters and their influence on rider-motorcycle deceleration performance using the VBCG motorcycle.

4.2 EXPERIMENTAL OBJECTIVE

The typical motorcycle brake configuration consists of two independent control levers, one for the front brake and one for the rear brake. In order to decelerate the vehicle the rider applies force to, resulting in a displacement of, these control levers. For each lever, two steady-state control parameters can be defined, viz. the displacement/deceleration gradient and the force/deceleration gradient. These parameters largely determine the 'feel' properties of the brake system. The experimental objective was to investigate the effect of these control gradients on rider/motorcycle deceleration performance, and to study the interactions between front and rear brake control parameter settings.

A small-scale pilot study was seen as a necessary first step in pursuit of the experimental objectives. Before a large-scale study involving many subjects could reasonably be undertaken, it was necessary to evaluate the proposed experimental procedures and performance measures. It was also thought that the results from a pilot study, involving a wide range of brake system characteristics, might show that some combinations of characteristics were clearly unacceptable. These could then be eliminated from the full-scale study, thereby reducing the magnitude of that task.

In the limited time available to this project, it proved to be not possible to go on from the pilot study to carry out a full-scale experimental investigation.

4.3 EXPERIMENTAL DESIGN

Four independent variables were chosen for investigation. They were front brake force/deceleration gradient (FBF), front brake displacement/deceleration gradient (FBD), rear brake force/deceleration gradient (RBF), and rear brake displacement/deceleration gradient (RBD).

The technique used for analysing the contributions of the four chosen variables is called Response Surface Methodology (RSM). It was developed for the chemical industry to determine optimum operating conditions with multiple-variable processes (Box and Hunter, 1957). The method consists of defining a 'response surface' which is the functional relationship between the dependent variable being investigated and the independent variables selected for analysis. The procedure allows the minimum number of experimental points to be selected in order to define the response surface. This is where RSM has its great advantage over a factorial design, which would require all possible combinations of the independent variables to be tested. Having defined the response surface, the coordinates of the

TABLE 4.1 RSM CONFIGURATIONS

Block	Configuration	Front Brake Disp. Grad.	Front Brake Force Grad.	Rear Brake Disp. Grad.	Rear Brake Force Grad.
1	1.1	-1	-1	-1	-1
	1.2	1	1	-1	-1
	1.3	1	-1	1	-1
	1.4	-1	1	1	-1
	1.5	1	-1	-1	1
	1.6	-1	1	-1	1
	1.7	-1	-1	1	1
	1.8	1	1	1	1
	1.9	0	0	0	0
	1.10	0	0	0	0
2	2.1	1	-1	-1	-1
	2.2	-1	1	-1	-1
	2.3	-1	-1	1	-1
	2.4	1	1	1	-1
	2.5	-1	-1	-1	1
	2.6	1	1	-1	1
	2.7	1	-1	1	1
	2.8	-1	1	1	1
	2.9	0	0	0	0
	2.10	0	0	0	0
3	3.1	2	0	0	0
	3.2	-2	0	0	0
	3.3	0	2	0	0
	3.4	0	-2	0	0
	3.5	0	0	2	0
	3.6	0	0	-2	0
	3.7	0	0	0	2
	3.8	0	0	0	-2
	3.9	0	0	0	0
	3.10	0	0	0	0

maximum or minimum value of the dependent variable define the optimum combination of the independent variables.

With four independent variables, and assuming a second-order fit of the variables to the response surface, 30 trials are necessary, and five equispaced levels in each variable are required (Dorey, 1979). A factorial model of the same four variables would require 81 trials, nearly three times that using RSM. The actual value of each variable is normalized so that the five levels are ± 2, ± 1, and 0. The 30 configurations to be tested, arranged in 'blocked' form, are shown in Table 4.1. Blocking of the configurations allows the use of a different group of subjects for each block, thereby reducing the number of configurations which must be tested by an individual subject.

A variable not investigated in this study was the level of force-deceleration hysteresis of the brake system. With the VBCG, force hysteresis was measured to be in the range 40N to 120N for the front brake (corresponding to the normalized force configurations -2 and +2); and 40N to 200N for the rear brake (for the -2 and +2 normalized configurations respectively). This variable may be important in ergonomic design of brake controls.

4.4 SELECTION OF RANGE FOR VARIABLES INVESTIGATED

The RSM design dictated five equispaced levels for each of the independent variables FBF, FBD, RBF, and RBD. The VBCG design described in Chapter 3 set the maximum and minimum value of force and displacement to lock the wheel being braked, and therefore the maximum and minimum value for each control gradient was determined. The VBCG was designed so that the five different levels of displacement gradient were obtained by having a further three pulleys of appropriate increments in diameter between the maximum and minimum diameters. For each displacement gradient an associated spring was designed and manufactured; the radius at which it operated on the brake lever determined the force level.

Thus, the five different levels of force gradient were obtained by adding three holes at appropriate radii between those for the maximum and minimum force levels. Each pulley and associated spring was colour coded, labelled and stored in a compartmented box, shown in Figure 4.1. Due to manufacturing tolerances, the precise values of the independent variables were not known at this stage. Further calibration was therefore required, as described in the next section.

4.5 CALIBRATION OF VBCG

4.5.1 Selection Of Configuration For Calibration

Table 4.1 shows the combinations of the variables to be used in the RSM design. It can be seen that there are nine different combinations of FBF and FBD, and similarly nine combinations of RBF and RBD, as shown in Table 4.2. The front brake is independent of the rear brake. Therefore calibration of the VBCG system at the nine settings for the front brake and the nine for the rear would encompass all combinations used in the RSM experiments.

4.5.2 Description Of Calibration Experiments

(a) Instrumentation

The on-board data acquisition system described in Chapter 2 was used on the VBCG motorcycle to record rider imputs and the machine's response to these.

Rider inputs consisted of force and displacement at the front and rear wheel brake control levers. The brake force and displacement transducers were the same as those used for the braking behaviour experiments described in Chapter 2.

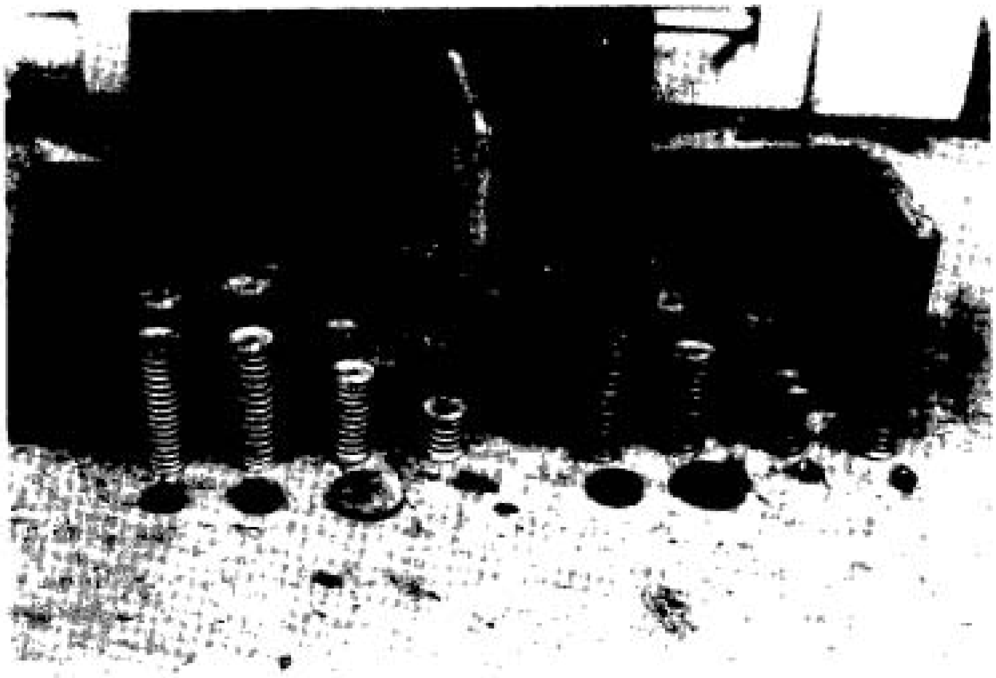

Figure 4.1 VBCG springs and pulleys used for varying the control gradients.

TABLE 4.2 VBCG CALIBRATION SETTINGS

Setting Number	Front Brake Displacement Gradient	Front Brake Force Gradient
1	2	0
2	-2	0
3	0	2
4	0	-2
5	0	0
6	1	1
7	-1	1
8	1	-1
9	-1	-1
Setting Number	**Rear Brake Displacement Gradient**	**Rear Brake Force Gradient**
10	2	0
11	-2	0
12	0	2
13	0	-2
14	0	0
15	1	1
16	-1	1
17	1	-1
18	-1	-1

TABLE 4.3 BRAKE CONTROL GRADIENT NORMALIZING EQUATIONS

Displacement Gradient

$$FDG = 1.19\ FBD + 3.39 \quad \mathrm{mm\ s^2/m}$$

where FDG = Front brake Displacement Gradient.
FBD = normalized value (±2, ±1, 0)

$$RDG = 2.79\ RBD + 6.39 \quad \mathrm{mm\ s^2/m}$$

where RDG = Rear brake Displacement Gradient
RBD = normalized value (±2, ±1, 0)

Force Gradient

$$FFG = 12.65\ FBF + 36.45 \quad \mathrm{N\ s^2/m}$$

where FFG = Front brake Force Gradient
FBF = normalized value (±2, ±1, 0)

$$RFG = 14.42\ RBF + 53.05 \quad \mathrm{N\ s^2/m}$$

where RFG = Rear brake Force Gradient
RBF = normalized value (±2, ±1, 0)

Different strain gauges were necessary for the VBCG brake levers, so the force transducers were recalibrated using a procedure similar to that described in Appendix A.

The motorcycle motion parameters measured were speed, acceleration and main frame pitch rate, using the transducers described in Appendix A.

(b) Test site

All data acquisition and experimental work for the calibration of the VBCG was conducted at the Australian Army Trials and Proving Wing facility located at Monegeetta and described in Section 2.4. The bitumen pads only were used for this work.

(c) Testing procedure

The low-frequency displacement modulation testing described in Section 2.5.3 was used to evaluate the displacement gradient and the force gradient for each of the nine front brake and rear brake configurations listed in Table 4.2.

(d) Data analysis and results of calibration experiments

The collected data were digitized and stored on magnetic disk using the PDP 11/23 computer system. The analog-to-digital converter sampling rate was 102.4 Hz per channel for these data.

A computer program was written which accessed the acceleration information and corrected it for motorcycle pitch effects. Figures 4.2 (a) and (b) show sample plots of deceleration versus brake lever displacement and force, respectively, for the front brake. The normalized configuration in this example is nominally -1 for displacement gradient and +1

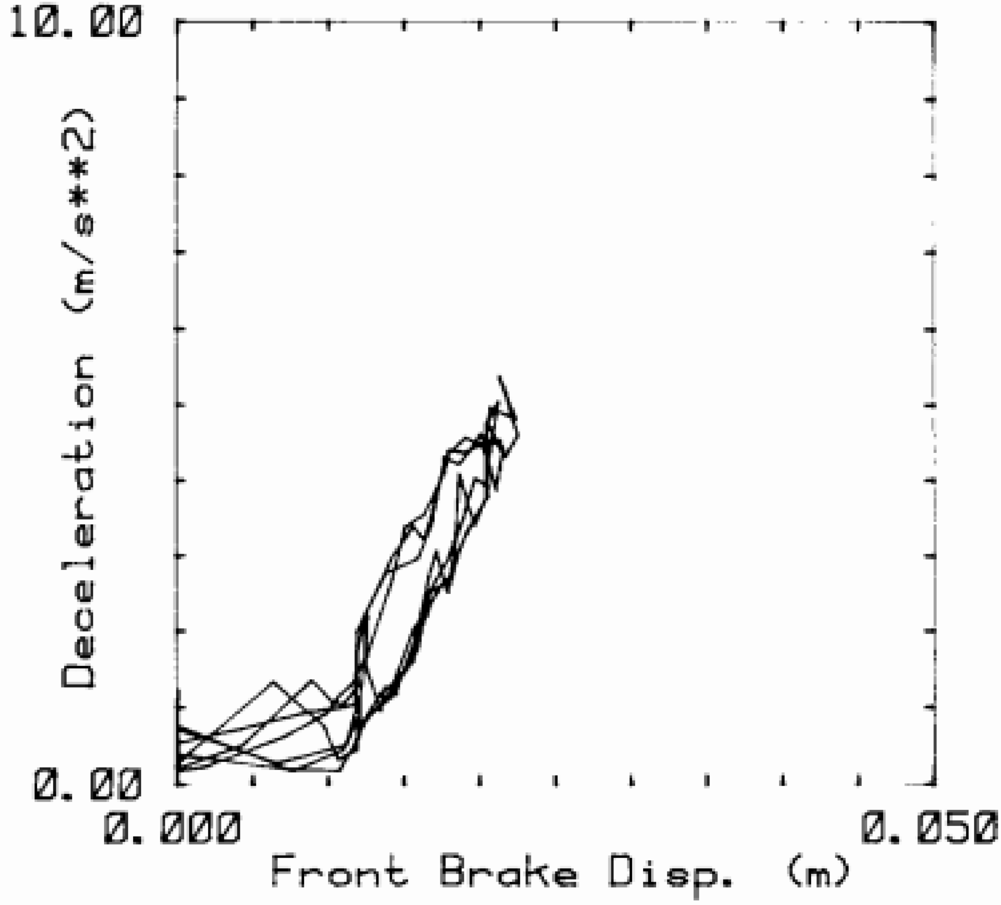

Figure 4.2 (a) Deceleration versus displacement, normalized front displacement gradient -1.

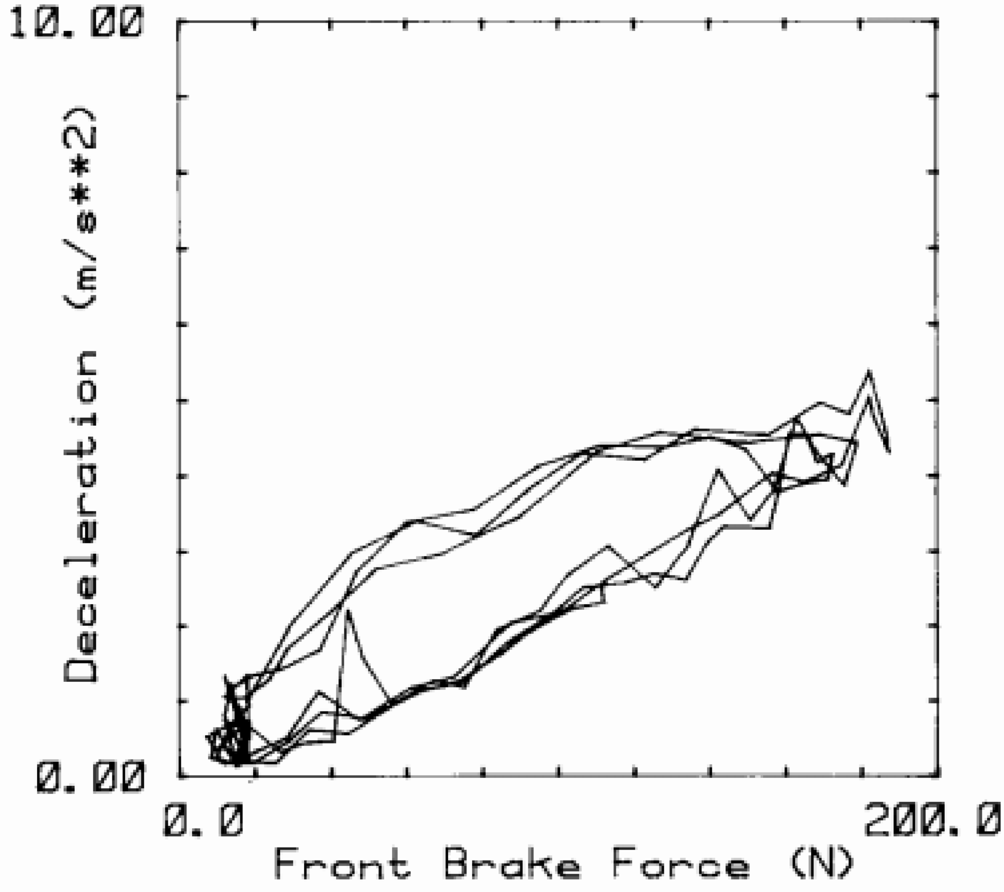

Figure 4.2 (b) Deceleration versus force, normalized front force gradient +1.

for force gradient. A small amount of displacement-deceleration hysteresis can be seen (about 3.0 mm for this example). This is due to a lag in the pressure controller output in response to its plunger depression. The force-deceleration hysteresis is larger (about 80 N for the case shown). However this compares favourably with the levels found to exist with the standard motorcycles tested in Chapter 2 (70 N to 80 N typically), and with that found by Zellner, 1980 (25 N to 120 N). Further discussion of VBCG force hysteresis may be found in Section 4.3.

The gradient of the deceleration-displacement graph during the brake application phase is the displacement gradient for that configuration. The force gradient may be calculated from the displacement gradient if the system stiffness is known. Alternatively the gradient of the deceleration-force data may be used directly. These gradients were determined in the manner described in Section 3.3.2.

Three calibration runs were made for each configuration and the resulting control gradients averaged. These average gradients were then plotted against the normalized values they were supposed to represent, as shown in Figure 4.3. It can be seen that there were some substantial departures from the ideal linear relationship. Changes in pulley diameter and, more particularly, spring stiffness would be necessary to bring the actual control gradients into closer agreement with those required by the RSM design. However, non-standard mandrels needed for manufacture of the appropriate springs were not available. Using the control gradients achieved with the VBCG system meant that some of the assumptions of the RSM design were not precisely met. However, if the underlying relationships between the performance measures and the independent variables were strong, these departures from the preferred RSM levels should still allow a reasonably accurable determination of the response surface.

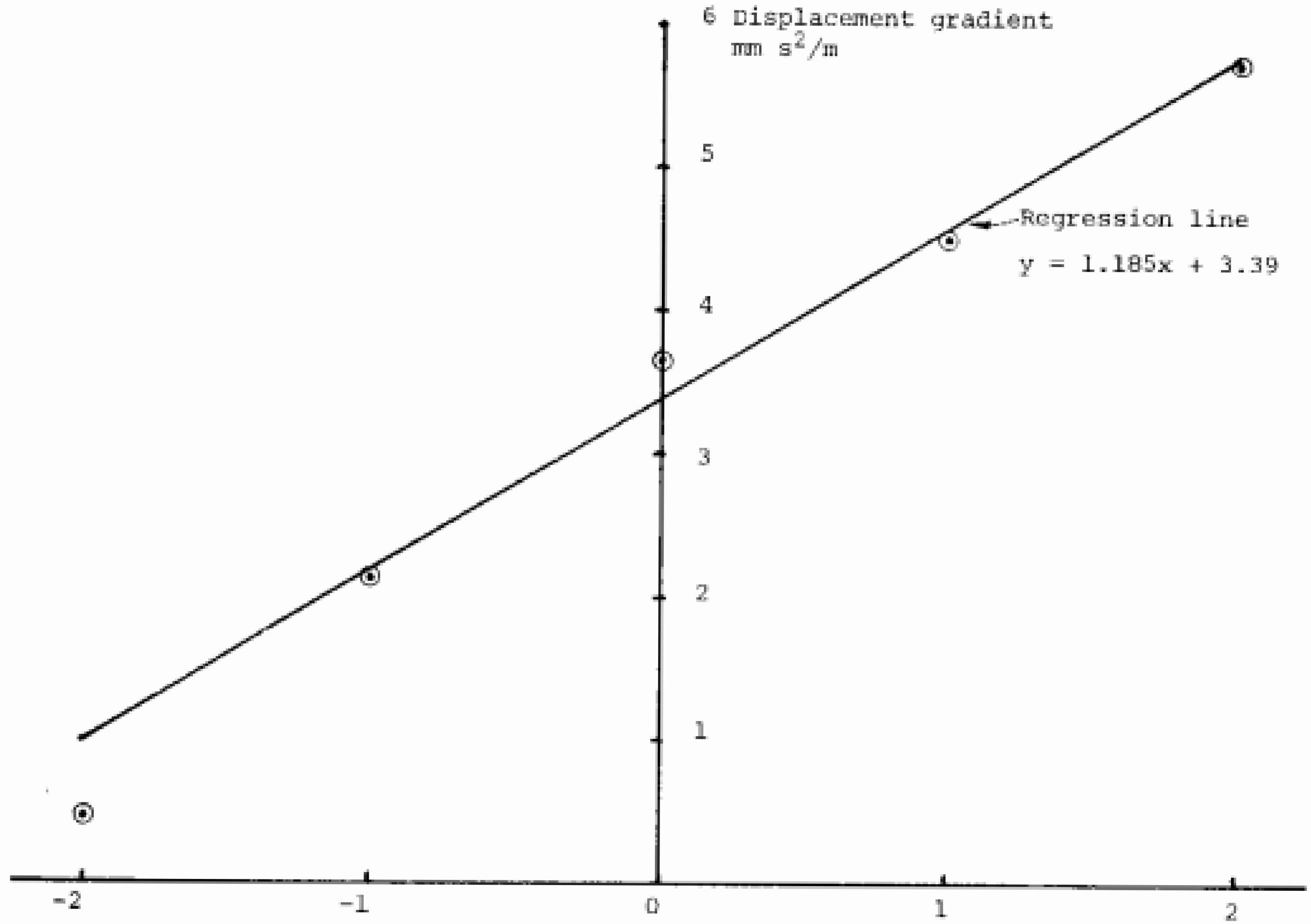

Figure 4.3 (a) Measured front brake displacement gradient versus normalized value.

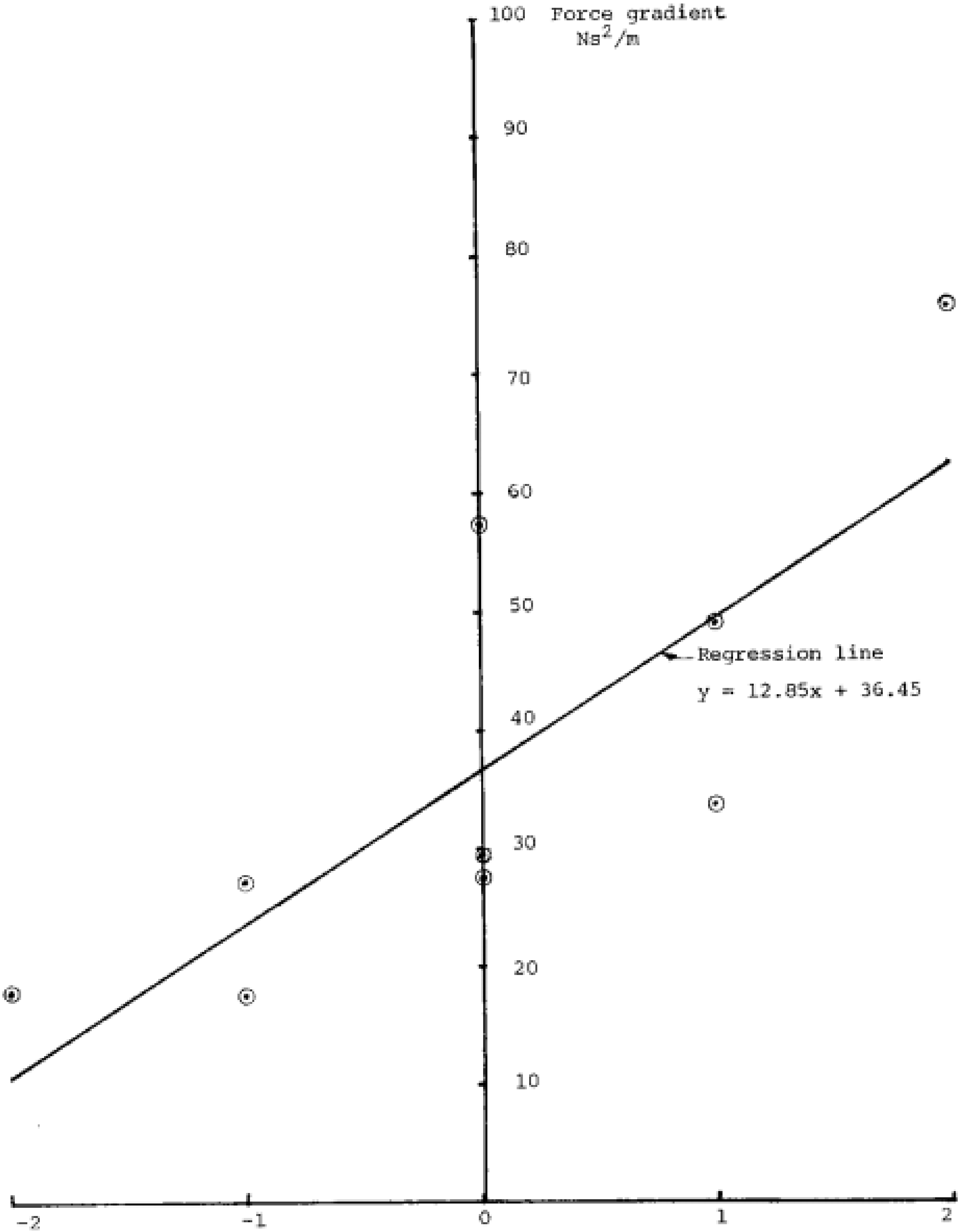

Figure 4.3 (b) Measured front brake force gradient versus normalized value.

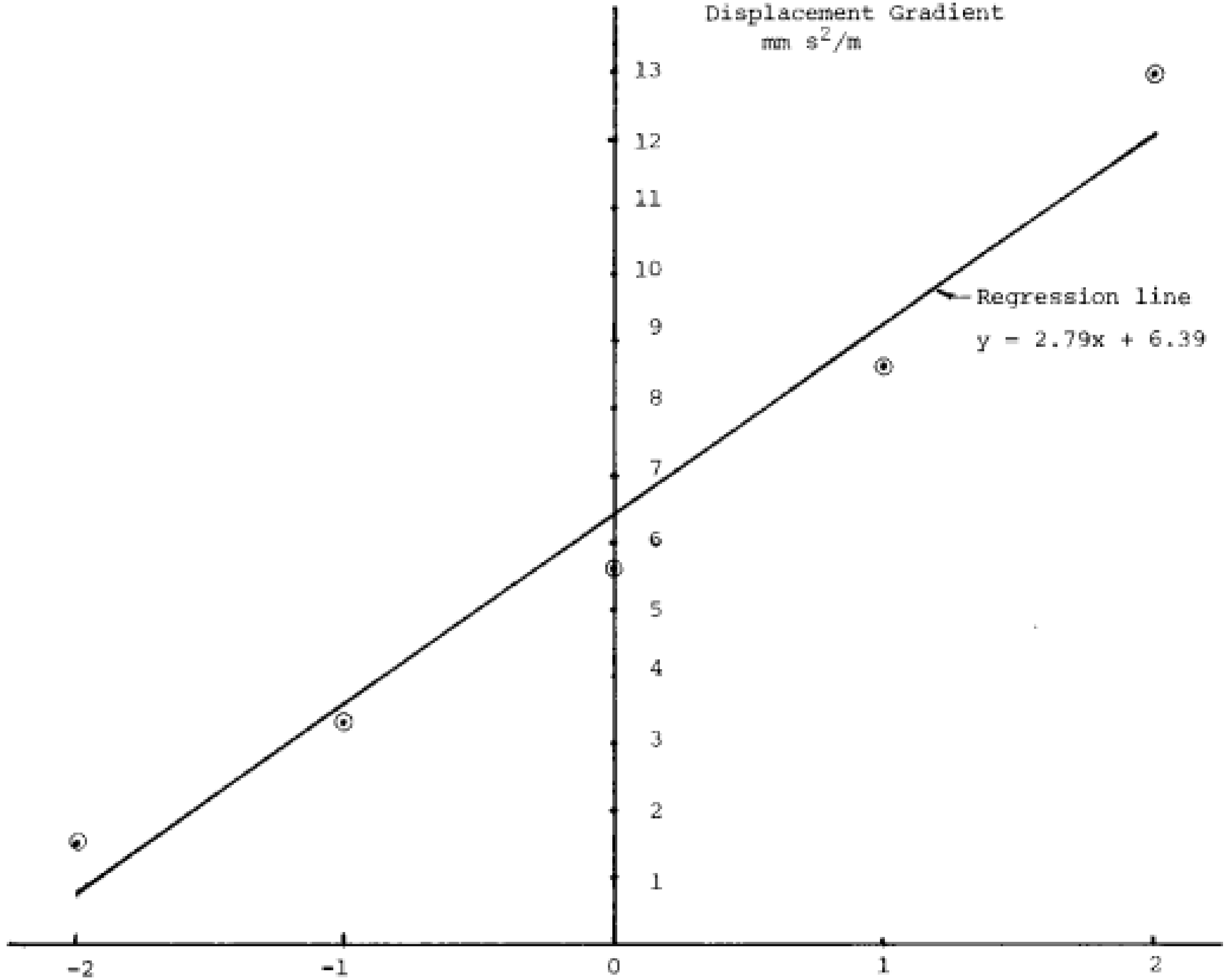

Figure 4.3 (c) Measured rear brake displacement gradient versus normalized value.

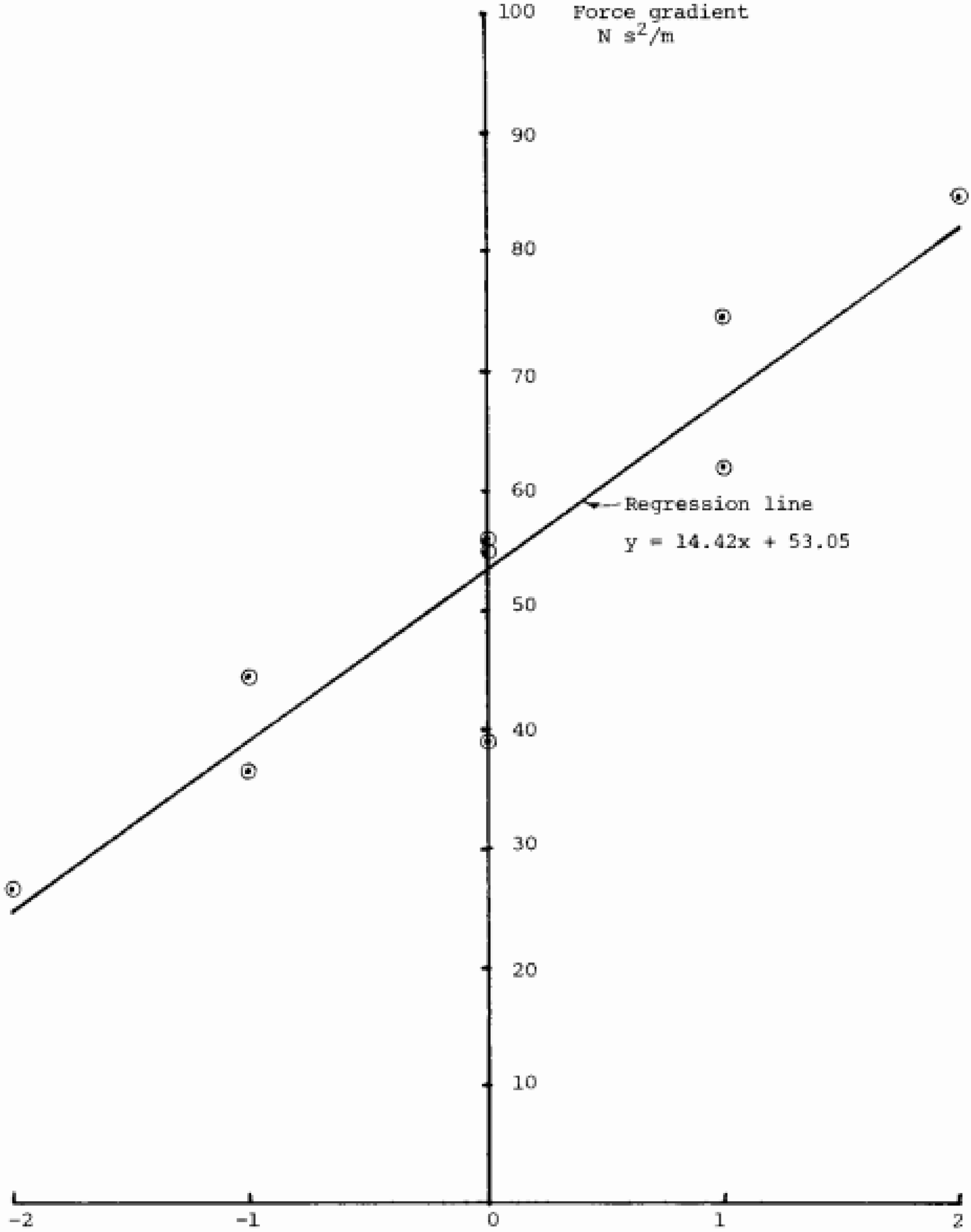

Figure 4.3 (d) Measured rear brake force gradient versus normalized value.

TABLE 4.4 VBCG ACTUAL NORMALIZED BRAKE CONTROL GRADIENTS

Block	Configuration	Front Brake Disp. Grad.		Front Brake Force Grad.		Rear Brake Disp. Grad.		Rear Brake Force Grad.	
		RSM	VBCG	RSM	VBCG	RSM	VBCG	RSM	VBCG
1	1.1	-1	-1.07	-1	-1.48	-1	-1.09	-1	-0.59
	1.2	1	0.93	1	0.99	-1	-1.09	-1	-0.59
	1.3	1	0.93	-1	-0.71	1	0.76	-1	-1.16
	1.4	-1	-1.07	1	0.21	1	0.76	-1	-1.16
	1.5	1	0.93	-1	-0.71	-1	-1.09	1	1.47
	1.6	-1	-1.07	1	0.21	-1	-1.09	1	1.47
	1.7	-1	-1.07	-1	-1.48	1	0.76	1	0.63
	1.8	1	0.93	1	0.99	1	0.76	1	0.63
	1.9	0	0.22	0	0.84	0	-0.28	0	0.20
	1.10	0	0.22	0	0.84	0	-0.28	0	0.20
2	2.1	1	0.93	-1	-0.71	-1	-1.09	-1	-0.59
	2.2	-1	-1.07	1	0.21	-1	-1.09	-1	-0.59
	2.3	-1	-1.07	-1	-1.48	1	0.76	-1	-1.16
	2.4	1	0.93	1	0.99	1	0.76	-1	-1.16
	2.5	-1	-1.07	-1	-1.48	-1	-1.09	1	1.47
	2.6	1	0.93	1	0.99	-1	-1.09	1	1.47
	2.7	1	0.93	-1	-0.71	1	0.76	1	0.63
	2.8	-1	-1.07	1	0.21	1	0.76	1	0.63
	2.9	0	0.22	0	0.84	0	-0.28	0	0.20
	2.10	0	0.22	0	0.84	0	-0.28	0	0.20
3	3.1	2	1.97	0	0.51	0	-0.28	0	0.20
	3.2	2	-2.03	0	0.68	0	-0.28	0	0.20
	3.3	0	0.22	2	3.13	0	-0.28	0	0.20
	3.4	0	0.22	-2	-1.39	0	-0.28	0	0.20
	3.5	0	0.22	0	0.84	2	2.35	0	-0.99
	3.6	0	0.22	0	0.84	-2	-1.73	0	0.13
	3.7	0	0.22	0	0.84	0	-0.28	2	2.18
	3.8	0	0.22	0	0.84	0	-0.28	-2	-1.89
	3.9	0	0.22	0	0.84	0	-0.28	0	0.20
	3.10	0	0.22	0	0.84	0	-0.28	0	0.20

In order to assign normalized values to the actual control gradients, straight lines were fitted to the data in Figure 4.3, yielding the normalizing equations given in Table 4.3. The normalized value for a given pulley-spring combination may be obtained by substituting the actual control gradient into the appropriate equation in Table 4.3. For example, for the nominal (0,0) front brake configuration, the displacement and force gradients were 3.65 mm s^2/m and 47.3 Ns^2/m, respectively, and the normalizing equations yielded RSM values of (0.22, 0.84). Table 4.4 shows the RSM preferred values and the actual normalized values for all the experimental configurations.

4.6 DESIGN OF RSM EXPERIMENTAL BRAKING TASK

4.6.1 The Stopping Task

On most occasions a motorcyclist applies the brakes on his machine in a non-hurried manner, as he will have anticipated the need to stop well before the desired stopping point. At the other end of the scale, it will be necessary for him to stop the motorcycle as rapidly as possible in an accident avoidance manoeuvre. Hurt et al.'s (1981) study showed that in an accident situation the rider typically has less than two seconds in which to take evasive action. With these considerations, three kinds of stop were identified; namely 'slow stop', 'medium stop', and 'quick stop'. It was thought that the experimental braking task should cover all of these situations so as to allow complete objective and subjective assessment of the rider-motorcycle configuration.

As with all the motorcycle experiments conducted in this study, rider safety was of paramount importance. This fact had a strong influence on the choice of an appropriate quick stop task. Three candidates were considered:

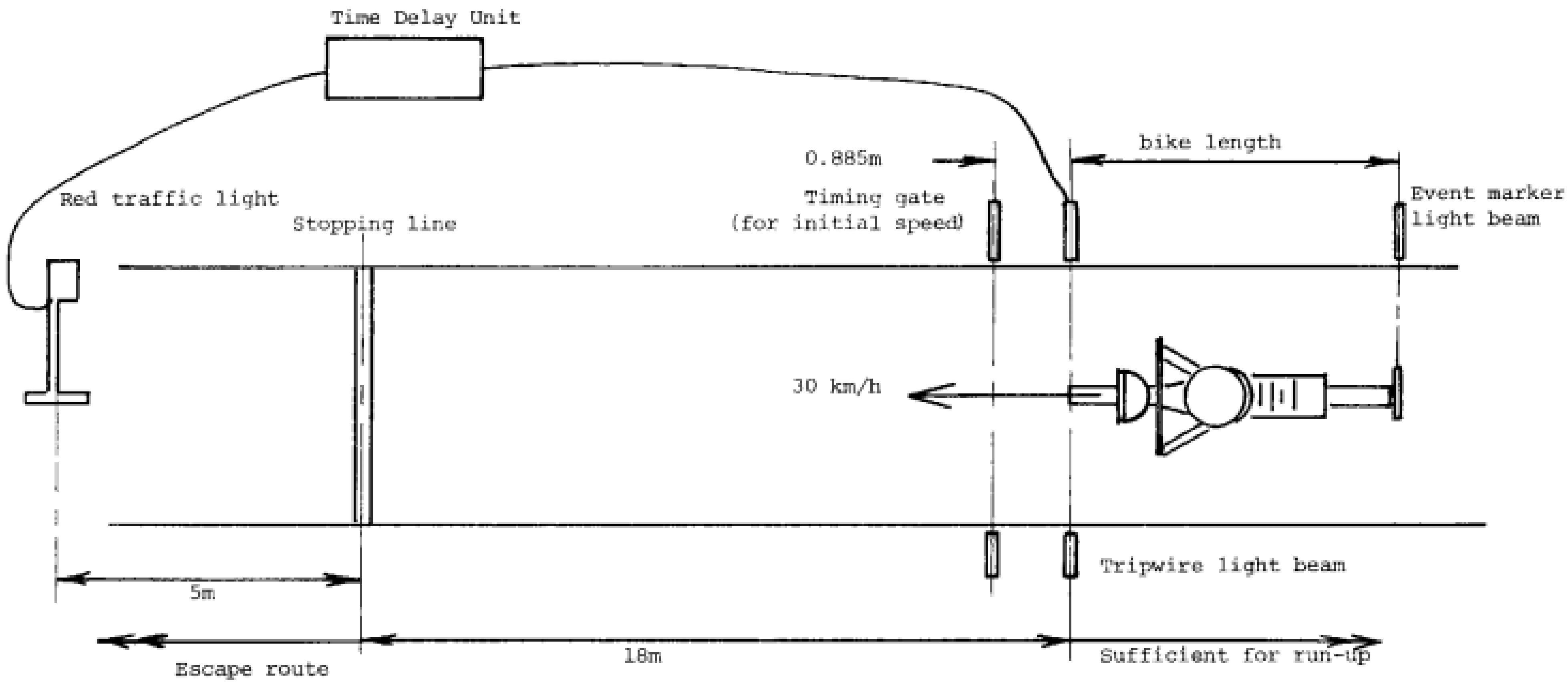

Figure 4.4 Layout of test track used for experimental braking task.

* 'Dropped box' situation, where the motorcycle is travelling in a straight line or a curve and, without warning, an obstacle appears in his path. The rider must use the brakes to avoid the obstacle.

* Car-following task, where the motorcycle is following another vehicle and, without warning, the latter stops rapidly. The motorcyclist must use his brakes to prevent a collision.

* Traffic light task. Here, the motorcycle approaches a set of traffic lights. If the lights change to red, the rider must respond by applying the brakes and attempt to stop the machine before reaching the lights.

The first two of the above quick stop tasks were rejected on safety grounds due to the greater possibility of loss of control and capsize or collision than for the traffic light task. Furthermore, the use of a 'tripwire' and a variable time delay to operate the traffic light enabled slow stop, medium stop and quick stop conditions to be set up with one apparatus and test track layout. The trip wire employed consisted of a lightbeam directed across the roadway and focussed on to a phototransistor. Interruption of the lightbeam by the motorcycle caused a change of state of the transistor. This signal was used to trigger a variable time delay circuit, which ultimately switched on the power supply to the traffic lights.

Figure 4.4 shows a diagramatic representation of the layout used for the braking task. The rider was instructed to keep the motorcycle at constant speed as he approached the tripwire area. In the event of the traffic lights turning on, the rider was to apply the brakes and attempt to stop on a line marked across the roadway. The task could be made more or less difficult depending on the selected time delay (longer delay being more difficult). In the interests of rider safety and to minimize potential equipment damage in the event of loss of control, the motorcycle speed was restricted to 30 km/h. The slow stop average deceleration was nominally 0.2 g, and the time delay for this task was zero. Thus the distance from the tripwire to the stopping line was determined as 18 m. The quick stop time delay was found by trial and error. The aim was that the rider should overshoot the stopping line on most occasions. This was found to occur with a time delay of 1.2 seconds, which implied an average deceleration of 0.5 g (including rider reaction time). A 0.6 second time delay was used for the medium stop, corresponding to an average deceleration of 0.3 g. An infinite time delay was also used, which meant the rider was not required to stop. This uncertainty was introduced to prevent the rider from anticipating a quick stop and thereby modifying his reaction time. The 'no-stop' task was randomly mixed with the medium and quick stop tasks.

4.6.2 Instrumentation

The on-board data acquisition system was used to record rider inputs and system responses during the RSM experiments. The transducers have been described in Appendix A.

It was necessary to have a mark on the recorded information to identify the passage of the motorcycle through the tripwire, so that initial speed, average deceleration during braking manoeuvre and rider reaction time could be determined. To do this an event marker system was designed and constructed. It switched the motorcycle speed trace off for 300 ms when the machine passed through the tripwire location. A phototransistor was mounted inside a blackened, 12.5 mm diameter by 150 mm long tube and attached to the motorcycle. A strong light beam was set at the same height as the tube, and directed across the motorcycle path at the tripwire location. When the light was incident on the phototransistor, a change of state occurred, and this signal was used to operate a relay on the speed trace which switched it to zero volts for 300 ms.

4.7 EXPERIMENTAL PROCEDURE

4.7.1 Test Site

The site for the RSM experiments with the VBCG motorcycle was at the rear of the Australian Road Research Board complex at Vermont South, Victoria. The track consisted of about 200 m of smooth hot mix bitumen in good condition with one flat straight section about 60 m long. Excellent garage and vehicle preparation areas were made available. Furthermore, the use of on-site 240V power simplified electricity requirements for the traffic lights and instrumentation.

4.7.2 Subjects

Two expert riders were used for the pilot experiments, in order to minimize performance variations due to insufficient riding and braking skills. Because some of the brake configurations to be tested were expected to be far from ideal, it was also considered prudent to have the first evaluations made by experts.

Both riders were everyday motorcycle commuters, one riding a 750ml large touring machine and the other a 500ml trail/street machine. They each had about ten years riding experience, and were members of motorcycle clubs. One had had closed club racing experience, and both were accustomed to long touring. Moreover they both had a technical background and were employed in research establishments.

4.7.3 Test Supervision

One person (Juniper) supervised the conduct of the experiments. He configured the motorcycle for the test riders, set the time delay for the traffic lights, and indicated to the rider when to begin the test. He also measured vehicle overshoot and noted the occurrence of wheel locks.

The two test riders assisted with setting up and dismantling the equipment on each day of the experiments. No other assistance was found necessary.

4.7.4 Test Logistics

A total of ten configurations per rider per day were tested. Each rider tested all thirty combinations required by the RSM design. The configurations for each day were randomly selected from the thirty to be covered, except that two of them were the 0, 0, 0, 0 'centre point' settings.

For a particular configuration the rider first completed three slow stops to allow familiarization with the new set up. Then followed one quick stop, one medium stop and (sometimes) a 'no stop' run, randomly ordered so as to prevent anticipation of a quick stop. The subject then filled out the rider rating form for that configuration while the other subject went through the same sequence of tests.

4.8 BRAKING PERFORMANCE MEASURES

Many motorcycle and rider related performance measures were used in the pilot study with a view to determining those most sensitive to brake control gradients. The measures included both objective measures of rider input and machine responses, and subjective measures of the riders' opinions about the brake configurations.

4.8.1 Subjective Measures

Rider ratings were obtained for seven different aspects of the braking system. On completion of the braking task, the riders were required to give an impression of the front and rear brake force and displacement requirements for that configuration. They were then asked to give an overall impression of the front and

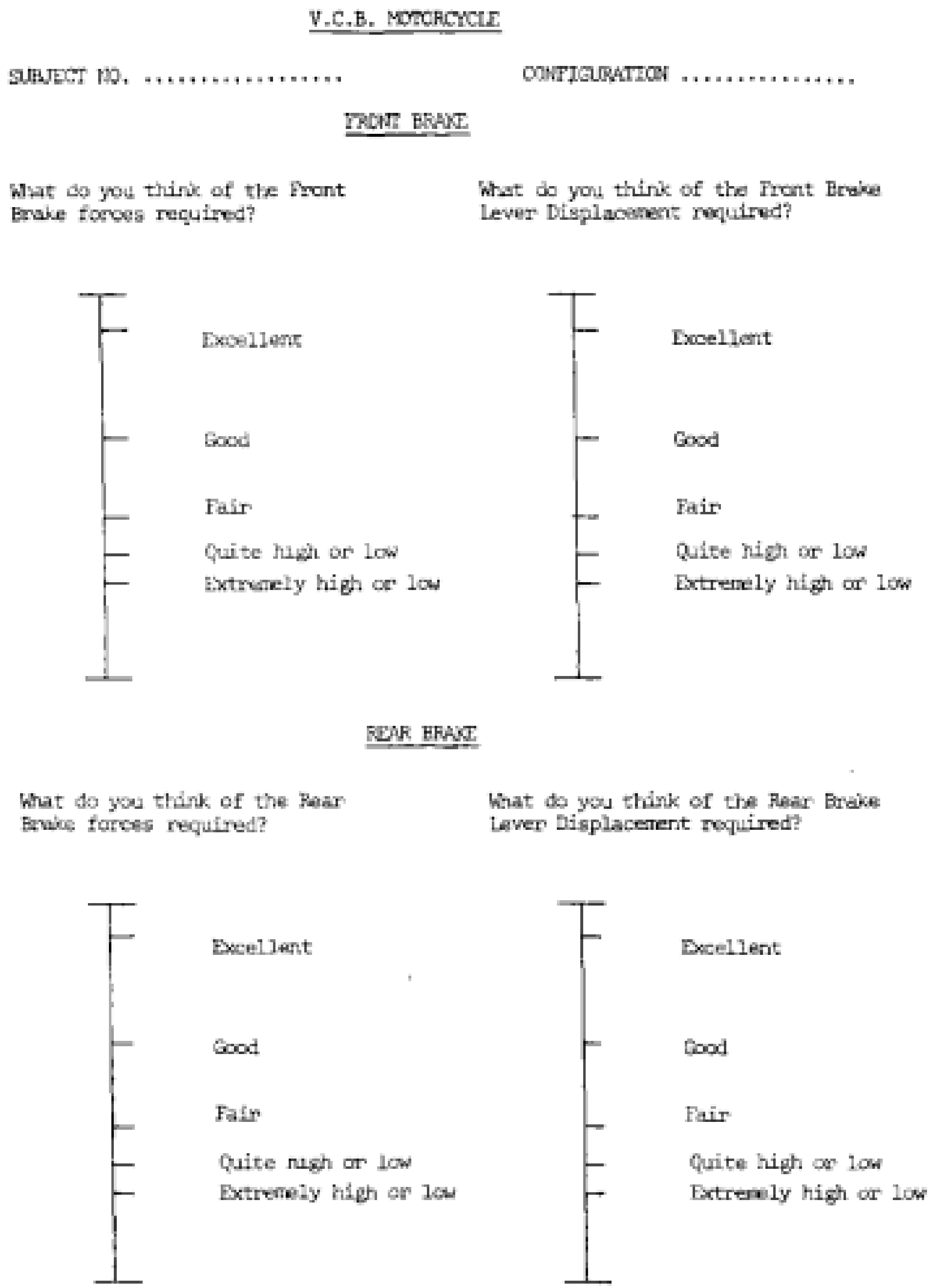

V.C.B. MOTORCYCLE

SUBJECT NO. .... CONFIGURATION ....

FRONT BRAKE

What do you think of the Front Brake forces required?

Excellent

Good

Fair

Quite high or low

Extremely high or low

What do you think of the Front Brake Lever Displacement required?

Excellent

Good

Fair

Quite high or low

Extremely high or low

REAR BRAKE

What do you think of the Rear Brake forces required?

Excellent

Good

Fair

Quite high or low

Extremely high or low

What do you think of the Rear Brake Lever Displacement required?

Excellent

Good

Fair

Quite high or low

Extremely high or low

Figure 4.5 Subjective rating form used in VBCG stopping task (reduced x 0.7)

How difficult was each task with this vehicle?

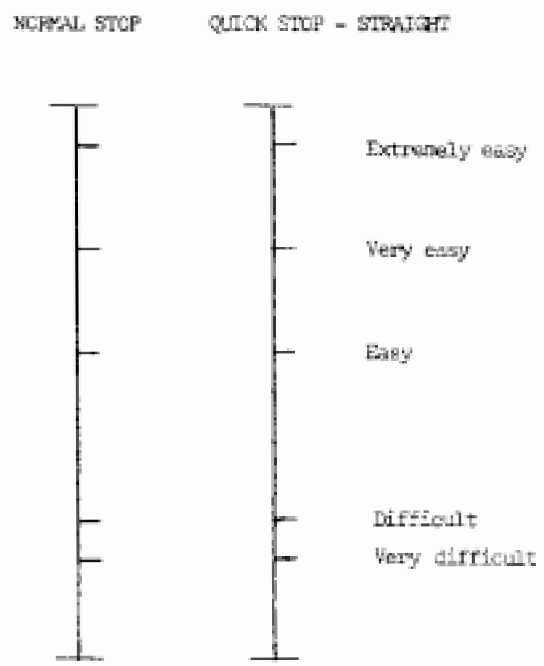

How does the braking of this vehicle compare with that of your own motorcycle.

Figure 4.5 (cont.)

TABLE 4.5 SUMMARY OF SUBJECTIVE AND OBJECTIVE PERFORMANCE MEASURES

Objective Performance Measures		
Number	Description	Symbol
1	Average deceleration during quick stop, from accelerometer	AVAC1
2	Average deceleration during quick stop, from speed trace	AVAC2
3	Average deceleration from front brake during quick stop	F
4	Average deceleration from rear brake during quick stop	R
5	Overshoot of stopping line during quick stop	OS
6	Reaction time during quick stop	TR

Subjective Performance Measures		
Number	Description	Symbol
7	Front brake force rating	FBFR
8	Front brake displacement rating	FBDR
9	Rear brake force rating	RBFR
10	Rear brake displacement rating	RBDR
11	Normal stop rating	NSR
12	Quick stop rating	QSR
13	Own motorcycle comparison rating	OMCR

rear brake combination in the normal stops (that is, the slow stop and medium stop tasks) and in the quick stop. Finally, they compared the braking ability of the machine with that of their own motorcycle.

The rating scales were derived from those used by Dorey (1979), which in turn were adapted from those developed for aircraft handling assessment (McDonnell, 1969). The adjectives on the scales are positioned in such a way as to provide an interval scale for the underlying psychological continuum (McDonnell, 1969). The rating form is shown in Figure 4.5. Each rider filled out one form for each configuration tested. They were instructed to put a mark on each rating scale in accordance with their opinion. The distance along the scale as a proportion of its total length was interpreted as a number between 0 and 100. The scale used for comparison with the rider's own motorcycle was horizontal, with adjectives only at either end, with zero at the left hand end, and 100 at the right hand end. A summary of the subjective performance measures can be found in Table 4.5.

4.8.2 Objective Measures

Several objective measures were used, all of which relate to rider-motorcycle performance in the quick stop task. Rider input force and displacement at each brake control was recorded, so that the separate contributions to the deceleration from the front and rear brakes could be determined. The ratio of front to rear wheel brake torque could also be calculated from these data. The lever input measurements, together with the event mark on the speed trace allowed rider reaction time to be measured. The average deceleration during the quick stop was determined both from the accelerometer, and from the average slope of the speed trace during the braking phase of the test.

Finally, the experimenter noted the distance by which the motorcycle over-shot (or under-shot) the stopping mark, and whether or not the rider locked the wheels at any stage. A summary of the objective performance measures is given in Table 4.5.

4.9 RESULTS AND DISCUSSION

The results obtained for all performance measures for both riders are tabulated in Appendix E.

In accordance with the RSM design, a second-order response surface model was fitted to the data for each performance measure, at first for each rider separately. The form of equation fitted was:

$$
\begin{aligned}
Y = b_0 &+ b_1\,(FBD) + b_2\,(FBF) + b_3\,(RBD) + b_4\,(RBF) \\
&+ b_{11}\,(FBD)^2 + b_{22}\,(FBF)^2 + b_{33}\,(RBD)^2 + b_{44}\,(RBF)^2 \\
&+ b_{12}\,(FBD.FBF) + b_{13}\,(FBD.RBD) + b_{14}\,(FBD.RBF) \\
&+ b_{23}\,(FBF.RBD) + b_{24}\,(FBF.RBF) \\
&+ b_{34}\,(RBD.RBF)
\end{aligned}
$$

where: Y = performance measure

FBD = normalized front brake displacement gradient

FBF = normalized front brake force gradient

RBD = normalized rear brake displacement gradient

RBF = normalized rear brake force gradient

The coefficients in the equation were determined using the SPSS Multiple Regression program (Nie et al., 1975). In this program the independent variables are entered into the regression in step-wise fashion, the next variable to be entered at each step being determined on the basis of the most significant increase in the measure of the proportion of the total variance explained by the regression (r^2). The statistical significance of each coefficient (probability of null hypothesis H_o:b_{ij}=0) is recalculated at each step. The regression results for all performance measures are tabulated in Appendix E. Example results, for both riders' deceleration performance in the quick stop, and their ratings of the brake configuration in that task, are shown in Tables 4.6 and 4.7.

One of the difficulties in interpreting these multi-variate data is the graphical presentation of the characteristics of a five-dimensional response surface. In order to facilitate the exploration and display of the nature of the response surfaces, a program was developed for the PDP 11/23 computer system which allowed plotting of response surface contours and of the variation of the predicted response with any given independent variable for selected constant values of the other independent variables. Example plots are shown in Figures 4.6 - 4.9.

4.9.1 Subjective Measures

The seven subjective measures listed in Table 4.5 were subjected to the analyses described above. The raw data together with the regression results are presented in Appendix E.

Reviewing the r^2 values in Appendix E reveals that, for none of the measures, was a large proportion of the total variance explained by the fitted response surface. The highest value of r^2 obtained was 0.675, being for rider RDH's front brake force rating; the lowest value of 0.273 was also for RDH, but for his rear brake force rating.

Of all the subjective measures, the quick stop rating (QSR) is perhaps of the greatest interest, for it represents the rider's overall assessment of the brake configuration in the most demanding braking task. The QSR regression results for both riders are shown in Table 4.7. It can be seen that less than 60% of the total variance in quick stop ratings was explained by the regressions.

TABLE 4.6 (a) DECELERATION PERFORMANCE IN QUICK STOP TASK, RDH

RESULTS OF SPSS MULTIPLE REGRESSION ANALYSIS

MEASURE: AVERAGE DECELERATION IN QUICK STOP FROM SPEED TRACE (AVAC2, m/s^2)

SUBJECT: RDH SIGNIFICANCE OF REGRESSION: 0.183 r SQUARE: 0.621

Coefficient	Independent Variable	Value of Coefficient	Significance	Entered On Step Number	r Square Change
b_0	Constant	6.68			
b_1	FBD	-0.41	.007	1	.122
b_2	FBF	0.11	.369	8	.029
b_3	RBD	0.04	.785	13	.002
b_4	RBF	0.08	.536	12	.009
b_{11}	$(FBD)^2$	-0.11	.366	6	.037
b_{22}	$(FBF)^2$	-0.11	.144	4	.065
b_{33}	$(RBD)^2$	0.08	.542	11	.008
b_{44}	$(RBF)^2$	-0.14	.225	3	.067
b_{12}	FBD.FBF	-0.02	.916	14	.000
b_{13}	FBD.RBD	-0.34	.090	2	.149
b_{14}	FBD.RBF	0.11	.499	10	.014
b_{23}	FBF.RBD	0.20	.308	7	.031
b_{24}	FBF.RBF	0.22	.201	5	.073
b_{34}	RBD.RBF	0.21	.298	9	.017

TABLE 4.6 (b) DECELERATION PERFORMANCE IN QUICK STOP TASK, BG

RESULTS OF SPSS MULTIPLE REGRESSION ANALYSIS

MEASURE: AVERAGE DECELERATION IN QUICK STOP FROM SPEED TRACE (AVAC2, m/s^2)

SUBJECT: BG SIGNIFICANCE OF REGRESSION: 0.456 r SQUARE: 0.461

Coefficient	Independent Variable	Value of Coefficient	Significance	Entered On Step Number	r Square Change
b_0	Constant	6.19	-		
b_1	FBD	0.28	.075	1	.167
b_2	FBF	-			
b_3	RBD	0.08	.642	6	.014
b_4	RBF	0.19	.239	3	.061
b_{11}	$(FBD)^2$	-0.02	.872	13	.001
b_{22}	$(FBF)^2$	-0.05	.575	9	.007
b_{33}	$(RBD)^2$	-0.08	.591	11	.004
b_{44}	$(RBF)^2$	-0.12	.364	5	.014
b_{12}	FBD.FBF	0.13	.471	7	.010
b_{13}	FBD.RBD	-0.22	.323	4	.035
b_{14}	FBD.RBF	-0.07	.723	12	.004
b_{23}	FBF.RBD	0.41	.053	2	.125
b_{24}	FBF.RBF	0.11	.529	8	.010
b_{34}	RBD.RBF	-0.13	.562	10	.004

TABLE 4.7 (a) QUICK STOP RATING, RDH

RESULTS OF SPSS MULTIPLE REGRESSION ANALYSIS

MEASURE: QUICK STOP RATING (QSR)

SUBJECT: RDH SIGNIFICANCE OF REGRESSION: 0.122 r SQUARE: 0.583

Coefficient	Independent Variable	Value of Coefficient	Significance	Entered On Step Number	r Square Change
b_0	Constant	52.86	-		
b_1	FBD	4.22	.156	6	.040
b_2	FBF	1.17	.671	11	.004
b_3	RBD	-0.01	.998	4	.044
b_4	RBF	3.11	.308	10	.026
b_{11}	$(FBD)^2$	-			
b_{22}	$(FBF)^2$	-2.83	.091	2	.104
b_{33}	$(RBD)^2$	3.25	.248	1	.144
b_{44}	$(RBF)^2$	-3.91	.116	3	.043
b_{12}	FBD.FBF	-6.09	.118	7	.032
b_{13}	FBD.RBD	-1.31	.734	12	.003
b_{14}	FBD.RBF	-			
b_{23}	FBF.RBD	-8.01	.080	8	.031
b_{24}	FBF.RBF	-6.72	.068	9	.075
b_{34}	RBD.RBF	-7.24	.106	5	.038

TABLE 4.7 (b) QUICK STOP RATING, BG

RESULTS OF SPSS MULTIPLE REGRESSION ANALYSIS

MEASURE: QUICK STOP RATING (QSR)

SUBJECT: BG SIGNIFICANCE OF REGRESSION: 0.081 r SQUARE: 0.559

Coefficient	Independent Variable	Value of Coefficient	Significance	Entered On Step Number	r Square Change
b_0	Constant	66.46	-		
b_1	FBD	-			
b_2	FBF	1.71	.719	10	.003
b_3	RBD	19.02	.003	1	.238
b_4	RBF	7.32	.194	2	.089
b_{11}	$(FBD)^2$				
b_{22}	$(FBF)^2$	-1.73	.566	9	.006
b_{33}	$(RBD)^2$	-9.84	.071	4	.057
b_{44}	$(RBF)^2$	-6.23	.185	6	.044
b_{12}	FBD.FBF	11.86	.084	3	.062
b_{13}	FBD.RBD				
b_{14}	FBD.RBF	-5.55	.391	7	.020
b_{23}	FBF.RBD	-4.56	.477	8	.015
b_{24}	FBF.RBF	-0.64	.916	11	.000
b_{34}	RBD.RBF	-12.22	.125	5	.025

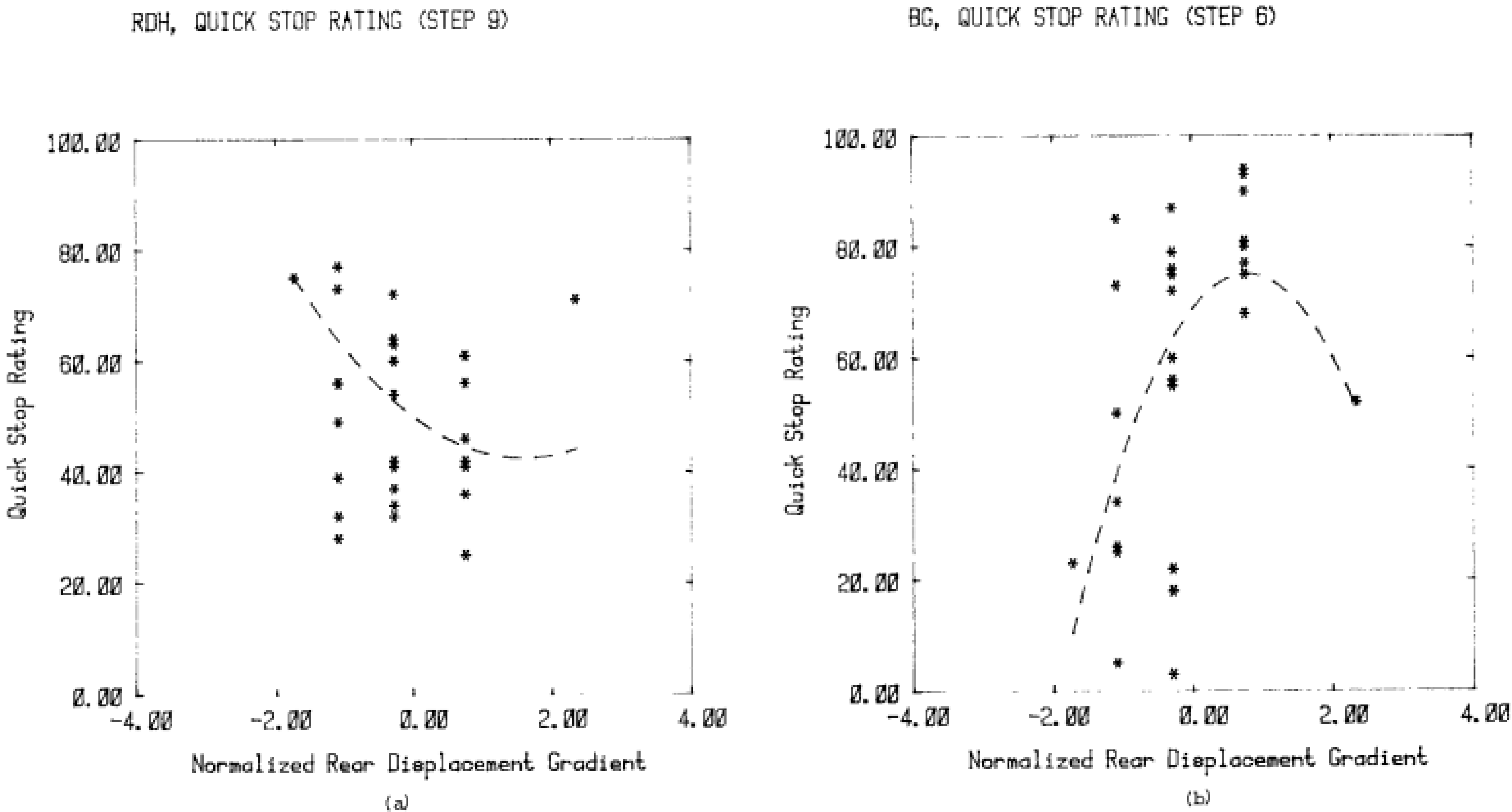

Figure 4.6 Subject quick stop rating versus rear displacement gradient.

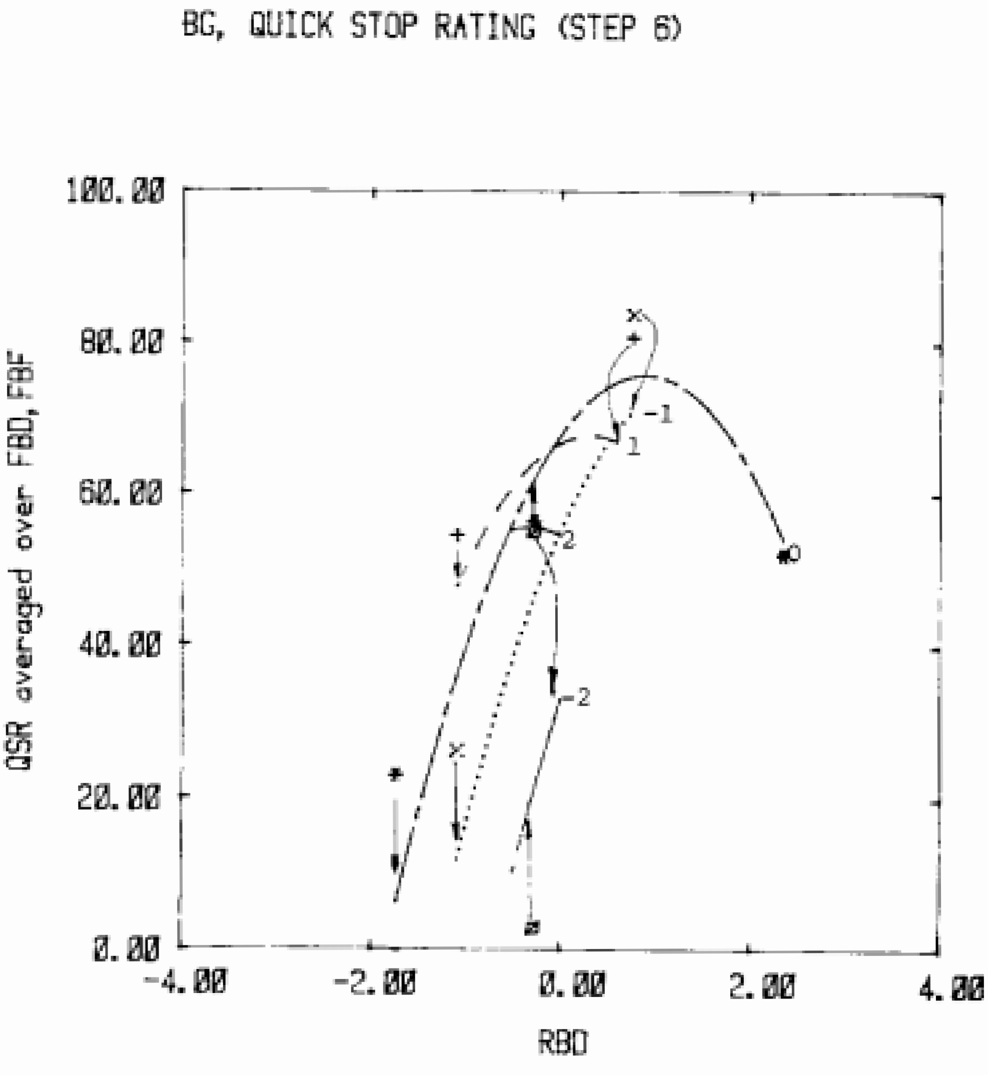

Figure 4.7 Quick stop ratings (averaged over front brake variables) versus rear brake displacement gradient, with rear brake force gradient shown parametrically, subject BG.

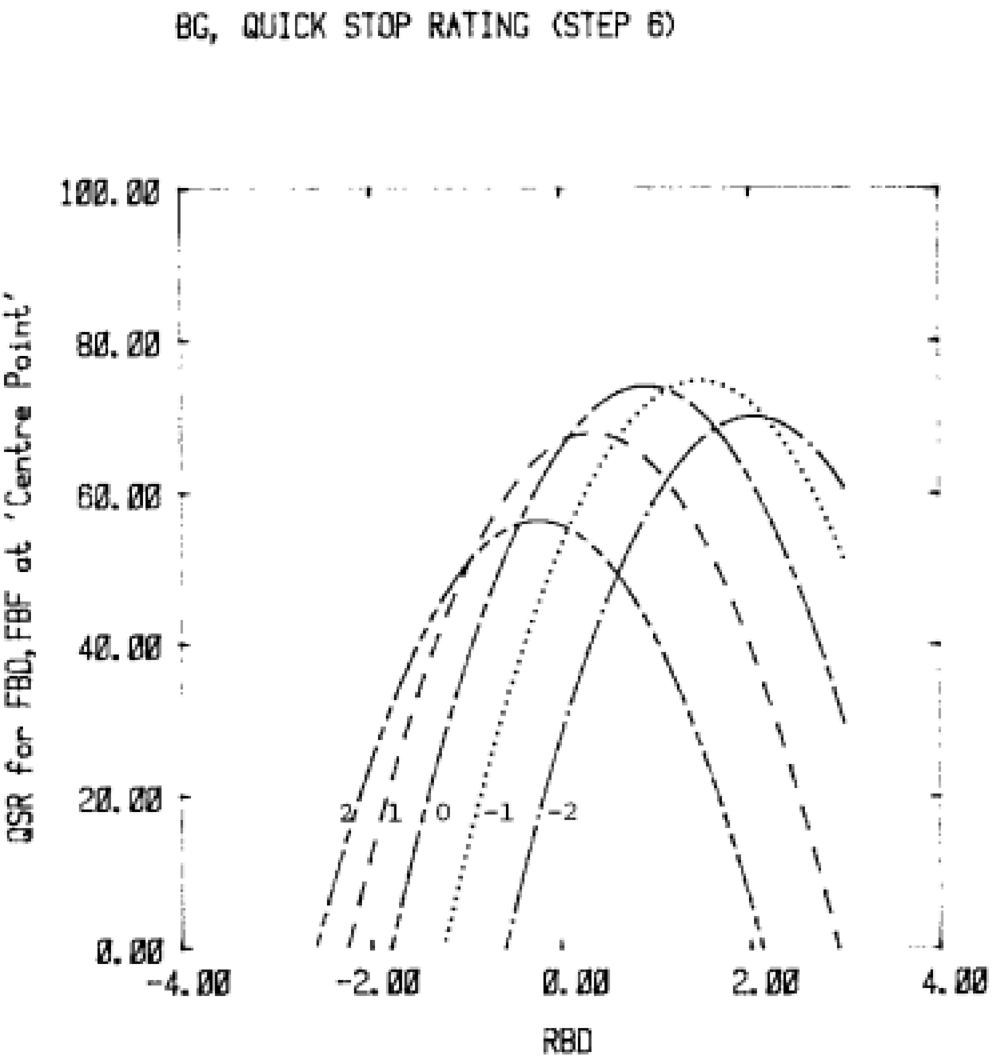

Figure 4.8 (a) Quick stop rating (with front brake variables at centre point) versus rear brake displacement gradient, with rear brake force gradient shown parametrically, subject BG.

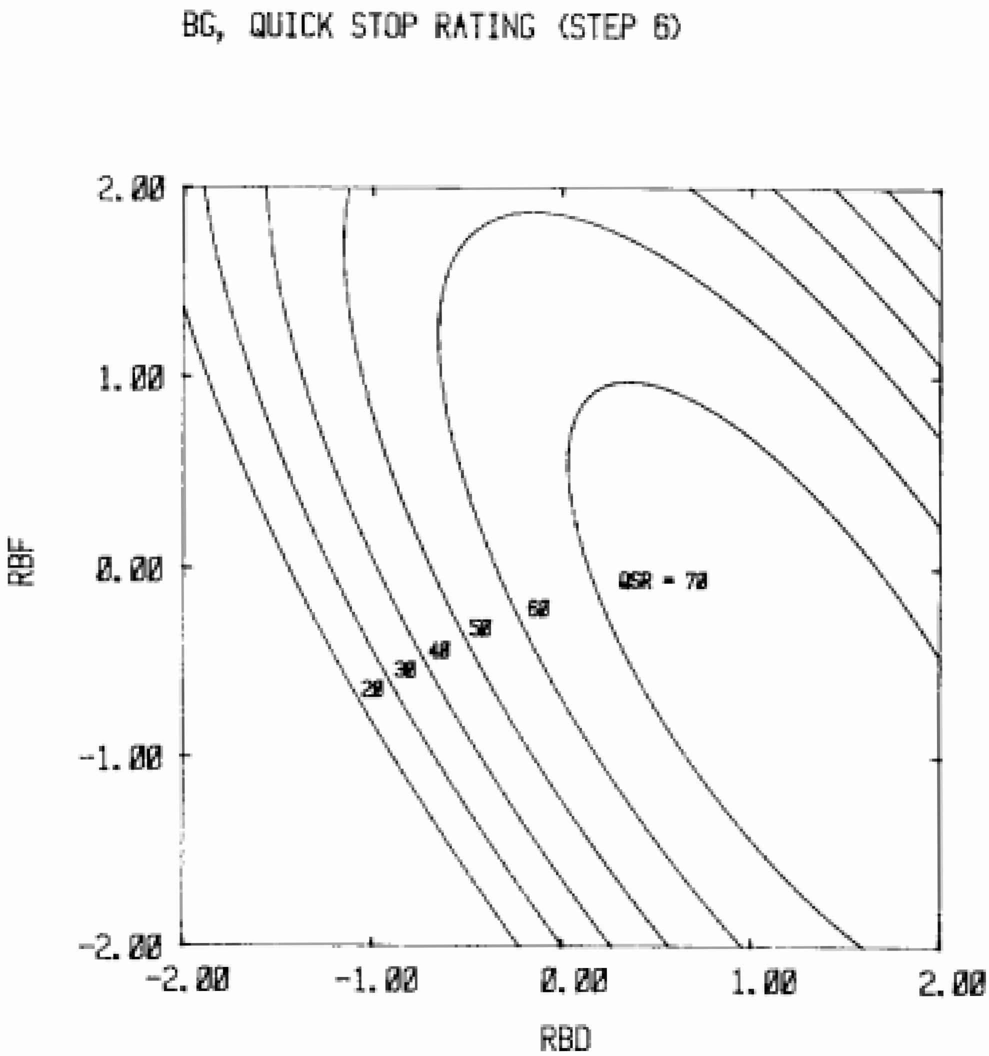

Figure 4.8 (b) Rear brake force gradient versus rear brake displacement gradient, showing quick stop rating contours (front brake variables at centre point).

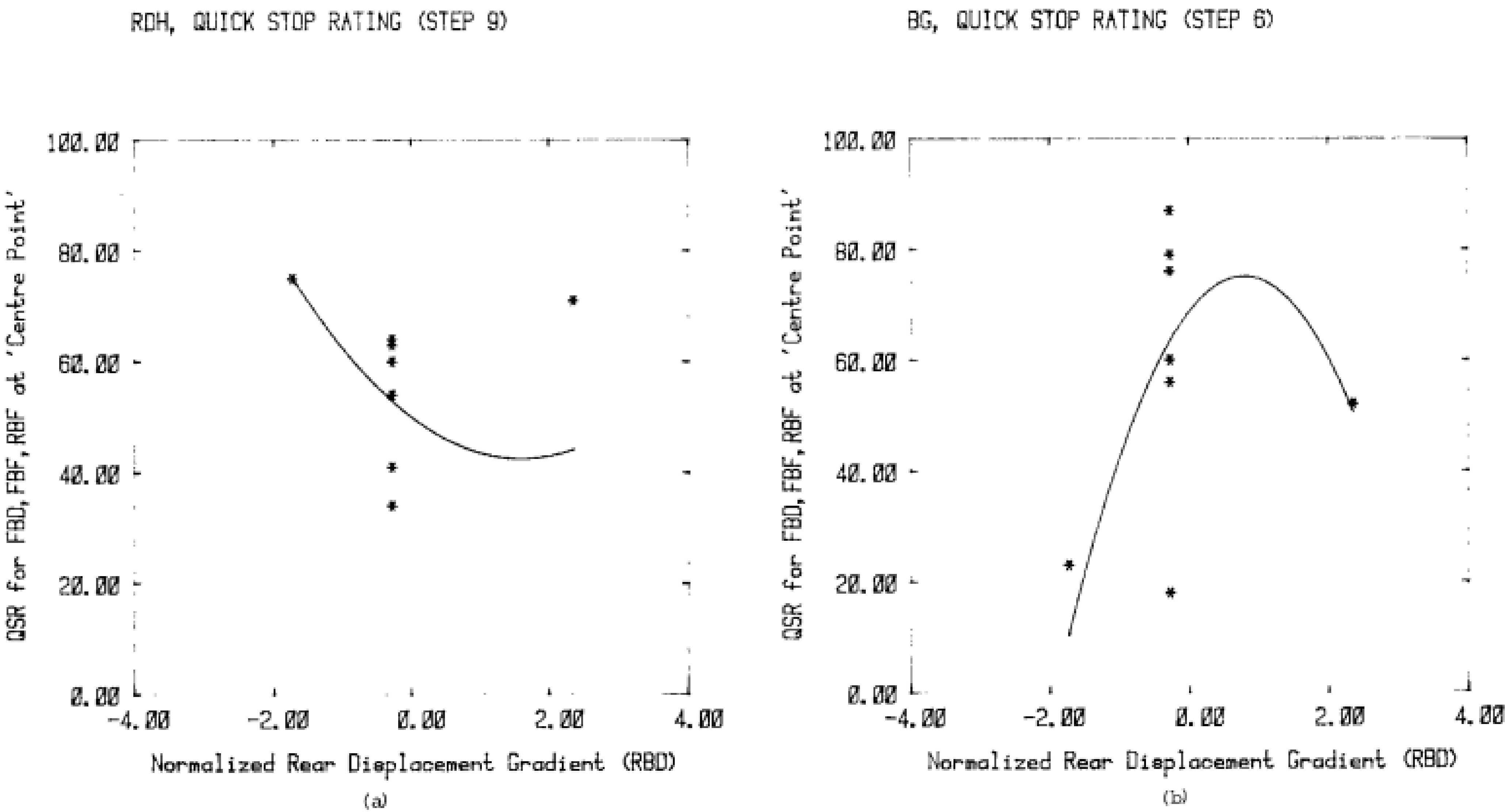

Figure 4.9 Quick stop rating versus rear displacement gradient, other independent variables at the centre point, both subjects.

Table 4.7 shows that, for both riders, the first variable to be entered into the QSR regressions was the rear displacement gradient RBD. Plots of QSR versus RBD, including all the measured data, are shown in Figure 4.6, together with the regression equation evaluated for the 'centre point' values of the other independent variables RBF, FBD and FBF: completely opposite trends are indicated for the two riders.

The 'scatter' of data points about the regression lines in Figure 4.6 could of course be related to the variation of QSR with the other independent variables. To explore this possibility, the data for BG's ratings were selected for further examination, because of his wider range of QS ratings. Figure 4.7 shows his QSR plotted against RBD for the five constant values of RBF, the data being averaged over the front brake configurations. The corresponding regression lines are also shown. The data are consistent in showing an increase in BG's rating as the normalized rear displacement gradient increases from -2 to +1, with the single data point at RBD = +2 being responsible for the decrease of the calculated QSR for higher values of RBD. However, the degree of correspondence between the average data points and the regression lines is not impressive. More as an illustration of the type of analysis it was hoped would be possible, rather than as a serious representation of BG's preferences, Figures 4.8 (a) and (b) show his QSR regression evaluated over the whole range of rear brake configurations, both as 'sections' of the response surface in (a), and as 'contours' in (b).

Figures 4.9 (a) and (b) reveal the reason for the lack of success of the response surface representations of the data. These show the QS ratings obtained for the six replications of the 'centre point' configuration (numbers 1.9, 1.10, 2.9, 2.10, 3.9, 3.10 in Table 4.1), and the two 'star point' configurations (3.5, 3.6) for which the RBD was the only variable with a value different from the centre point configuration. It can be seen that the variation in the ratings for the identical centre point configurations is as wide as that obtained over all configurations. Thus, the hoped-for consistency in ratings from 'expert' riders was not obtained. It is clear that the overall form of the regression equation (eg. whether it indicates a maximum or minimum for the response surface) depends critically on the values obtained for the star points. Given the variability of the replicated data, no confidence can be placed in the results obtained from the single observations at the star point configurations.

Analyses of the type illustrated for BG's QS ratings were pursued vigorously for any data which appeared to contain some trend of significance. These efforts were all ultimately frustrated by the problem epitomized in Figure 4.9 : the 'error variance' - shown by the variation in centre point results - was simply too large for the response surface methodology to yield useful results.

A further illustration of this unfortunate situation is that many of the statistically 'significant' regression results do not accord with common sense. For example, it would be expected that if a rider were asked to rate front brake force requirements, then the front brake force gradient would be highly correlated with this rating measure. This situation occurred only twice, with rider RDH when rating front brake force requirements, and BG when rating rear brake displacement requirements. The ratings given by rider BG were always highly correlated with rear brake displacement gradient without regard to the measure involved.

Possibly the main reason for the variability of the riders' ratings and the poor correlation between them and the control gradient settings was the short time they had to assess the motorcycle behaviour. They were restricted to five stops from 30 km/h, mainly due to the limited time available to conduct the RSM experiments. A rider may require more like half to one hour of testing at all speeds, in both straight and curved path braking tasks, to be accurate in his assessment of the system characteristics. As a further aid to judgement, referral to a standard, benchmark motorcycle throughout the tests, or a paired-comparison technique, may be required. Data collection on this basis for a full scale experiment involving 30 subjects would take 4 to 6 months to complete. Thus the minimum time for a rider to accurately assess the brake system behaviour is a factor requiring careful evaluation in the planning of any future full scale experiments.

Another factor requiring consideration in the design of future experiments is the brake system attributes which riders are asked to evaluate. One of the riders found that assessing the brake feel properties in terms of the brake force and displacement requirements was particularly difficult. It may be that riders judge feel characteristics on the basis of system 'stiffness' (i.e. force/displacement) rather than force and displacement separately. This matter warrants further consideration. The variability of the present data precludes such an investigation now.

As has been seen, the quick stop ratings for the two riders were poorly correlated with the brake control gradients : for RDH, $r^2 = 0.583$, overall significance $= 0.122$; for BG, $r^2 = 0.559$ and overall significance $= 0.081$. It was thought that the riders' quick stop rating might be influenced by their performance in this task: that is, if they were successful with a particular configuration they might rate it highly. In order to investigate this hypothesis, overshoot in the quick stop was included in the multiple regression analysis of quick stop ratings as an independent variable. For rider RDH, the inclusion of this additional independent variable was of no consequence. With BG, however, the first variable entered into the equation was overshoot, the coefficient of which was negative and highly significant. This variable alone accounted for half of the variance in BG's ratings. This implied that if the rider had a large overshoot in the quick stop, he then down-rated the configuration. It is shown in the next section that overshoot was virtually constant, apart from random variations about the mean value (of zero). Thus, although this regression relationship is statisically significant, it does not help to elucidatethe nature of rider preferences for control gradients.

4.9.2 Objective Measures

The average deceleration in the quick stop was calculated by two different procedures. The first, represented by AVAC1, was computed from the accelerometer trace. It was corrected for pitch effects and then averaged between when the brakes were applied and when the speed became zero. The second procedure involved determining the average speed just before the brakes were applied, and the time taken to stop after the brakes were applied, from which the average deceleration AVAC2 was computed. These procedures yielded virtually indentical results, as shown in Figure 4.10. However, there was some scatter, particularly for rider RDH's data, so it was decided to use AVAC2 as the measure of average deceleration in the quick stop, as fewer calculations (and, presumably, errors) were involved in its determination.

The AVAC2 data were processed by SPSS Multiple Regression with the results shown in Table 4.6. It can be seen that, for neither of the riders, was the variation in average deceleration adequately explained by the control gradient variations: rider RDH yielded $r^2 = 0.62$; BG gave $r^2 = 0.46$.

The most significant independent variable in the AVAC2 regression for both riders was the front brake displacement gradient FBD (for RDH, $p < 0.007$; for BG, $p < 0.075$). However, RDH yielded a negative regression coefficient, implying a marginally better braking performance for lower front brake displacement gradients, while BG gave a positive coefficient, again in contradiction of RDH's results. The AVAC2 data for both

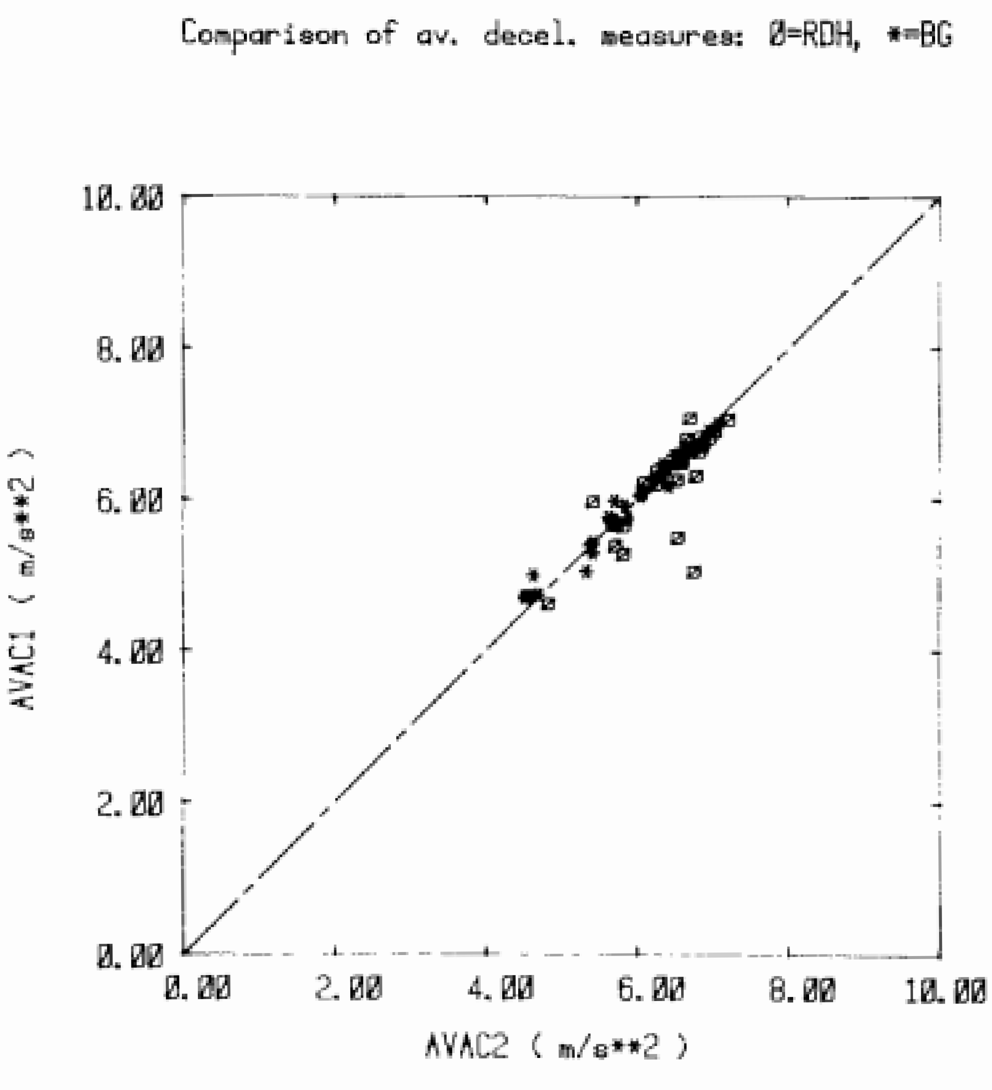

Figure 4.10 Quick stop average deceleration from accelerometer trace versus average deceleration calculated from speed transducer.

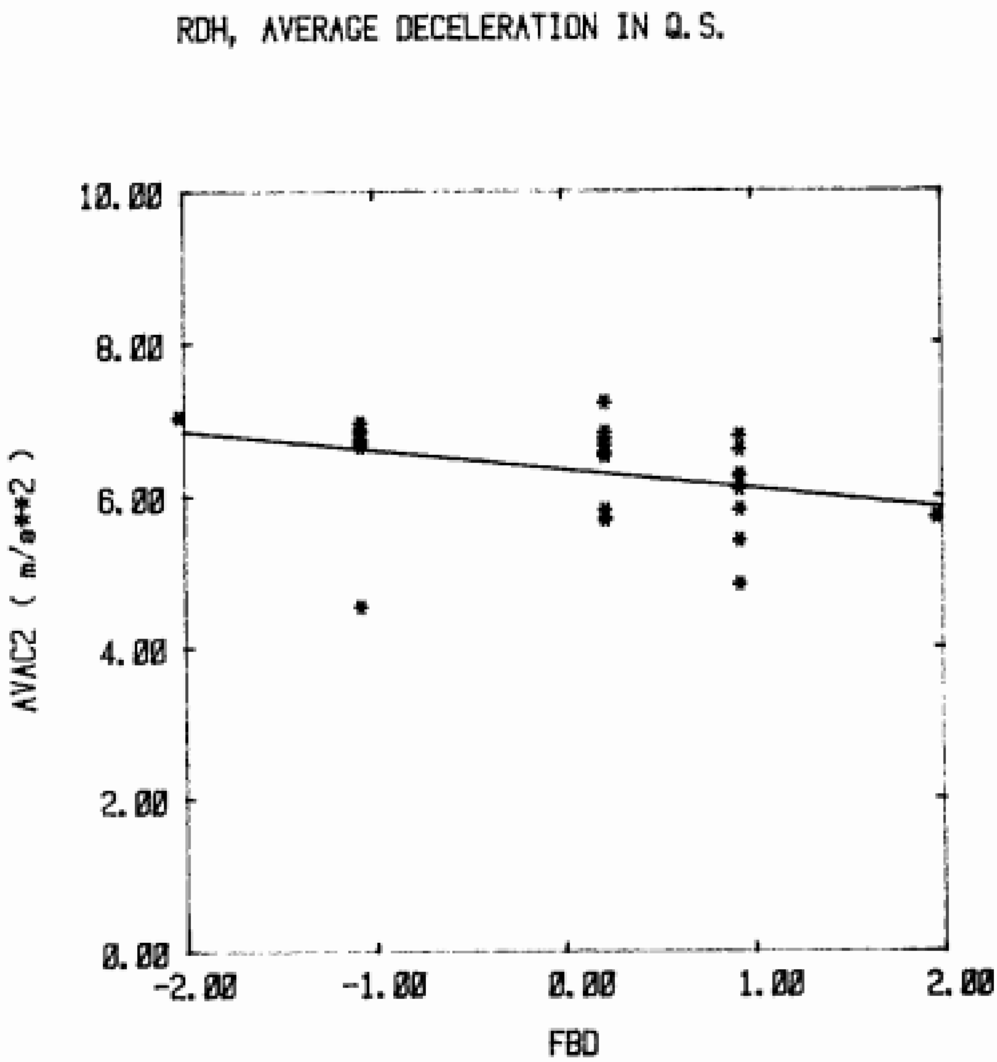

Figure 4.11 (a) Average deceleration in quick stop versus front brake displacement gradient, subject RDH.

BG, AVERAGE DECELERATION IN Q.S.

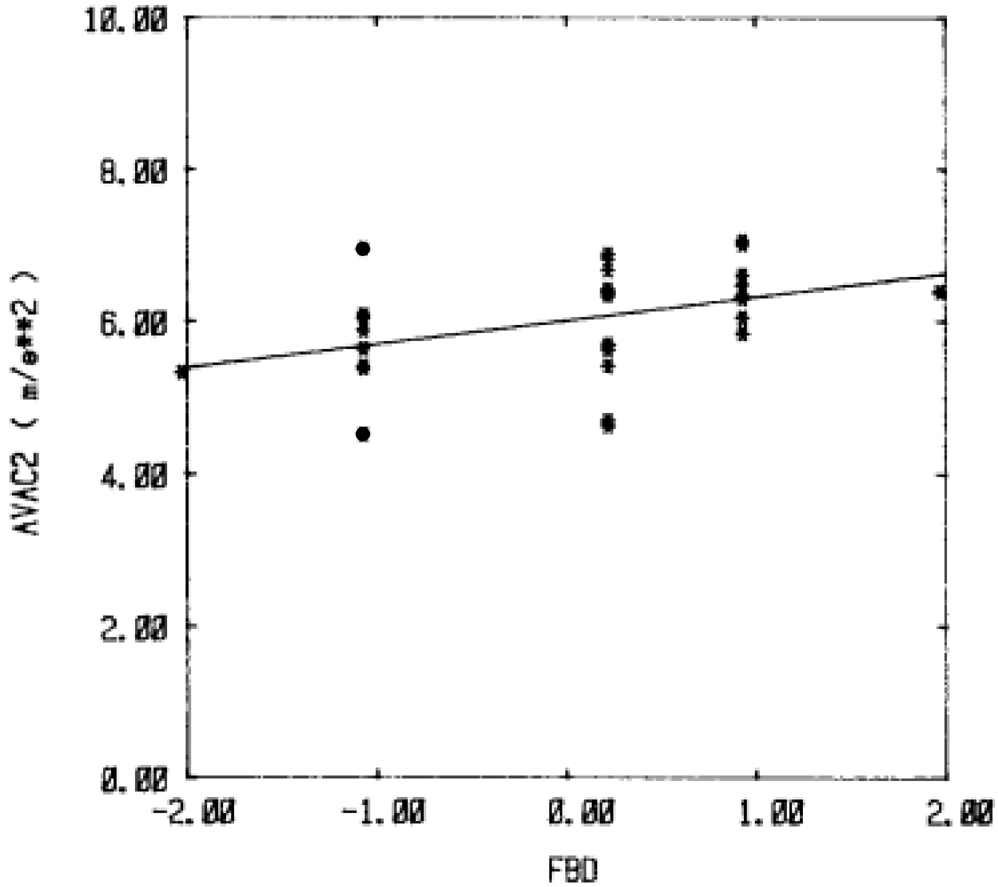

Figure 4.11 (b) Average deceleration in quick stop versus front brake displacement gradient, subject BG.

riders are plotted in Figure 4.11, together with the linear regressions on FBD. In both cases, the variation of AVAC2 with FBD is not large, while the remaining variation of AVAC2 is not satisfactorily explained by the other independent variables.

On average, then, both riders were able to achieve similar levels of braking performance over a wide range of brake system characteristics. This is further demonstrated by the regression results for the overshoot in the quick stop, shown in Appendix E. Variations in this measure were not related to configuration variations, and the value of the constant b_0 in the relationship had a high probability of being zero. This implies that the motorcycle mostly stopped on the stopping line marked across the roadway, and that a change of control gradient did not make much difference to the result. Braun et al.(1982) found a similar situation exists for gain factors in motor vehicle brake systems. Tests were carried out with a number of drivers in a car with a selectable gain factor. On dry surfaces, their results did not show any significant influence of the gain factor on the stopping distance under full braking. They concluded that because of the great adaptability of the drivers to the test conditions, no guides to design modifications of brake systems could be given. Such consistency of objective measures of task performance, a result of the human operator's great adaptability, is not uncommon in investigations of this sort (Good, 1977). There is also the possibility that, perhaps unconsciously, the riders used the stopping line as a target, rather than an upper bound for stopping distance. If this was the case, and the stopping distance was within their capabilities for all the brake configurations presented, the effects of the different control gradients would have been masked. However, further testing with more severe stopping requirements would be required to test this hypothesis.

One aspect of performance with a two-point braking system that is of considerable importance is the proportioning of braking effort between the front and rear brakes. Because of load-transfer effects, the optimum proportioning (to achieve equal utilization of available tyre/road friction at each wheel) varies with the level of deceleration. Investigation of the contributions made to the total deceleration from the front and rear brakes revealed a deficiency in the experimental procedure. To determine these contributions, the average lever displacement, D_{av}, and the displacement at which a brake torque was first applied, D_o, were required for each brake. Then, from the average useful lever displacement, $D_{av} - D_o$, and the displacement/deceleration gradient calibration for the given brake configuration, the average deceleration contribution from that brake could be computed. In setting up the spring-pulley arrangements for each configuration, care was taken to adjust the amount of 'slack', D_o, to be roughly the same for each set up. However, because the need for this information was not anticipated at the time of the experiments, the adjustment was not made precisely. What was really required was that a low-frequency displacement modulation calibration of each brake be performed prior to each rider's tests with a given configuration. Had such tests been performed it would have been possible to accurately determine the threshold displacement D_o for each case. In the event, it was necessary to estimate D_o by the following procedure: The force-displacement relationship for each brake was examined for each run, and the displacement at which the force began to increase was found by overlaying a line with a slope determined from the appropriate stiffness calibration. An example is shown in Figure 4.12(b). It was then necessary to assume that the experimenter had adjusted the slack correctly, so that the brake force would rise at the same time as the brake actually applied a torque to the wheel. As already indicated, this assumption would not always have been precisely met. A second source of uncertainty arose from the fact that the brake application in the quick stop was extremely rapid, so that there were only a few sampled data points during the rise of brake force and displacement, and it was consequently difficult at times to fit the stiffness calibration line. Again, Figure 4.12(b) illustrates this difficulty.

The contributions to the average deceleration in the quick stop from the front and rear brakes determined by the procedure just described were denoted F and R, respectively. Results of regression of F and R on the RSM independent variables are given in Appendix E. For both riders, the first variable to be entered into the regression equation for F was the front brake displacement gradient, FBD, as was the case for the measured deceleration AVAC2.

Figure 4.13 shows simple linear regressions of F and R on FBD for both riders. Also shown is the sum of these, F+R, for comparison with the measured total deceleration AVAC2 (shown as the plotted data points and the solid regression line). For rider RDH the sum of the calculated deceleration contributions, F+R, agrees well with the measured data. For BG, however, the calculated sum considerably underestimates the actual total deceleration. The reason for this discrepancy appears to lie in BG's braking strategy. He was observed to modulate the brakes in the quick stop, as illustrated in Figure 4.14. Because of the hysteresis associated with the displacement-deceleration cycling, the use of the simple 'stiffness' calibration to calculate the average deceleration would underestimate the actual contribution from the given brake. Rider RDH did not exhibit the same cycling behaviour in the quick stop (Figure 4.12 is representative).

It was indicated previously that the proportioning of the total braking effort between the front and rear brakes is of considerable importance. Parts (a) and (b) of Figure 4.15 respectively show the calculated deceleration contributions F and R plotted against FBD for rider RDH. The corresponding data for rider BG are shown in Figure 4.16. The solid lines in these

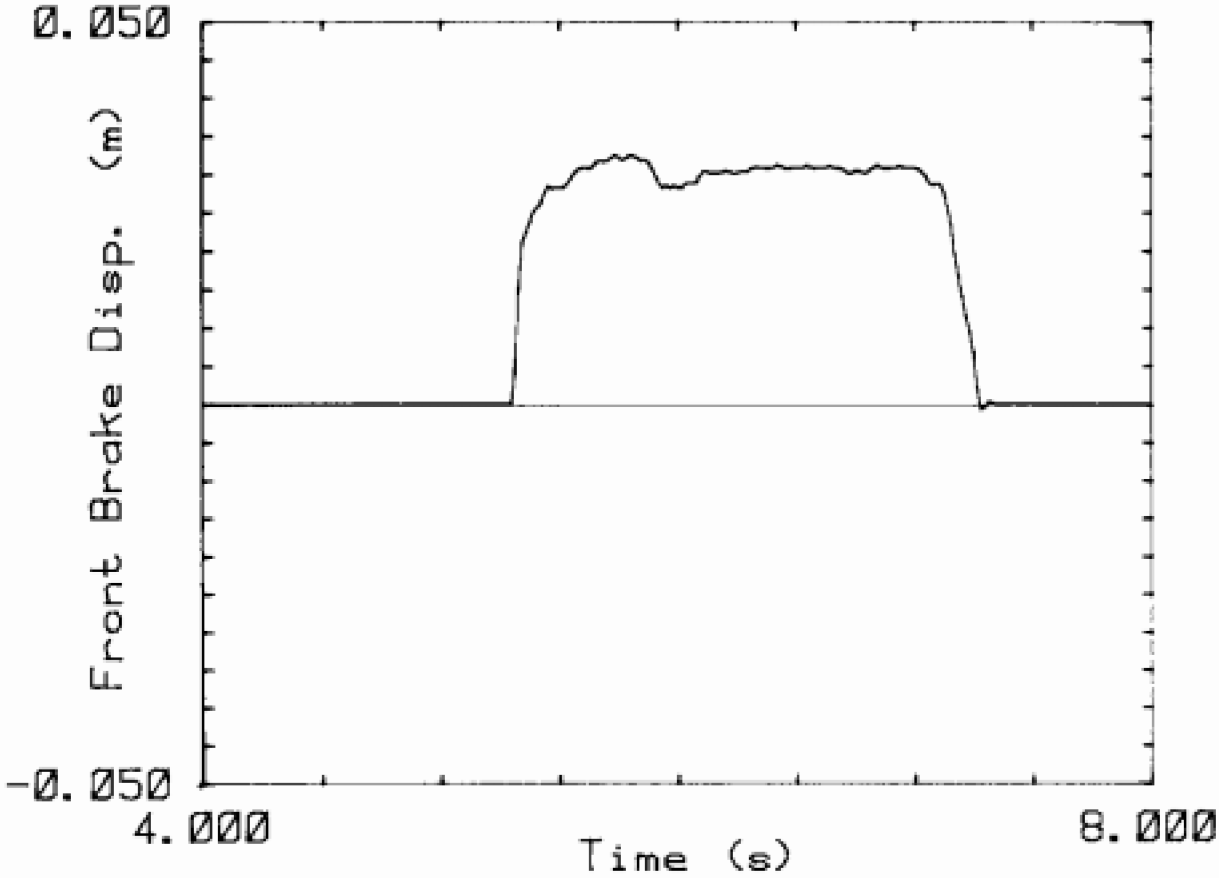

Figure 4.12 (a) Front brake displacement during a quick stop manoeuvre, subject RDH.

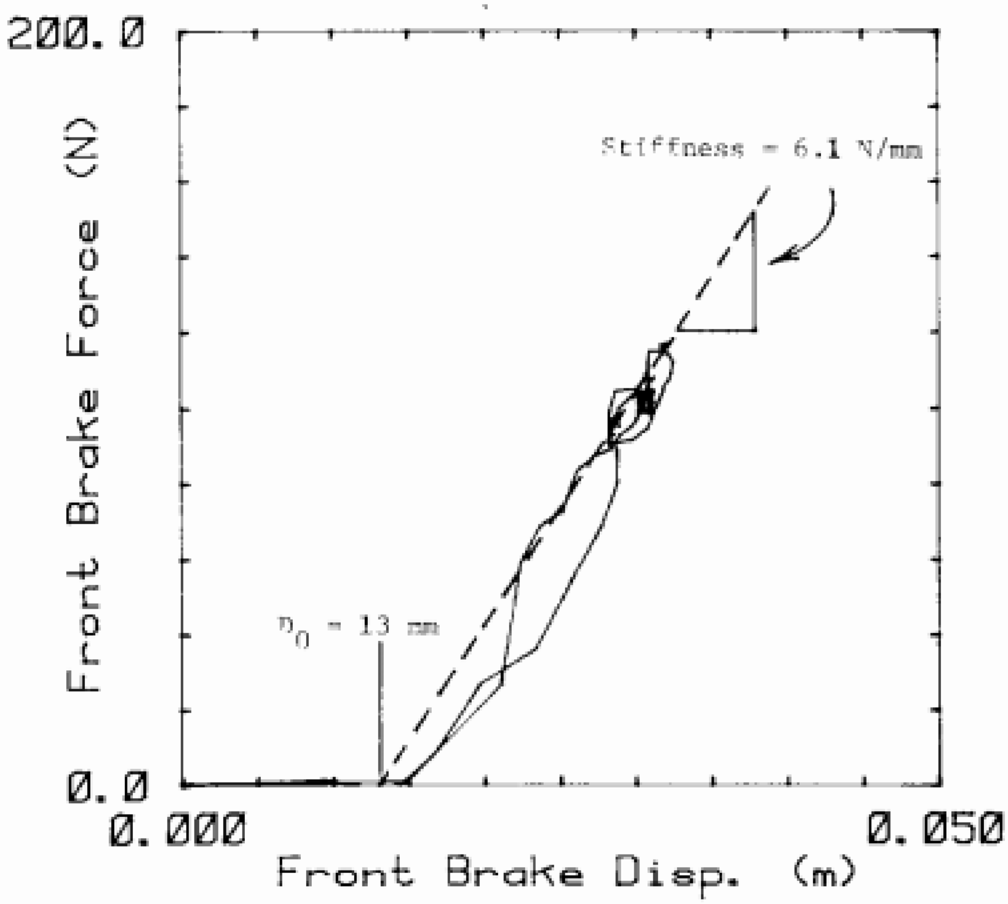

Figure 4.12 (b) Front brake force versus front brake displacement during a quick stop manoeuvre, subject RDH.

RDH, AVERAGE DECELERATION IN Q.S.

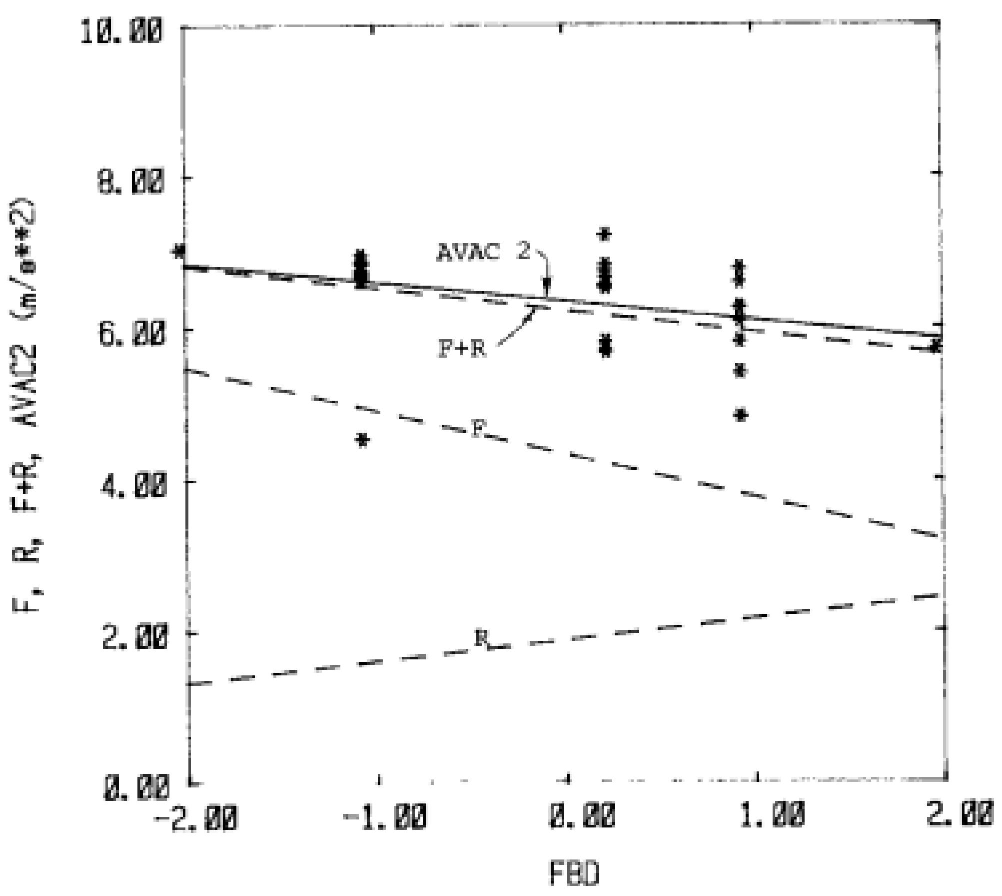

Figure 4.13 (a) Front brake deceleration contribution, rear brake contribution and total deceleration in quick stop task versus front brake displacement gradient, subject RDH.

BG, AVERAGE DECELERATION IN Q.S.

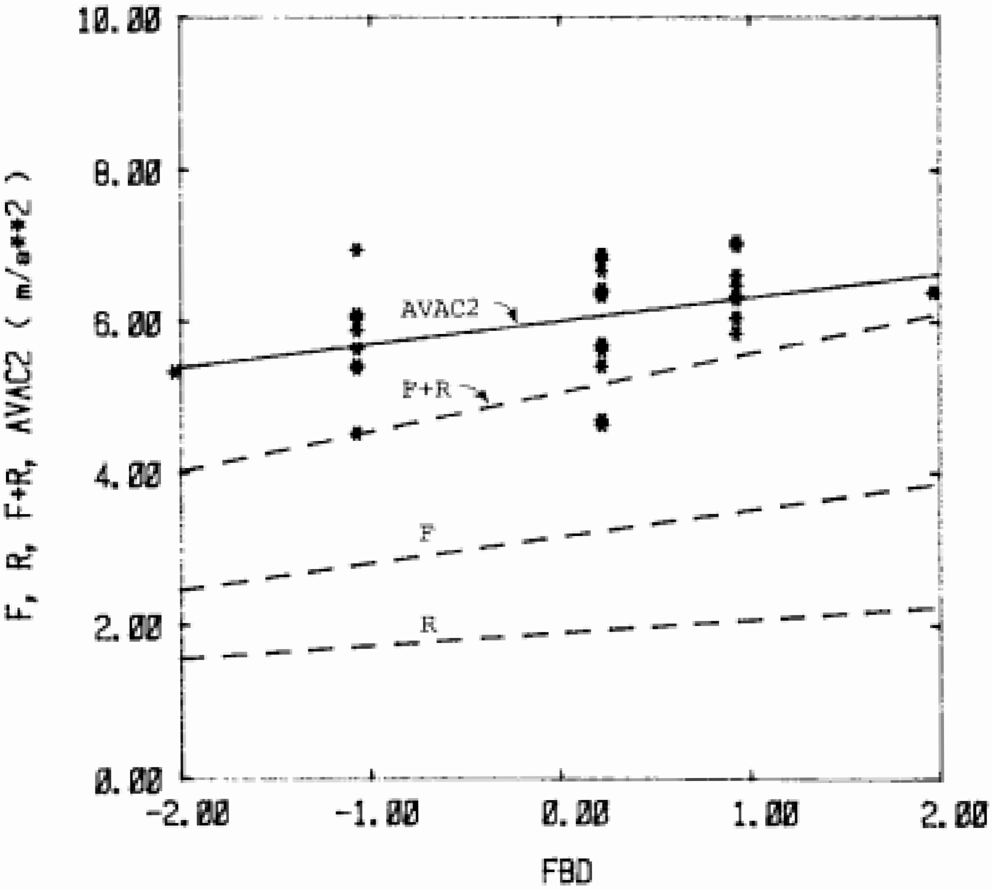

Figure 4.13 (b) Front brake deceleration contribution rear brake contribution and total deceleration in quick stop task versus front brake displacement gradient, subject BG.

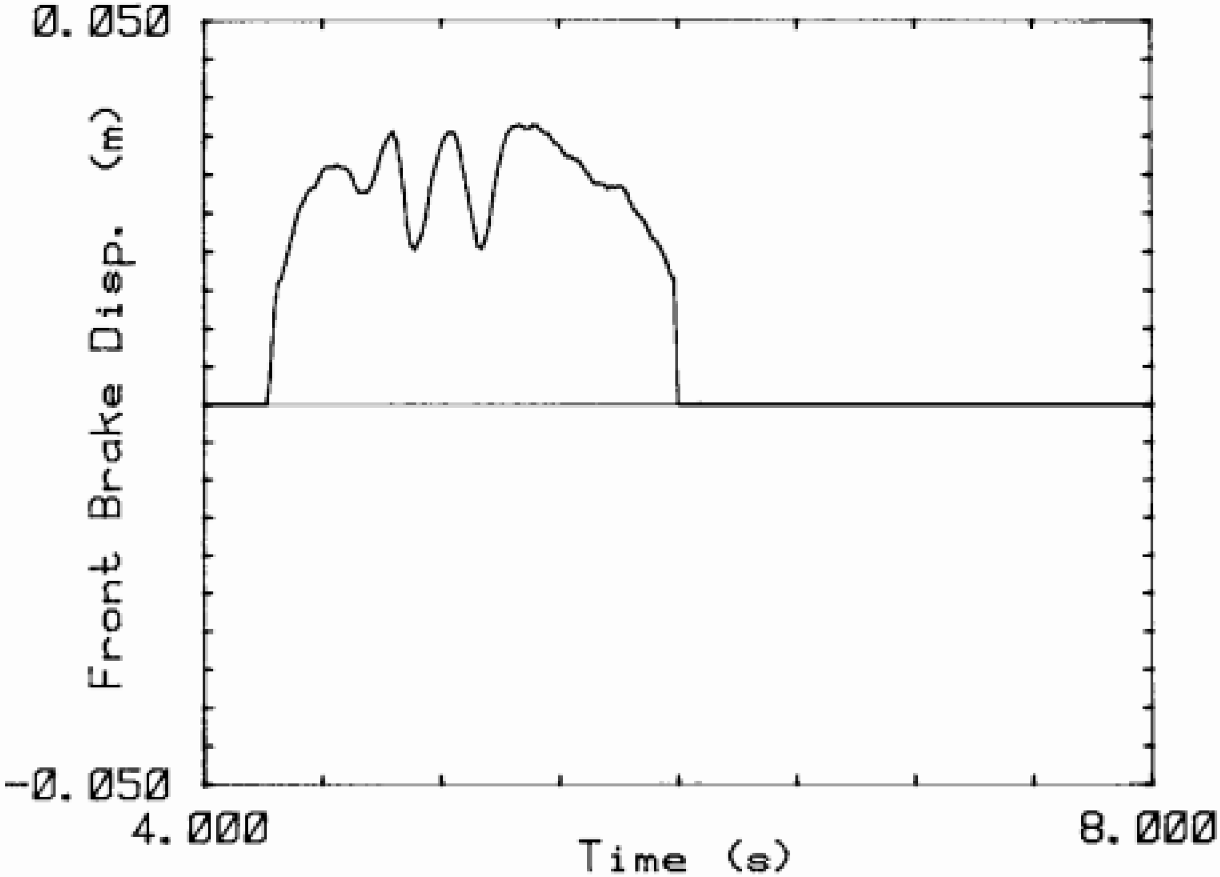

Figure 4.14 (a) Front brake displacement during a quick stop manoeuvre, subject BG.

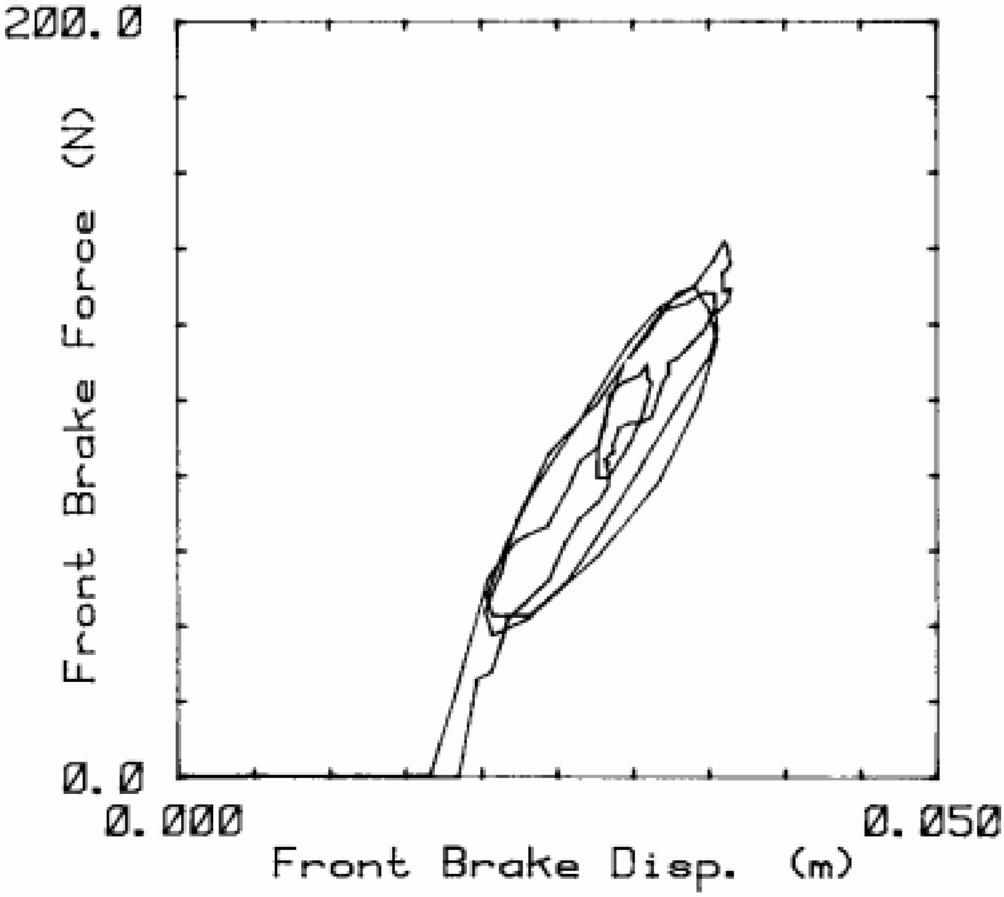

Figure 4.14 (b) Front brake force versus front brake displacement during a quick stop manoeuvre, subject BG.

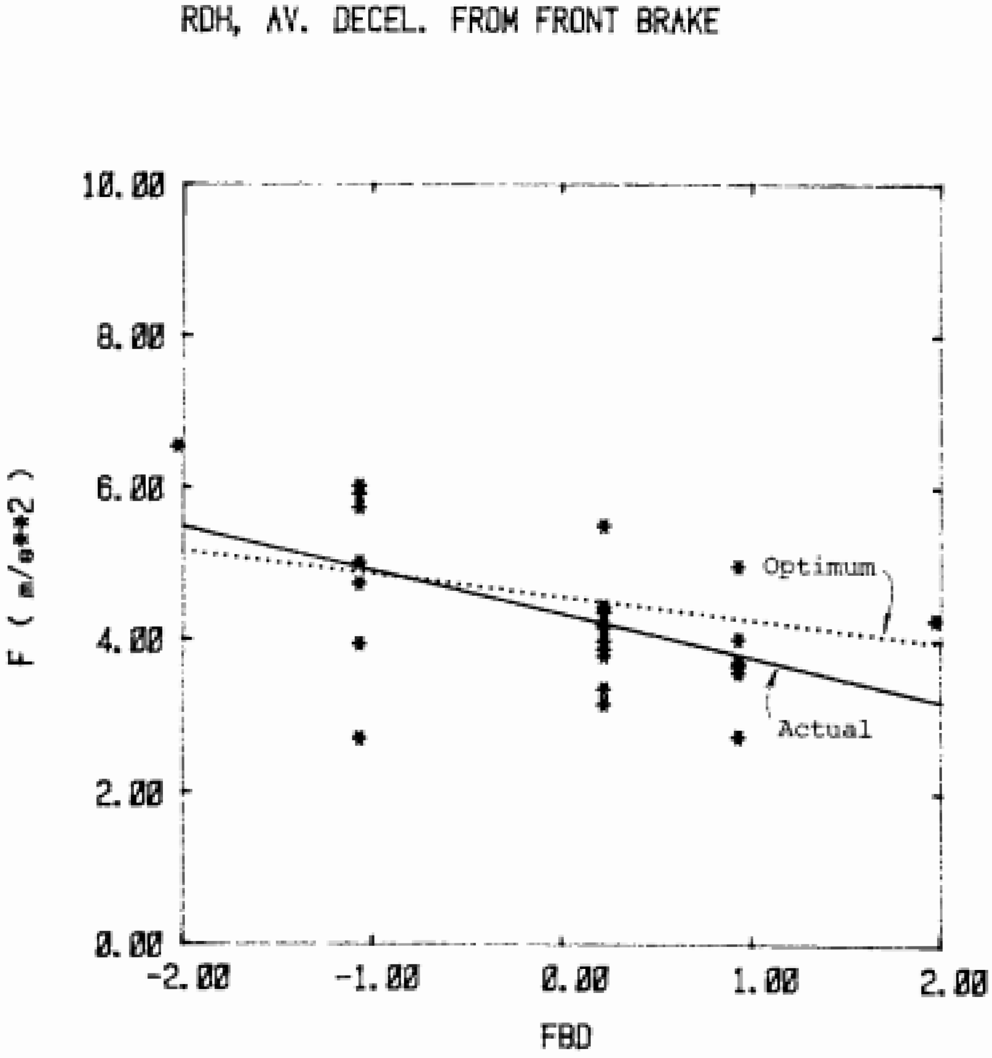

Figure 4.15 (a) Front brake deceleration contribution in quick stop versus front brake displacement gradient, subject RDH.

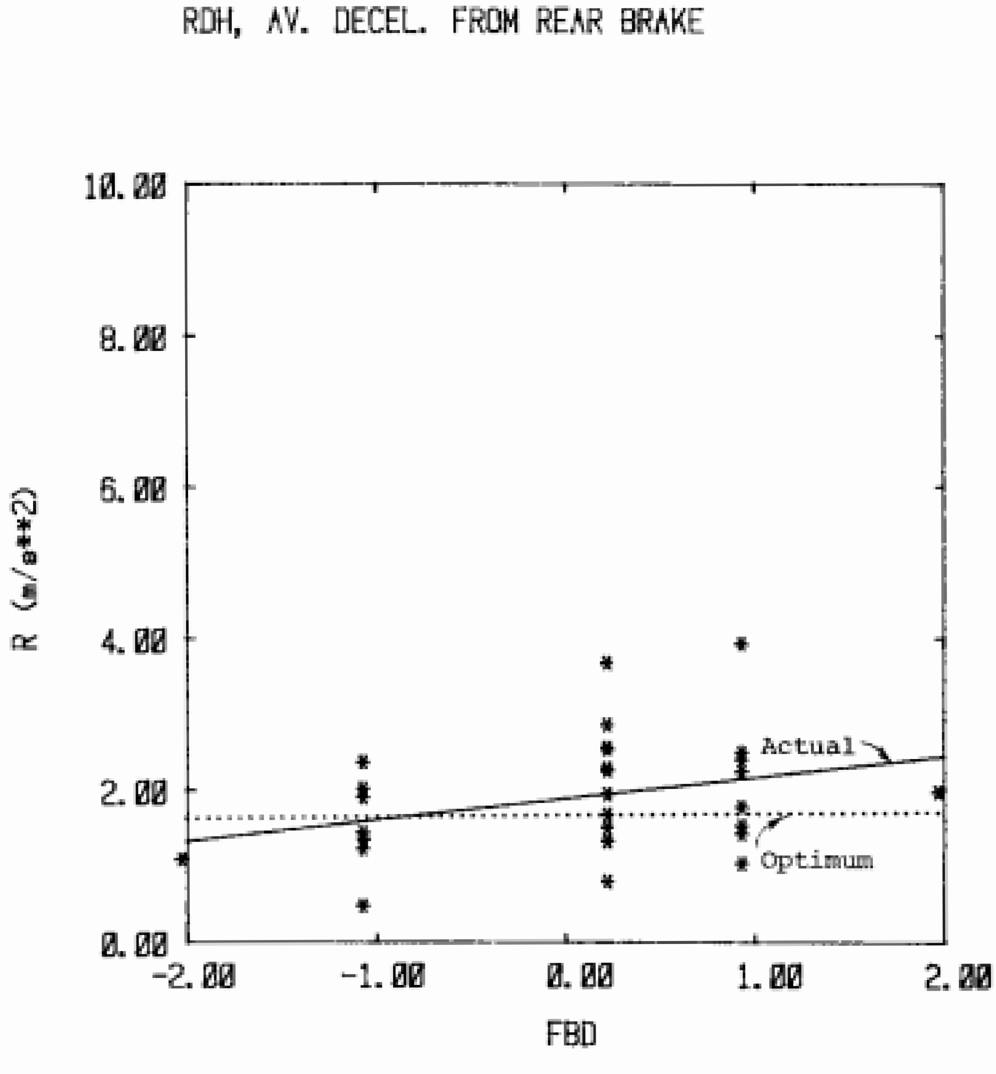

Figure 4.15 (b) Rear brake deceleration contribution in quick stop versus front brake displacement gradient, subject RDH.

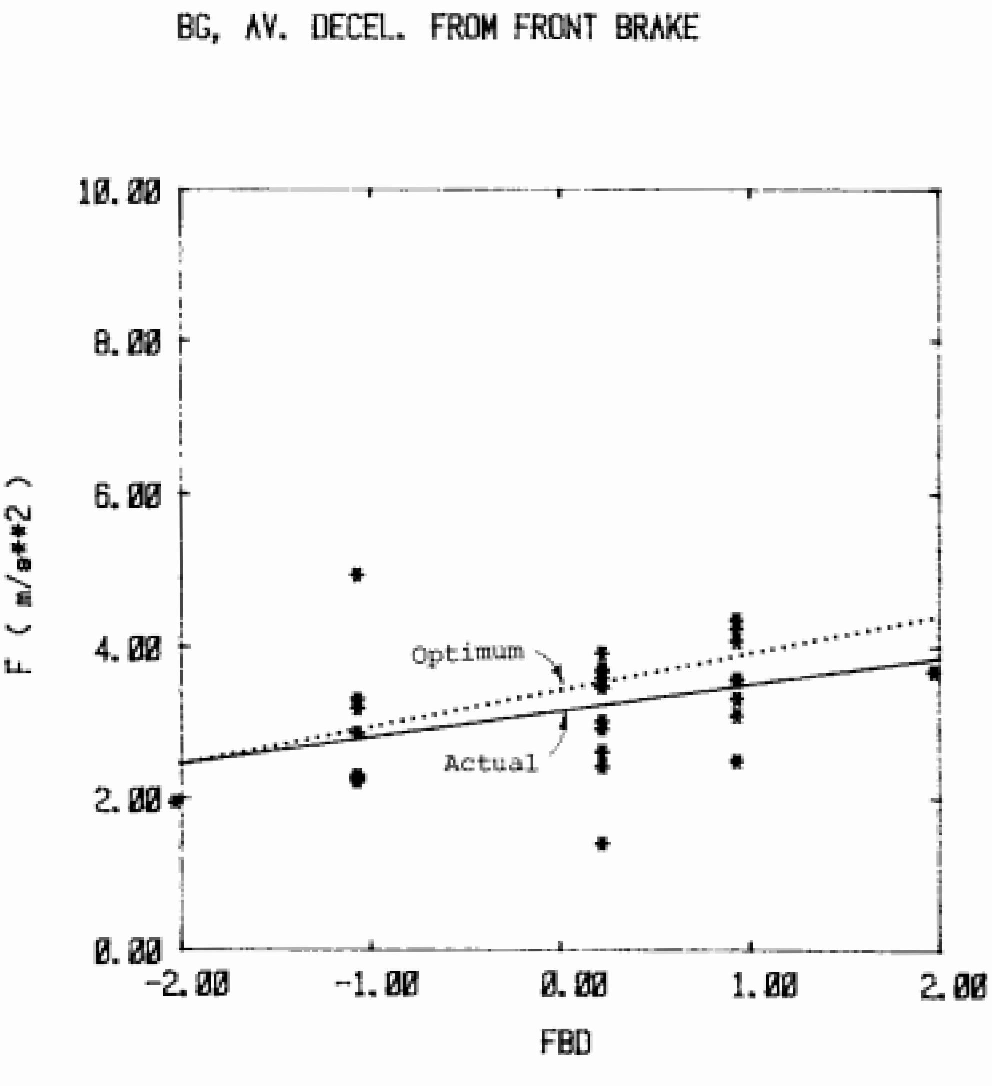

Figure 4.16 (a) Front brake deceleration contribution in quick stop versus front brake displacement gradient, subject BG.

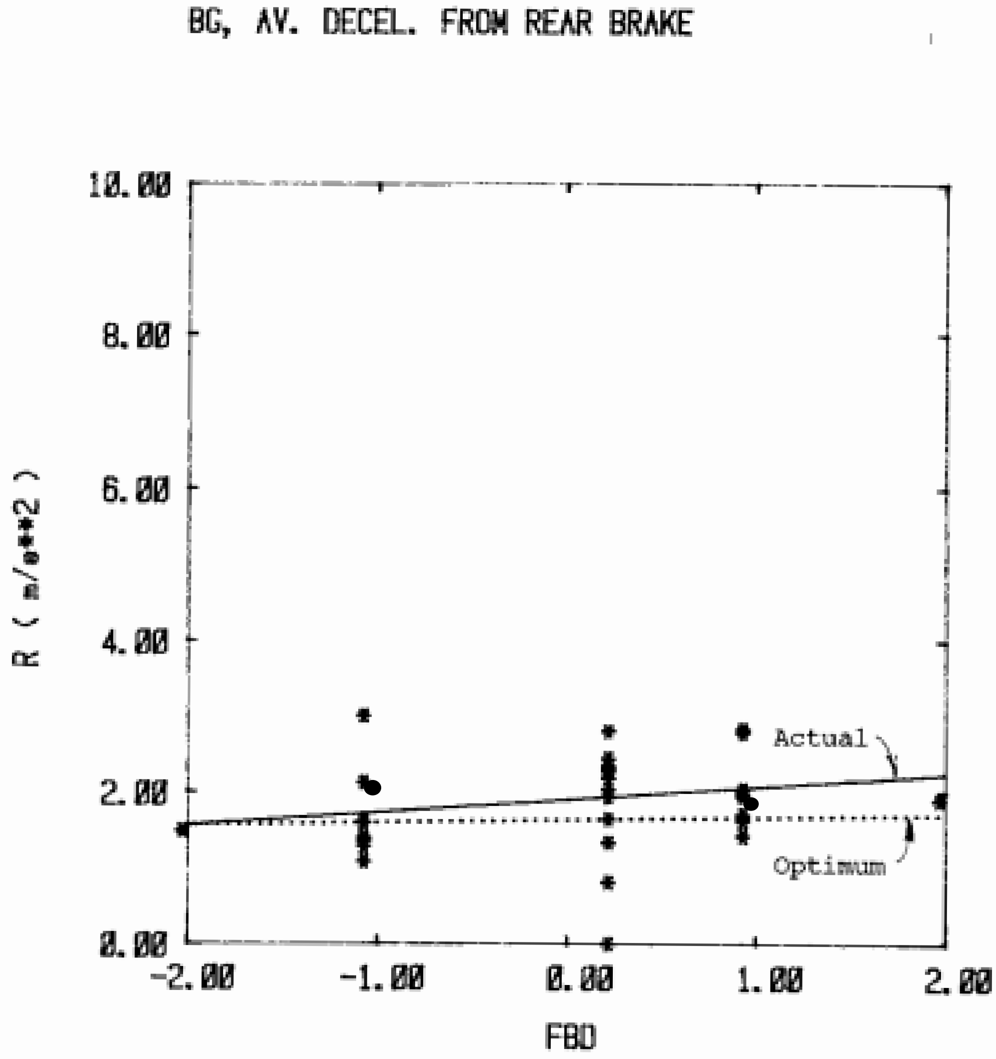

Figure 4.16 (b) Rear brake deceleration contribution in quick stop versus front brake displacement gradient, subject BG.

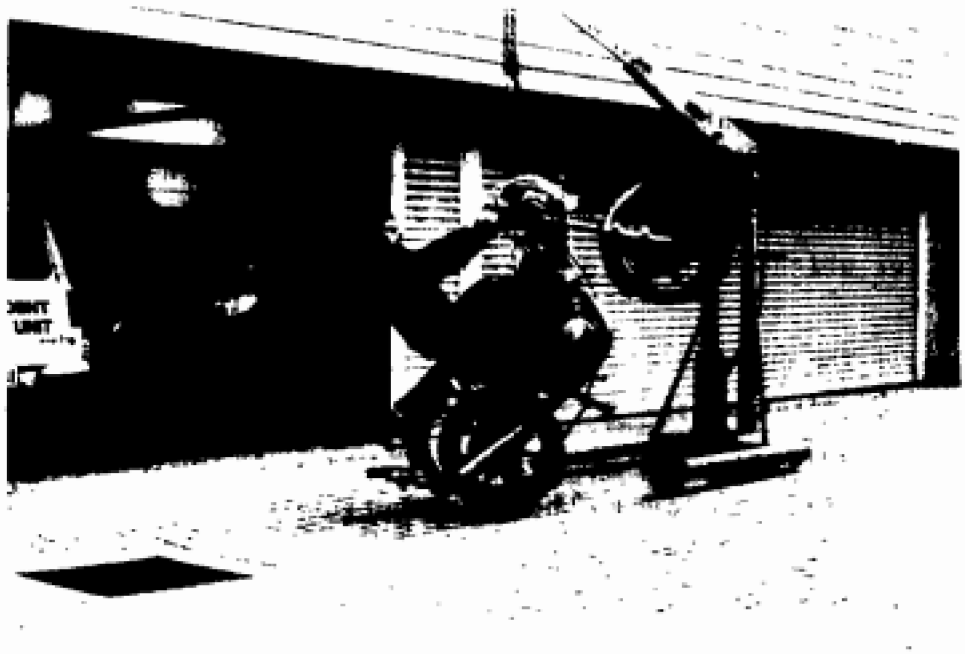

Figure 4.17 Photograph of procedure used to locate the centre of gravity (plumb line is vertical white line)

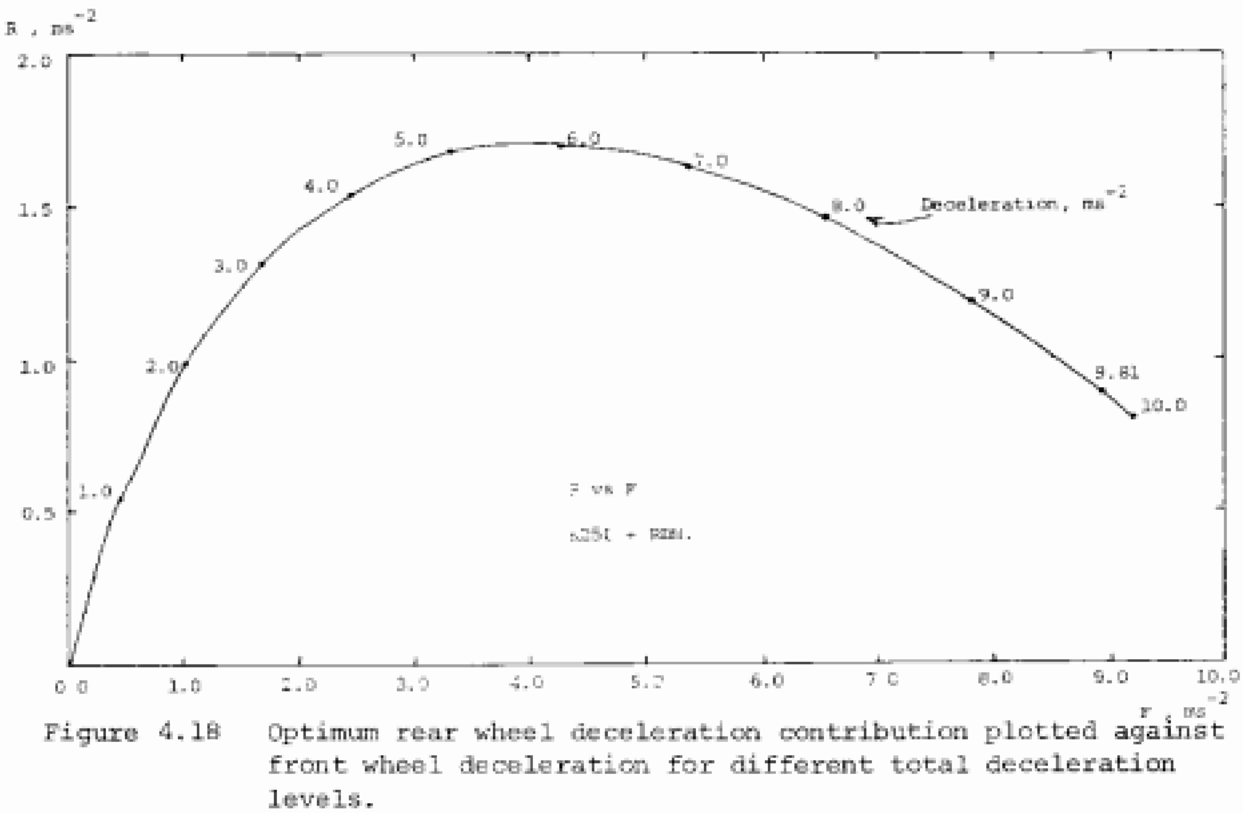

Figure 4.18 Optimum rear wheel deceleration contribution plotted against front wheel deceleration for different total deceleration levels.

plots represent simple linear regressions of the data on FBD. The dotted lines show the <u>optimum</u> partitioning of the calculated total F+R into front and rear contributions. (The calculated total F+R was partitioned in preference to the measured AVAC2 because it allowed a more consistant comparison for BG's data, for which the total decelerations were not in good agreement.)

The optimum front and rear contributions were calculated with the criterion that the fraction of the total tyre-road friction coefficient utilized be the same at each wheel. At any given deceleration level, the contributions from the front and rear that will achieve this may be calculated if the total rider/vehicle mass and centre of gravity location are known (see Appendix F). The centre of gravity was found using a photographic method. The motorcycle with rider was successively suspended from two different points with a portable jib crane. A plumb line was attached at the suspension point, and a photograph was taken of each case. The two negatives were superimposed and the intersection of the two plumb lines marked the centre of gravity. A print of one of the negatives is given in Figure 4.17. The locus of optimum front and rear deceleration contributions is plotted in Figure 4.18 with the total deceleration level as a parameter.

Returning to Figures 4.15 and 4.16, it can be seen that (on average) both riders adjusted their brake control inputs to achieve a roughly optimal front/rear distribution, over the very wide ranges of brake sensitivity with which they were presented. Both riders possibly under-utilized the front brake for most configurations, although the uncertainties in the calculations do not allow this finding to be asserted very strongly.

This result again attests to the remarkable adaptability of these two skilled riders, and again does not provide an insight into the particular brake control gradients which would yield the easiest and best braking performance for most riders. Experiments with less skilful riders may be more revealing.

Another aspect of braking performance investigated was the rider's reaction time: the time delay between the signal light being turned on and a control response from the rider. The time between the 'tripwire' event mark on the speed-trace, and either front or rear brake application (whichever occurred first) was extracted from the recorded data. The reaction time was found by subtracting 1.2 seconds (the signal light time delay for the quick stop). The average values are of interest: Rider RDH had a mean reaction time of 408 ms with a standard deviation of 33 ms; for BG it was 377 ms with a standard deviation of 58 ms.

The reaction time data were also processed by SPSS Multiple Regression, with the results shown in Appendix E. For rider BG, this was the most successful of the objective data regressions, with 72.6% of the variance being explained. The front and rear displacement gradients and the rear force gradient all made significant contributions, of similar magnitude, to the explained variance. However, it is difficult to draw any useful conclusions from these results. For example, although BG's reaction time tended to increase with FBD, so did his average deceleration, and there was no net effect on the overshoot measure. Rider RDH's reaction times showed no strong relationship with the independent variables.

4.10 SUMMARY AND CONCLUSIONS

This chapter has presented the results of a pilot study conducted to investigate ergonomic aspects of motorcycle deceleration control. The VBCG motorcycle was developed for this purpose.

Four independent brake control parameters were investigated. They were front brake displacement/deceleration gradient (FBD), front brake force/deceleration gradient (FBF), rear brake displacement/deceleration gradient (RBD), and rear brake force/deceleration gradient (RBF).

Response Surface Methodology (RSM) was employed as the experimental design. RSM offered the most efficient procedure for investigating relationships and interactions with the independent variables. A second-order response surface was fitted to the data to allow optimum brake configurations to be defined.

The RSM design dictated five levels for each of the independent variables. The VBCG was calibrated accordingly. The range of control gradients explored in this study was:

FBD	1.00	-	5.7	mm s^2/m
FBF	17.5	-	76.7	N s^2/m
RBD	1.6	-	12.9	mm s^2/m
RBF	25.8	-	84.6	N s^2/m

The control gradients of the three production motorcycles tested (see Chapter 2) fell within these ranges.

An experimental braking task was developed. It involved the motorcycle travelling in a straight line at constant speed with the rider monitoring traffic lights ahead. In response to the red lights turning on the rider applied the brakes and attempted to stop before a line across the roadway. A variable time delay was used to change the difficulty of the task. Three types of stop were used: a slow stop at a nominal 0.2 g average deceleration, a medium stop at 0.3g and a quick stop at 0.5g.

Two expert riders were used for the pilot study. It was hoped that expert riders would exhibit consistent behaviour and provide meaningful subjective ratings.

Seven subjective and five objective measures were derived from the experimental measurements. A summary of these is given in Table 4.6.

SPSS Multiple Regression was used to obtain the coefficients defining the response surface and statistical measures of the strength and significance of the observed relationships.

The main conclusions from this work are as follows:

(i) The two riders were able to modify their control inputs so as to (on average) achieve roughly the same braking performance over the whole range of brake configurations.

(ii) On average, both riders distributed the braking effort between the front and rear wheels in an optimal manner, again despite the wide ranges and combinations of front and rear brake sensitivities with which they were presented.

(iii) All the data exhibited a large error variance which generally precluded the definition of significant relationships between response measures and the brake configuration variables.

(iv) Performance in the quick stop task was primarily affected by the front brake displacement gradient. However, only small and contradictory trends were obtained from the two riders: for one, average deceleration increased marginally with a more displacement sensitive front brake; for the other it decreased slightly.

(v) Subjective ratings of the brake system were primarily influenced by the rear brake displacement gradient. Again, however, quite contradictory results were obtained from the two riders.

(vi) Future experimental investigations should allow the riders a longer period to become familiar with each new braking configuration. A paired-comparison experimental design should also lead to more consistent subjective ratings than were obtained in the present study.

(vii) Experiments with less-skilled riders would probably yield performance measures that were more strongly affected by the brake system variables than was the case in this study.

REFERENCES

BOX, G.E.P., and HUNTER, J.S. (1957). Multi-factor experimental designs for exploring response surfaces. Annals of Math. Stat., Vol. 28, 1957, p. 195-241

BRAUN, H. et al. (1982) Optimal gain factors in brake systems. Deutsche Kraftfahrtforschung und Strassenverkehrstechnik, No. 274

CANNON, R.H. (1967). Dynamics of physical systems. McGraw Hill Inc.

DOREY, A.D. (1979). Free control variables and automobile handling. Ph.D. Thesis, University of Melbourne, 1979

ERVIN, R.D., MacADAM, C.C., and WATANABE, Y. (1977). A unified concept for measurement of motorcycle braking performance. Proc. International Motorcycle Safety Conference, December 1975, U.S. DOT, Washington DC, p. 205-220

GOOD, M.C., (1977). Sensitivity of driver-vehicle performance to vehicle characteristics revealed in open-loop tests Vehicle System Dynamics, 6, 245-277

HOUSE OF REPRESENTATIVES Standing Committee on Road Safety (1978). Motorcycle and bicycle safety. Australian Government Publishing Service, Canberra

HURT, H.H. Jr., OUELLET, J.V., and THOM, D.R. (1981). Motorcycle accident cause factors and indentification of countermeasures. Vol. 1: Technical Report. U.S. DOT National Highway Traffic Safety Administration, Washington DC, NTIS PB81-20-644-3

IRVING, P.E. (1978). Rich mixture. Sun Books Pty. Ltd., South Melbourne, Victoria

JUNIPER, R.G. and GOOD, M.C. (1983) Braking, stability and handling of motorcycles Australian Department of Transport Office of Road Safety Report CR29

McDONNELL, J.D. (1969). An application of measurement methods to improve the quantitive nature of pilot rating scales. IEEE Transactions of Man-Machine Systems, Vol. MMS-10, No. 3, September 1969

MORTIMER, R.G., SEGEL, L., DUGOFF, H., CAMPBELL, J.D., JORGENSON, C.M., and MURPHY, R.W. (1970). Brake force requirement study: driver vehicle braking performance as a function of brake system design variables. Highway Safety Research Institute, Report No. HuF-6

NIE, N.H., HADLAI HULL, C., JENKINS, J.G., STEINBRENNER, K., BENT, D.H. (1975). Statistical package for the social sciences. McGraw Hill Book Company

TAGUCHI, M., and SUNYAMA, K. (1973). Some considerations for safety of motorcycle brake systems. International Congress on Automotive Safety (2nd) Proceedings, Vol. 1 Part 2 Motorcycle Safety, Paper 73019, Washington, DC, 1973

WEIR, D.H., ZELLNER, J.W., and TEPER, G.L. (1978). Motorcycle handling. Volume II: Technical Report. Systems Technology, Incorporated. California. Report No. TR-1086-1-II.

ZELLNER, J.W. (1980). Recommendations for improved conventional motorcycle brake systems. Systems Technology, Incorporated, CaliforniaWorking Paper No. 1159-3

ZELLNER, J.W., and KLABER, K.M. (1981). Considerations for improvement of conventional motorcycle brake systems. Society of Automotive Engineers, SAE Paper 810408

APPENDIX A

TRANSDUCER DESIGN AND CALIBRATION

A.1 INTRODUCTION

In order to monitor motorcycle dynamic characteristics in response to rider braking inputs, a total of nine transducers were used. Implementation of these transducers involved adaption of commercially available units, and original design employing strain gauges and potentiometers as basic sensing elements.

This appendix contains the details of adaption, design and physical mounting of the transducers on the motorcycles. Also the calibration procedures used are described.

Finally, an analysis of motorcycle mainframe pitch effects on an accelerometer mounted to measure longitudinal deceleration is given. This results in a simple correction term (attained from a pitch rate gyroscope) which must be applied to the accelerometer trace.

A.2 TRANSDUCER DETAILS

A.2.1 Front Brake Force Transducer

Figure A.1 is a photograph of a typical front brake hydraulic master cylinder and its control lever. If strain gauges are positioned on the master cylinder actuating arm, they will always sense the force applied to the master cylinder piston. These strain gauges will thus actually indicate the torque the rider applies to the control lever. Their output will be (largely) independent of the position along the blade at which the rider input force is applied.

Four strain gauges were attached to each of the three motorcycle front brake levers at the location indicated in Figure A.1. The gauges were connected to form a full bridge, two being in compression and two in tension. The bridge output was amplified to a suitable voltage level (0 to 10 volt) using a 'pseudo-differential' amplifier circuit. It was found to be necessary to filter the output of this circuit, and an active fourth order Butterworth filter stage was added.

Static force calibration was performed for each lever, according to the scheme shown in Figure A.2. For universality, it is important to note that the calibration force was applied to the brake blade 115 mm from the fulcrum. This point was chosen to represent the usual position of the middle finger when applied to the brake lever. Masses were added in suitable increments from zero to approximately 25 kg, and then removed in the reverse order. The amplifier/filter output voltage at each point was recorded with a digital voltmeter. When this procedure was first employed, considerable force hysteresis was noted. This was largely due to coulomb friction in the fulcrum pin, as a drop of light machine oil in this area reduced the hysteresis to an acceptable level. This is demonstrated by Figure A.3 which shows the calibration curve obtained for the 250 ml motorcycle. A straight line was fitted by least-squares regression through all the data points. The force calibration sensitivites thus obtained can be found in Table 2.1.

The output amplifier filter was designed to have a linear phase-frequency characteristic. Figure A.4 shows the transfer function of the filter stage for the 750 ml motorcycle front brake force transducer, obtained with an HP 3582A Spectrum Analyzer. An almost linear relationship is observed. This means that the force transducer signals at all frequencies will be delayed by a constant time interval relative to an unfiltered signal. This time delay was compensated for after the data had been digitized and stored on computer files. The force traces

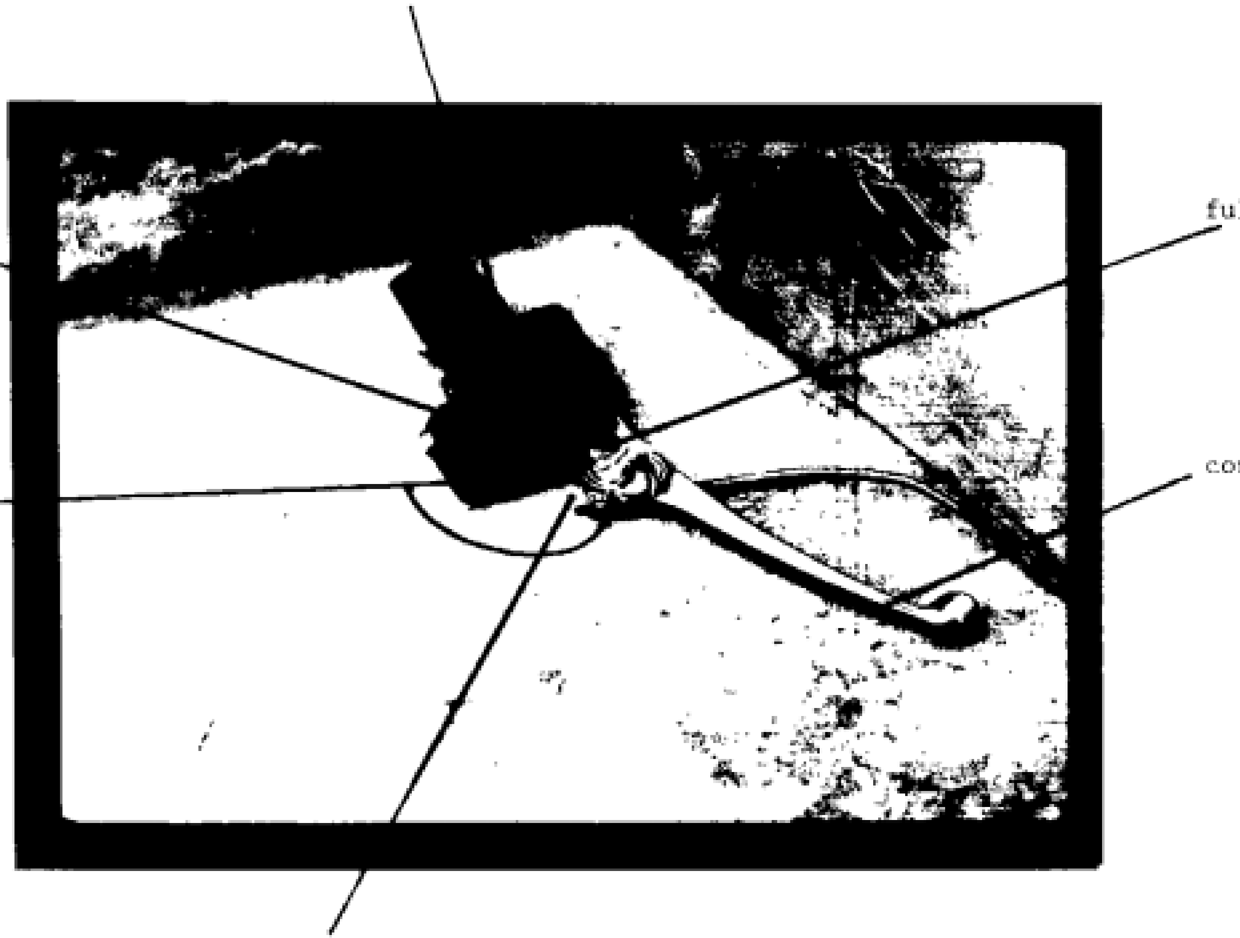

Figure A.1 Photograph of a typical front brake hydraulic master cylinder

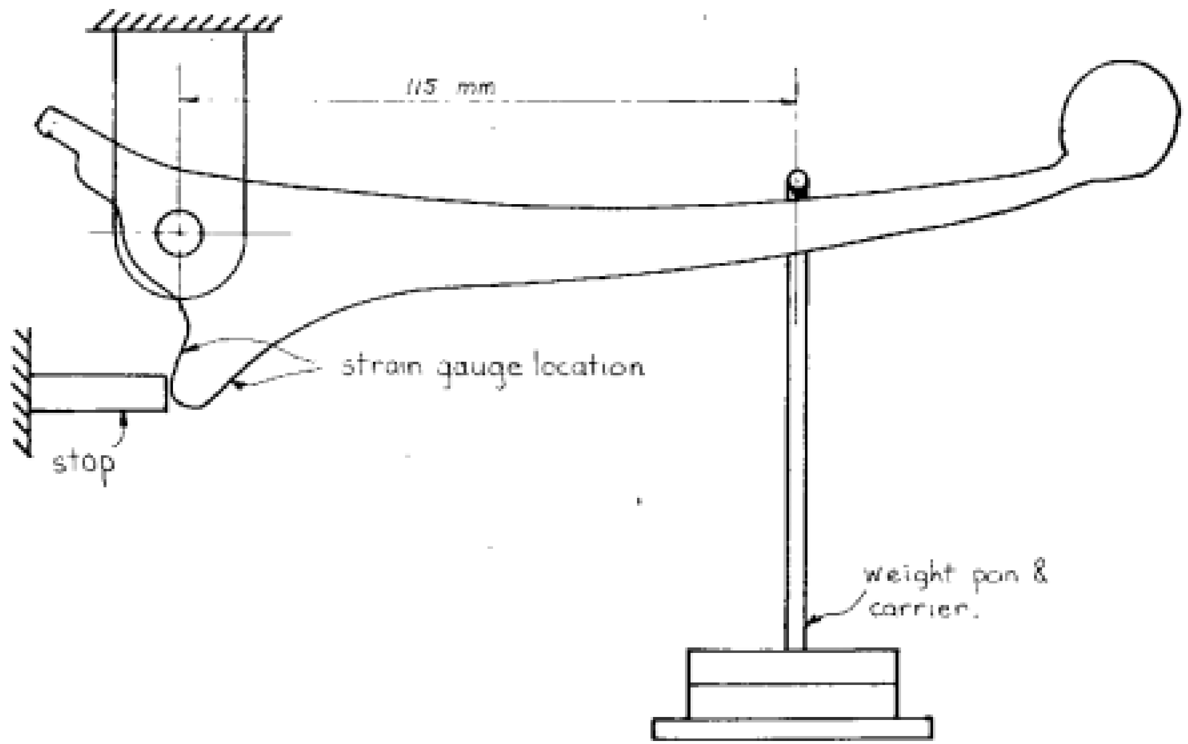

Figure A.2 Apparatus used for static force calibration of front brake lever

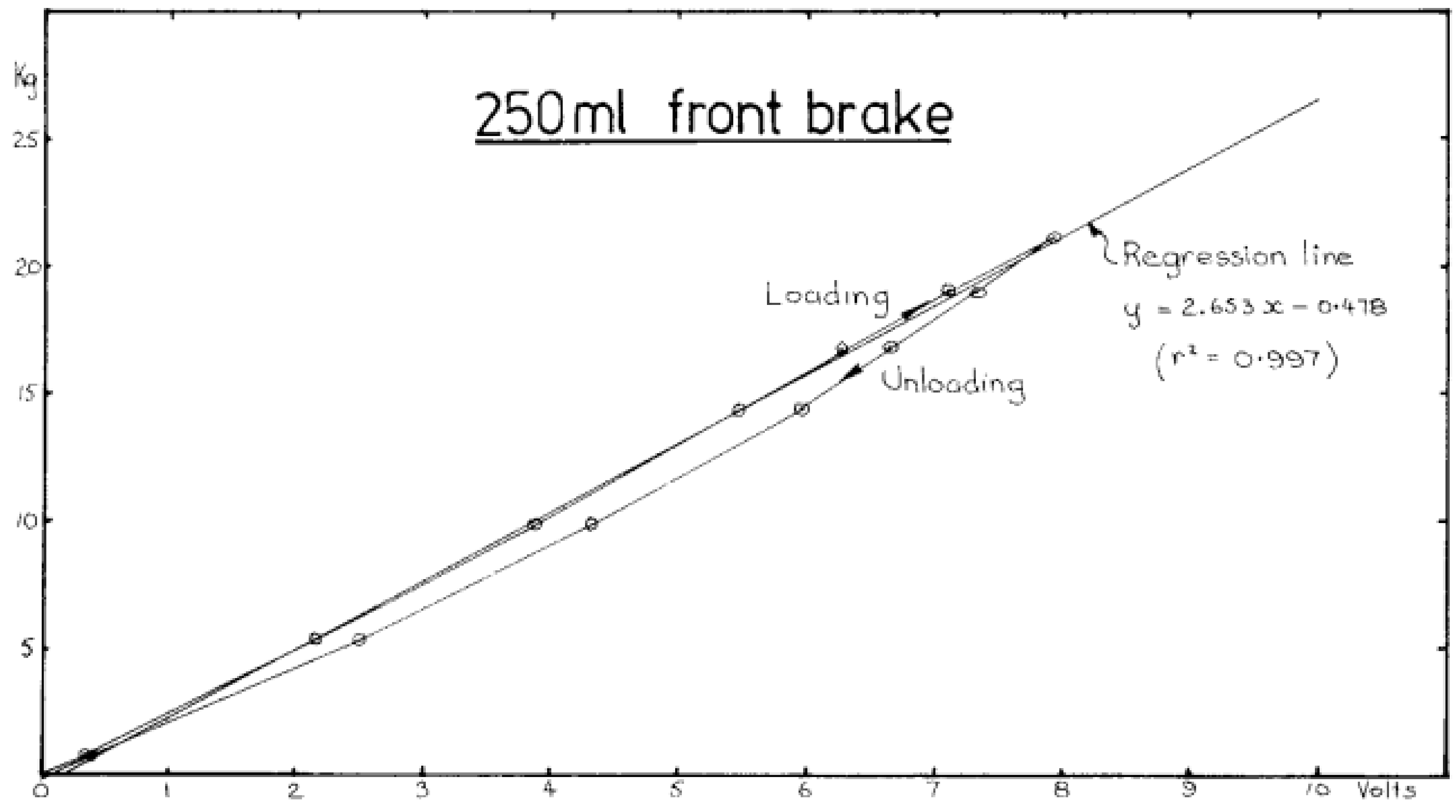

Figure A.3 Front brake force calibration curve, 250 ml motorcycle

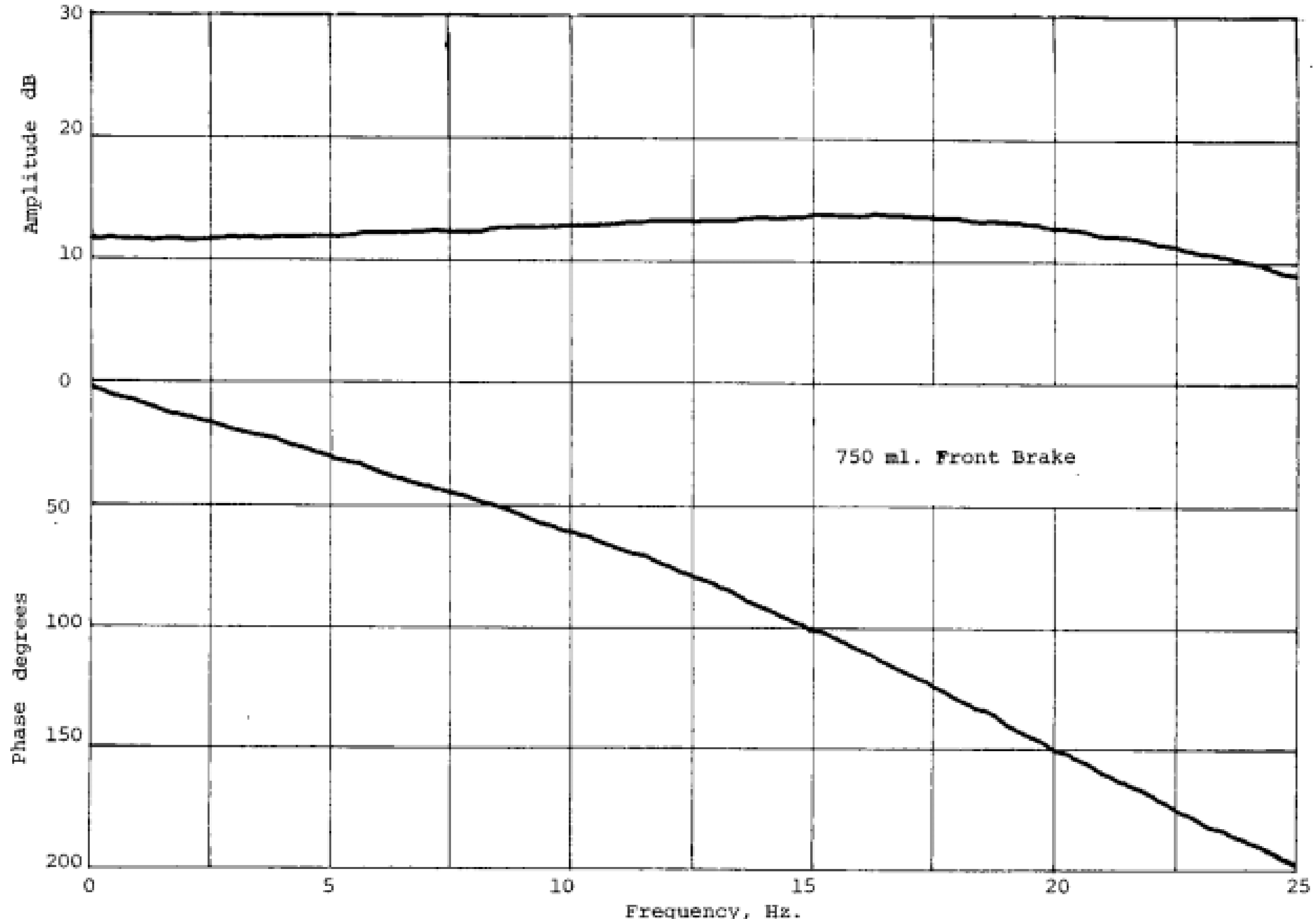

Figure A.4 Filter transfer function of force amplifier

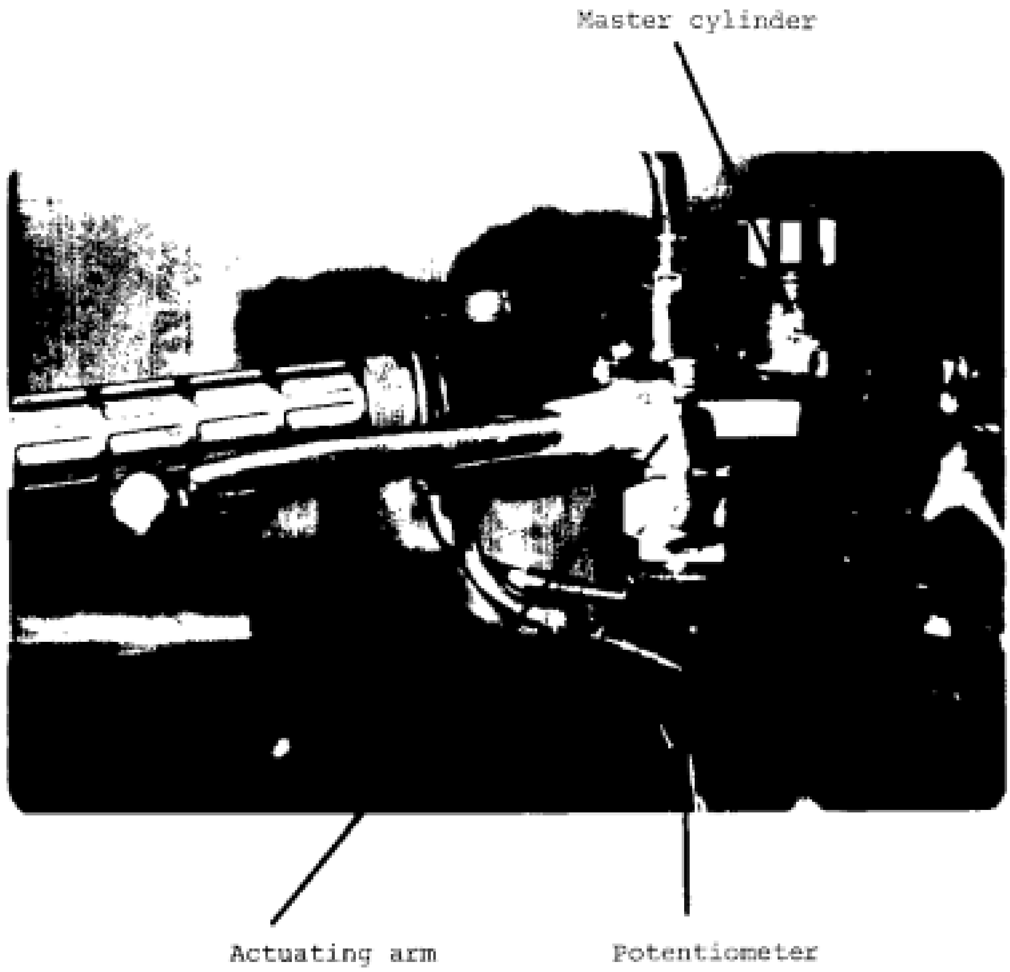

Figure A.5 Front brake displacement transducer.

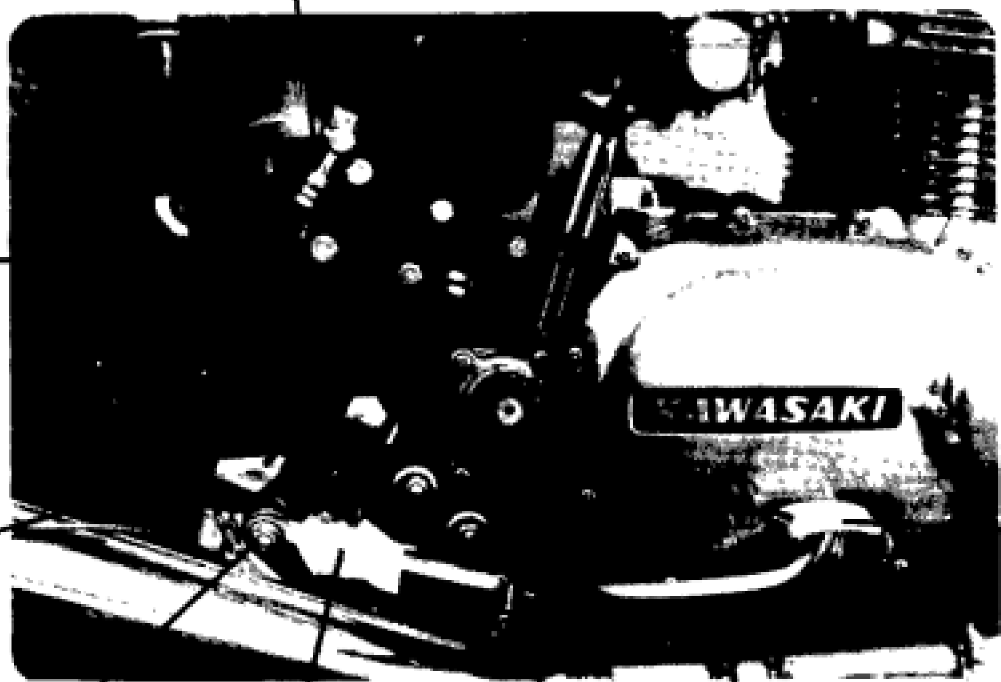

Figure A.6 Motorcycle hydraulic rear brake arrangement.

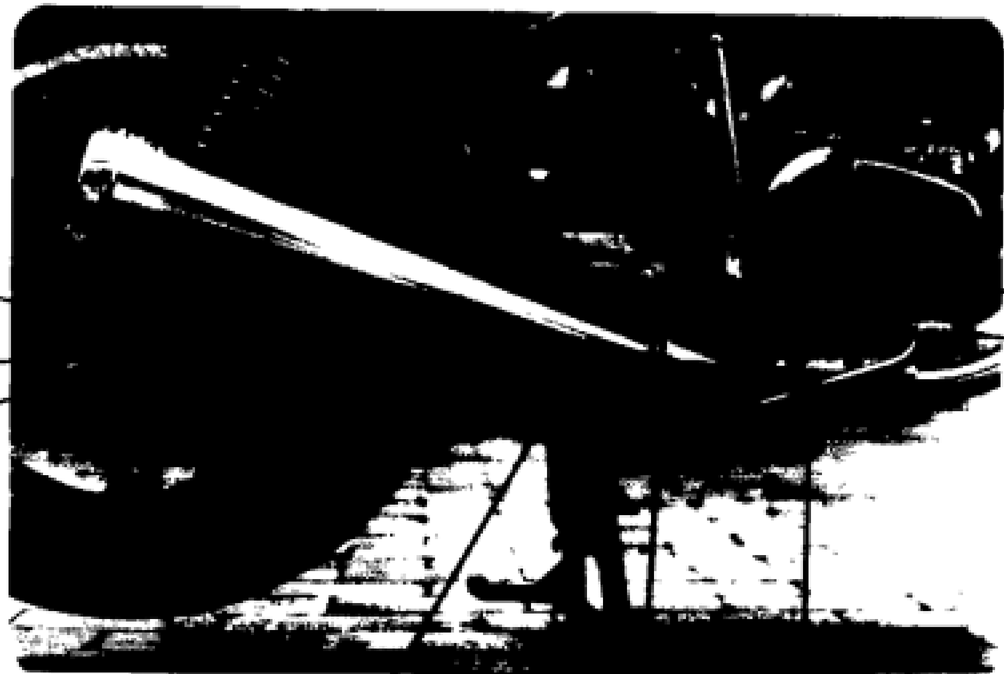

Figure A.7 400 ml mechanical rear brake.

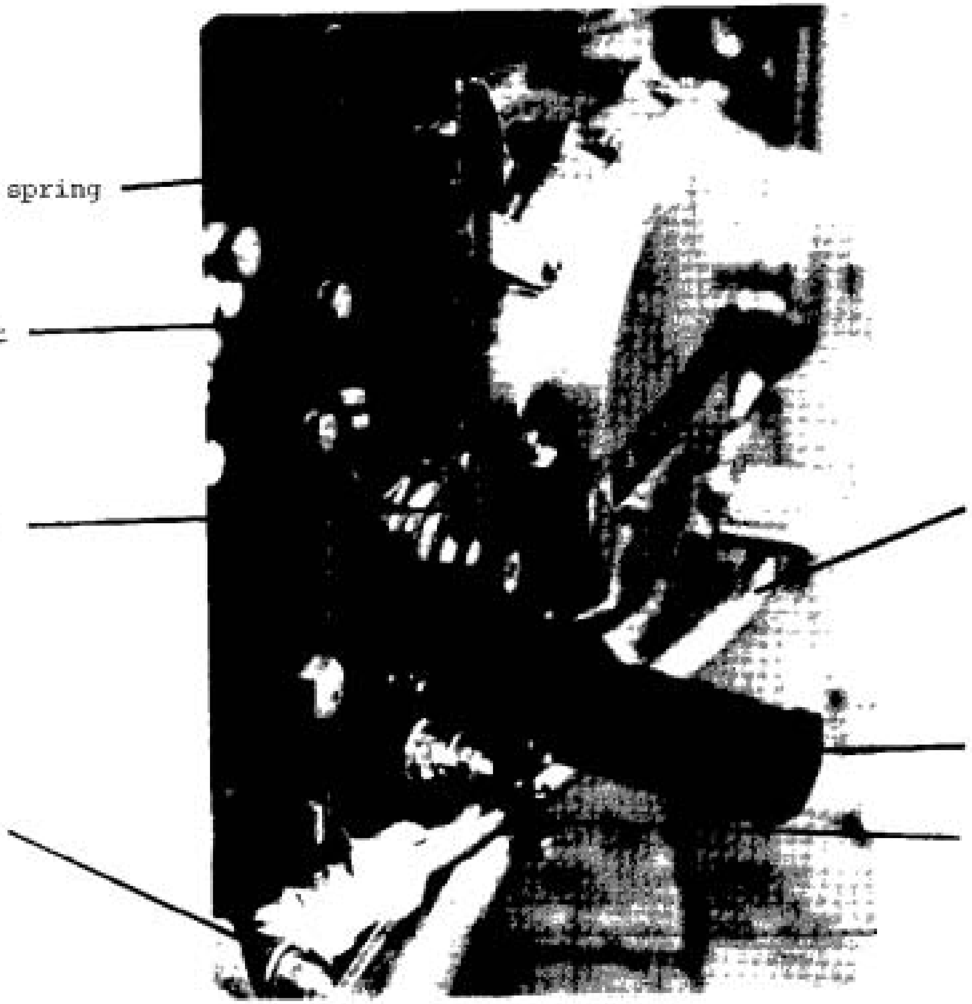

Figure A.8 Rear brake displacement transducer.

were shifted in time by the appropriate time interval as determined from the filter transfer function.

A.2.2 Front Brake Displacement Transducer

To sense front brake lever displacement, a wire-wound rotary potentiometer was mounted with its axis of rotation parallel to and intersecting the fulcrum pin axis, as shown in Figure A.5. A small actuating arm was then attached to the brake lever with adhesive tape. The potentiometer was connected in a voltage divider circuit, and the voltage output amplified to give 10 volts when the lever reached the limit of its travel (against the handlebar). The amplifier circuit had an offset facility to set zero voltage to zero displacement.

This transducer was calibrated against a vernier caliper to measure lever displacement at a point 115 mm from the fulcrum (cf., A.2.1) and the amplifier output monitored with a digital voltmeter. A straight line regression was applied to this data, with the resultant sensitivity being tabulated in Table 2.1.

A.2.3 Rear Brake Force Transducer

(a) Hydraulic disc brake system

Figure A.6 shows the usual arrangement for a rear brake lever and hydraulic master cylinder on a motorcycle. The point at which the rider applies force to the lever is typically 300 mm from the lever fulcrum. It was found that strain gauges could be adhered to the lever adjacent to the fulcrum and be relatively insensitive to small variations in the point of force application. Four gauges were used, connected in a full bridge, and the output amplified and filtered with a circuit similar to that used for the front brake force transducer (cf., A.2.1).

The amplifier output voltage was calibrated against standard masses applied to a weight pan hooked onto the centre point of the brake lever pad. Linear regression was used to obtain the force-voltage sensitivity. The results for the three motorcycles are presented in Table 2.1.

The rear brake force transducer amplifiers also contained a filter stage, similar to those used with the front brake force transducer. The time delay resulting from this filter was compensated for using the same technique as for the front brake force (cf., A.2.1)

(b) Mechanical drum brake system on the 400 ml motorcycle

Figure A.7 shows the mechanical drum brake employed for rear wheel braking on the 400 ml motorcycle. It was found to be necessary to sense the rider input force at both the lever fulcrum (as described in A.2.3) and at the drum actuating arm located at the rear wheel hub. The latter sensing position was used to monitor brake force during a step input of brake displacement, and is described more fully in Section 2.5.1.

Again, four strain gauges were adhered to the drum actuating arm, and the amplifier circuit and calibration procedure used were the same as those described in Section A.2.3.

A.2.4 Rear Brake Displacement Transducer

Figure A.8 shows the arrangement used for sensing rear brake lever displacement. A linear slider potentiometer, actuated by a tension member attached to the brake lever and working against a return spring, was used in a voltage divider circuit. The output was amplified to give 10 volts at maximum lever displacement, with a variable offset facility provided.

The transducer was calibrated against a vernier caliper which was used to measure brake lever foot pad displacement. The

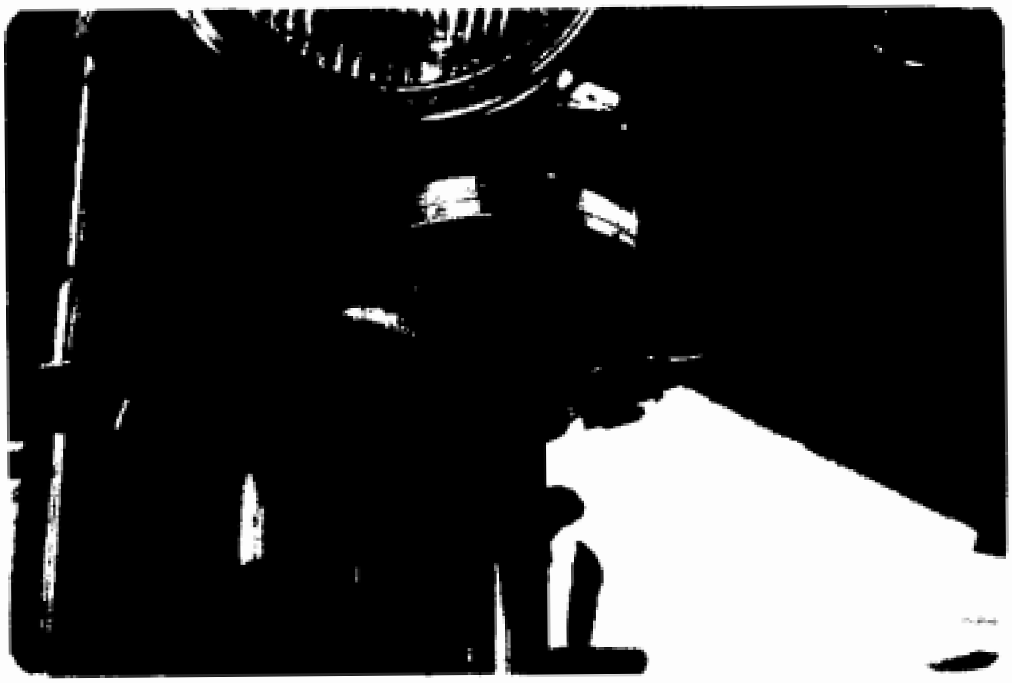

Figure A.9   Speed transducer mounted on 400 ml motorcycle.

amplifier output voltage was monitored with a digital voltmeter. Linear regression was used to obtain the voltage-displacement sensitivity, and the results for the three motorcycles are given in Table 2.1.

A.2.5 Motorcycle Forward Speed

Speed was monitored with a device driven by the odometer cable. Operation of the standard speedometer was unaffected, so that it was available for the rider to observe normally.

The device uses a rotating slotted disc, which interrupts the light path between a light-emitting diode and a phototransistor. The output of the phototransistor was electronically manipulated to provide a d.c. voltage, between 0 and 10 volts, proportional to motorcycle speed (the system was designed to give approximately 10 volts at 160 km/h). Figure A.9 shows the speed measuring device mounted on the 400 ml motorcycle.

Calibration was performed by recording transducer output voltage during several rider-controlled constant speed runs through a measured 200m distance at nominal speeds of 20, 40, 60, 80 and 100 km/h. Figure A.10 shows a plot of average transducer output voltage against calculated average speed over the 200 m distance, for the 400 ml motorcycle. Linear regression was used to fit a straight line to the data. The results of the calibration for the three motorcycles are given in Table 2.1.

A.2.6 Motorcycle Deceleration

Motorcycle deceleration was monitored with a closed-loop servo-accelerometer with a rated range of $\pm$ 1g (Schaevitz model number LSMP-1).

An accelerometer mounted on a motorcycle is in a very 'noisy' environment, due to engine and transmission vibrations, and

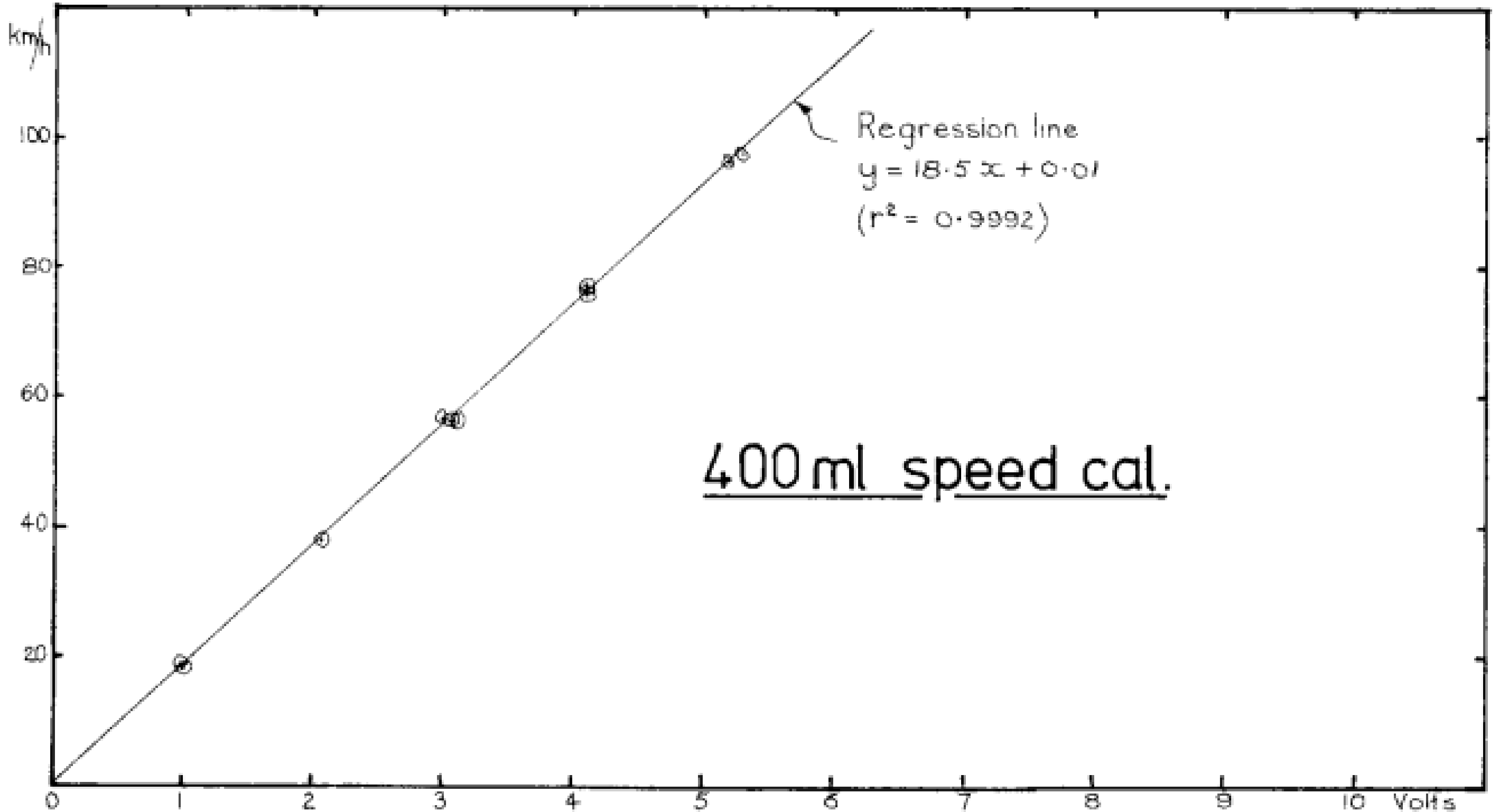

Figure A.10 Speed calibration curve for 400 ml motorcycle.

accelerations resulting from road surface irregularities. To minimize these effects, the accelerometer was mounted on the motorcycle main frame. Its output amplifier had, as its final stage, a fourth-order active filter with a corner frequency of 20 Hz. The output amplifier gain was set to give 0.1 g/volt. Figure A.11 shows the accelerometer and amplifier transfer function. This was obtained by mounting the accelerometer on an electromagnetic shaker driven by the random noise source from a Hewlett Packard HP3582A Spectrum Analyzer. The accelerometer's output was compared to that from a reference accelerometer mounted adjacent to it. The phase-frequency relationship is seen to be closely approximated by a straight line. This means that accelerometer signals at all frequencies will be delayed by a constant time interval relative to a transducer signal without the filter stage in its output. The same time delay compensation procedure used for the front brake force transducer (cf., A.2.1) was employed for the accelerometer signals.

Referring to Figure A.12, an accelerometer mounted on the main frame will sense the longitudinal acceleration of the rear axle, $\ddot{x}_B$ and will respond additionally to the horizontal component of the acceleration of point C relative to B due to rotation of the rear swing arm, θ_1 and the horizontal component of the acceleration of P relative to C due to pitching of the main frame, θ.

The x component of the acceleration of C relative to B is:

$$a_{C/B_x} = -x_C \dot{\theta}_1^2 - y_C \ddot{\theta}_1 \qquad \text{(A.1)}$$

The x component of the acceleration of P relative to C is:

$$a_{P/C_x} = -y_P \ddot{\theta} + x_P \dot{\theta}^2 \qquad \text{(A.2)}$$

Therefore the x component of the absolute acceleration of P is:

$$\ddot{x}_P = \ddot{x}_B - x_C \dot{\theta}_1^2 - y_C \ddot{\theta}_1 - y_P \ddot{\theta} + x_P \dot{\theta}^2 \qquad \text{(A.3)}$$

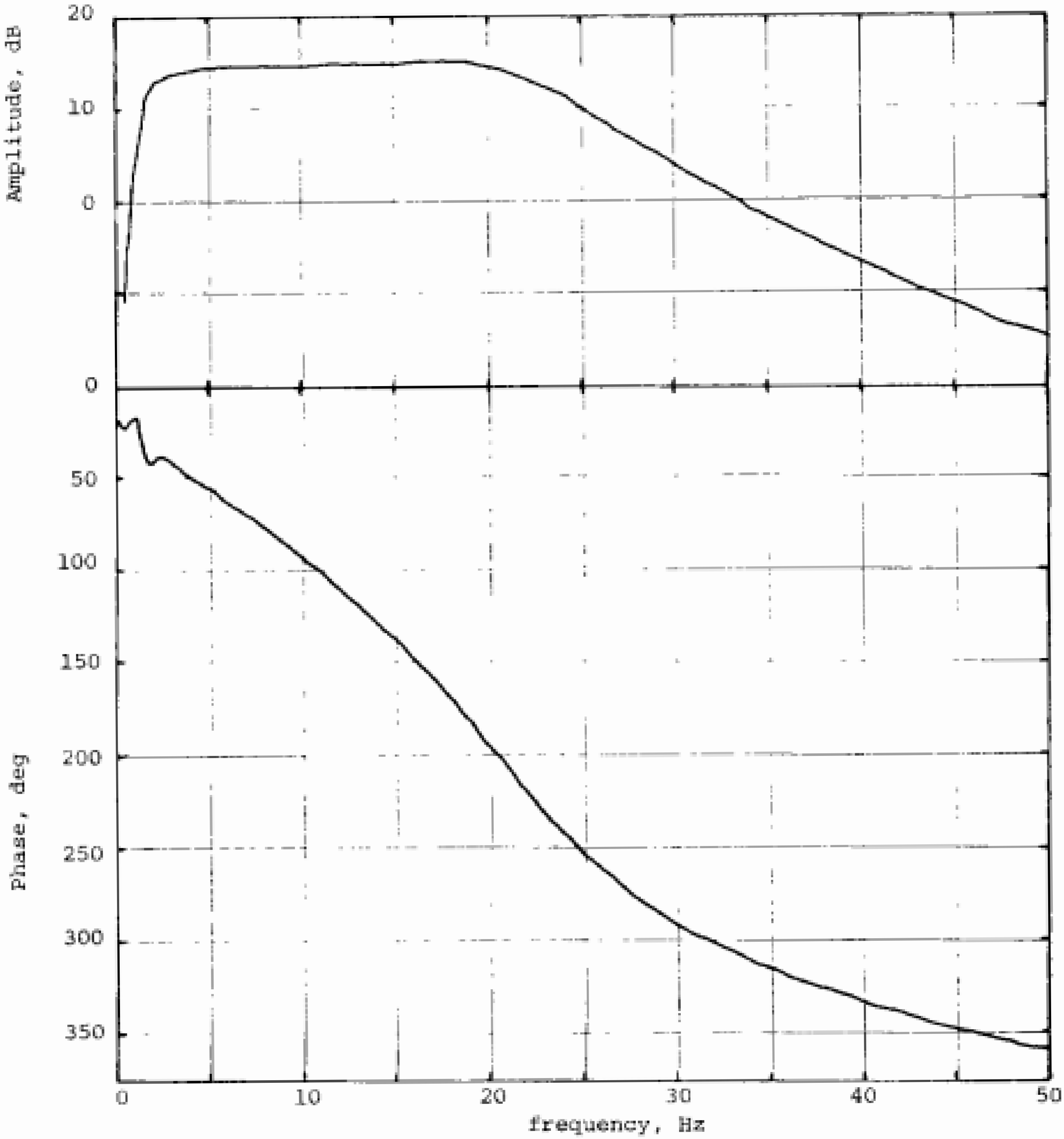

Figure A.11 Accelerometer amplifier and filter transfer function

Note: The motorcycle accelerometer had a flat amplitude response down to 0 Hz. The low frequency roll-off shown in this figure results from filtering during the calibration testing.

Furthermore, the accelerometer will respond to the component $g\sin\theta$ of the gravitational force along its sensitive axis as the main frame angle changes.

It follows therefore, that the accelerometer indicated acceleration is (for small pitch angles θ):

$$A_i = g\theta + \ddot{x}_B - x_C\,\dot{\theta}_1^2 - y_C\,\ddot{\theta}_1 - y_P\,\ddot{\theta} + x_P\,\dot{\theta}^2 \qquad (A.4)$$

Thus, provided θ, θ_1 and their rates of change are measured, the accelerometer output can be corrected as follows to yield the required longitudinal motorcycle acceleration, $\ddot{x}_B$:

$$\ddot{x}_B = A_i - g\theta + x_C\,\dot{\theta}_1^2 + y_C\,\ddot{\theta}_1 + y_P\,\ddot{\theta} - x_P\,\dot{\theta}^2 \qquad (A.5)$$

The motorcycle main frame has two degrees of freedom relative to the rear axle, and two independent co-ordinates are necessary to describe its position at any time. The quantities selected for measurement were the main frame pitch rate, $\dot{\theta}$ and the rear suspension deflection, l_r. The transducers used to measure these quantities are described in Sections A.2.7 and A.2.8.

An expression relating l_r and $\dot{\theta}$ to $\dot{\theta}_1$ can be derived as follows, with reference to Figure A.12:

$$\dot{l}_r = r(\dot{\theta}_1 - \dot{\theta}) \qquad (A.6)$$

where r = perpendicular distance from EB to C

so $$\dot{\theta}_1 = (\dot{l}_r/r + \dot{\theta}) \qquad (A.7)$$

and $$\ddot{\theta}_1 = (\ddot{l}_r/r + \ddot{\theta}) \qquad (A.8)$$

with the assumption that r does not change very much.

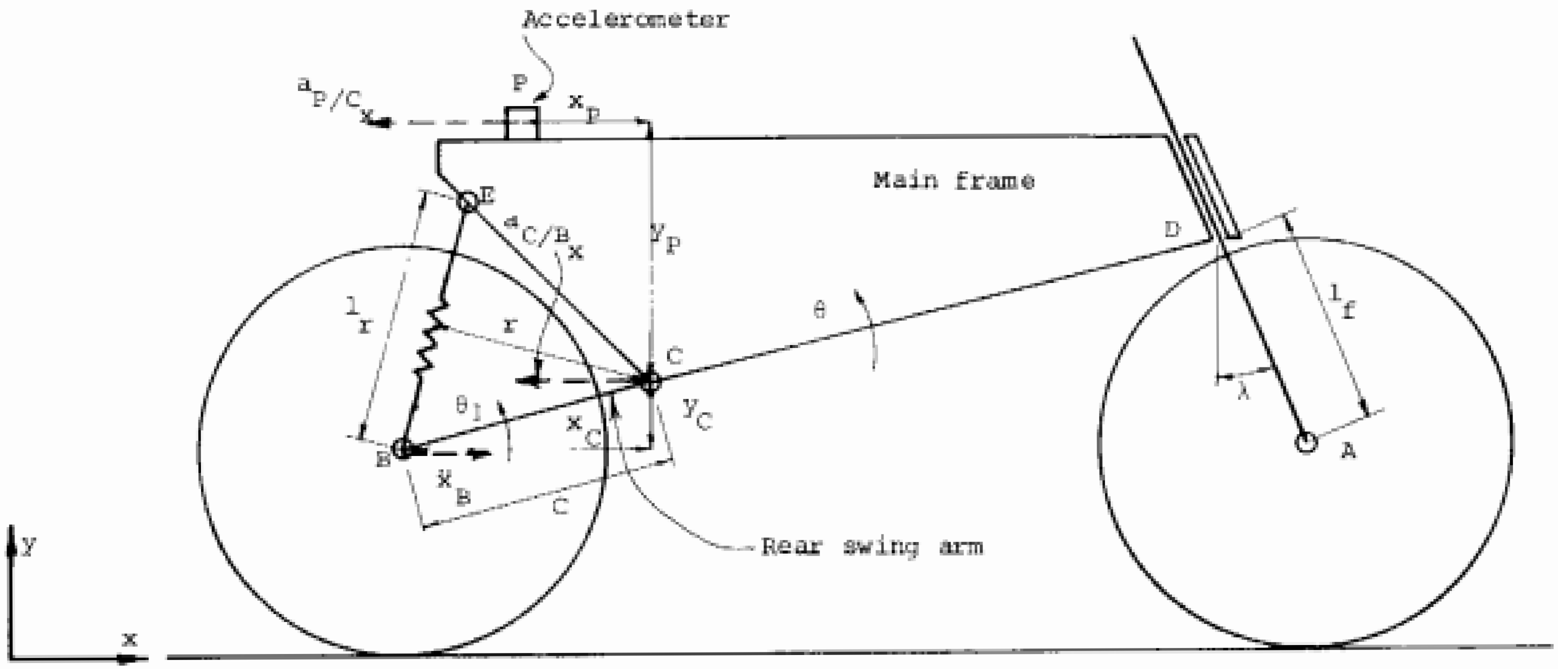

Figure A.12 Symbolic representation of a motorcycle with an accelerometer mounted on the main frame.

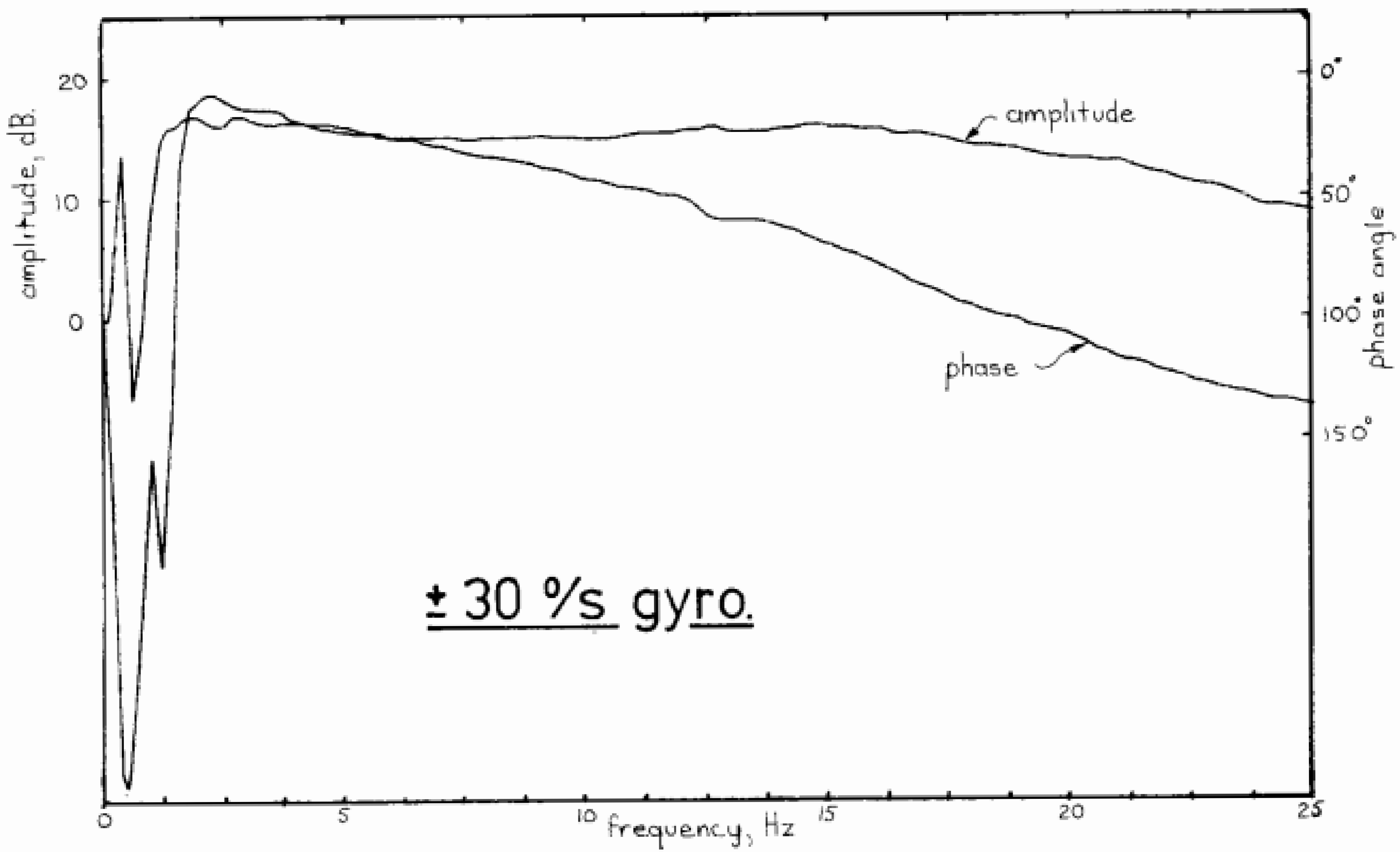

Figure A.13 Transfer function of rate gyroscope.

Note: The rate gyroscope had a flat amplitude response down to 0 Hz. The low frequency roll-off shown in this figure results from filtering during the calibration testing.

Therefore, in terms of the quantities to be measured on the motorcycle (A_i, $\dot{\theta}$, l_r), the required horizontal acceleration $\ddot{x}_B$ is:

$$\ddot{x}_B = A_i - g\theta + x_C[(\dot{l}_r/r)^2 + 2\dot{l}_r/r\ \dot{\theta} + \dot{\theta}^2] + y_C\ddot{l}_r/r + (y_C + y_P)\ \ddot{\theta} - x_P\ \dot{\theta}^2 \qquad (A.9)$$

The significance of the various correction terms in equation A.5 is discussed in Section A.3.

A.2.7 Motorcycle Mainframe Pitch Rate

A rate gyroscope was used to measure (Humphrey, model number RG51-0107-1, ± 30 deg/sec). This device was selected on the basis of its compact, lightweight design and easily-provided +28 volt d.c. power supply requirement. Furthermore the output signal is a varying resistance, and a simple regulated supply voltage was the only requirement to obtain a signal proportional to pitch rate. The gyroscope manufacturer supplied a calibration data sheet, which was assumed correct (± 0.3%). However, it was noted that this device had a nominal natural frequency of 10Hz, which is in the area of interest to this analysis. Therefore a gyroscope calibration rig was constructed which gave the transfer function found in Figure A.13. The natural frequency is 18.75 Hz (90° phase shift) and the phase-frequency relationship is non-linear. In this case, the high frequency $\dot{\theta}$ signals will be delayed by a greater amount than the low frequency signals. Therefore a more complex procedure for frequency compensation than that used for the force and acceleration signals (cf., A.2.1) would be required for the pitch rate signals. A plausible scheme would be to transform the $\dot{\theta}$ signals into the frequency domain (using a Fourier transformation) where the non-linear compensation could be applied. Returning to the time domain (using an inverse Fourier transformation) would yield the correct signal. Unfortunately time constraints have not allowed completion of this procedure, and a linear phase-frequency

The data collected from these experiments was digitized and stored in files on a DEC PDP 11/23 computer. The brake force and acceleration traces were shifted in order to compensate for the time delay arising from their output amplifier filter stages. The pitch rate signal was shifted to compensate for the (assumed linear) time delay caused by its resonant frequency being 18.75 Hz. Then use was made of a data manipulation facility developed for the PDP 11/23 computer, which includes a waveform calculator, a visual display system, and a hardcopy digital plotter. With this program, each of the terms in equation A.5 was calculated, and its contribution to the indicated deceleration assessed. As an example, the data for a typical front displacement modulation run is presented in Figure A.15. Figure A.15 (a) shows front brake displacement for the duration of the test. The initial speed was 18.5 m/s (67 km/h). The rear suspension deflection, l_r together with the main frame pitch rate, $\dot{\theta}$ allowed calculation of the rear swing arm rotational velocity and acceleration ($\dot{\theta}_1$ and $\ddot{\theta}_1$) by use of equations A.7 and A.8 respectively. Then, referring to equation A.5, the magnitude of each correction term to be applied to the indicated acceleration was assessed.

The validity of the measurements and calculation procedures was checked by comparing the measured front suspension deflection with that calculated from the equation:

$$\dot{l}_f = (L\,\dot{\theta} + C/r\,\dot{l}_r)/\cos\lambda \qquad\qquad (L = \text{wheel-base})$$

This equation follows from the same considerations which lead to equation A.5 The comparison showed excellent agreement, thereby giving some confidence in both the measurements and the calculations.

The $\dot{\theta}_1$, $\ddot{\theta}_1$and $\dot{\theta}^2$ terms in equation A.5 were each found to make a negligible contribution to the indicated acceleration. Thus, only $y_p\,\ddot{\theta}$ and $g\theta$ in equation A.5 were of any significance. Figures A.15 (b) and (c) show the magnitude of both these correction terms during this experimental run. Figure A.15 (d) shows the indicated acceleration, A_i, and the indicated acceleration after application of the correction terms $y_p \ddot{\theta}$ and $g\theta$. The latter is the required horizontal acceleration of the motorcycle, $\ddot{x}_B$. This figure demonstrates that the indicated acceleration and the corrected acceleration are not greatly different from one another. Furthermore the $g\theta$ term has, overall, a larger influence on A_i than $y_p\ddot{\theta}$. The latter term is seen to have an average value of nearly zero, and is of high frequency compared to the displacement input. Its main influence is on the magnitude of the acceleration peaks. On the other hand, the $g\theta$ term has an average value of about 0.8 m/s^2, and is of the same frequency as the displacement input. Also, as the $\dot{\theta}_1$ and $\ddot{\theta}_1$ terms were shown to be small compared to the others in equation A.5, there is no requirement to record suspension deflections in motorcycle deceleration tests.

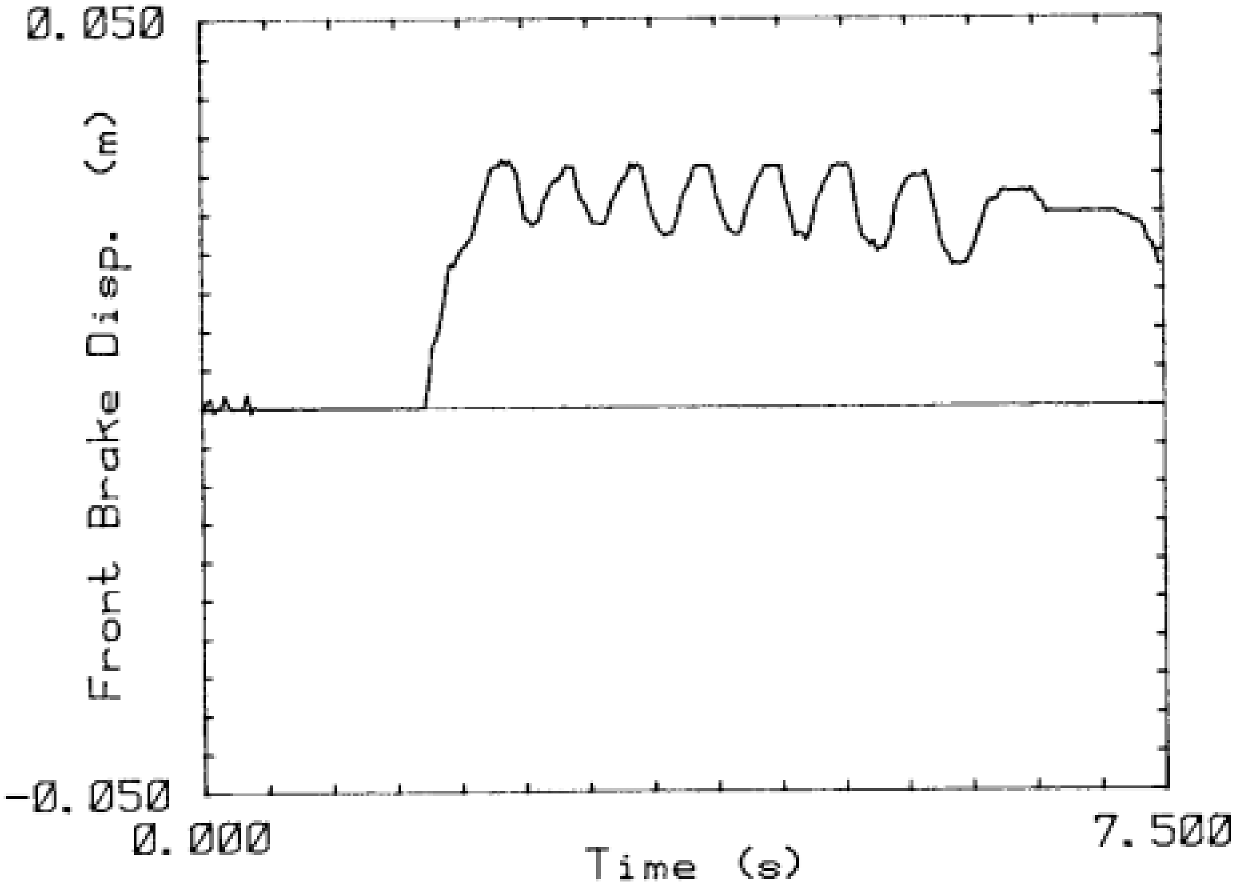

(a)

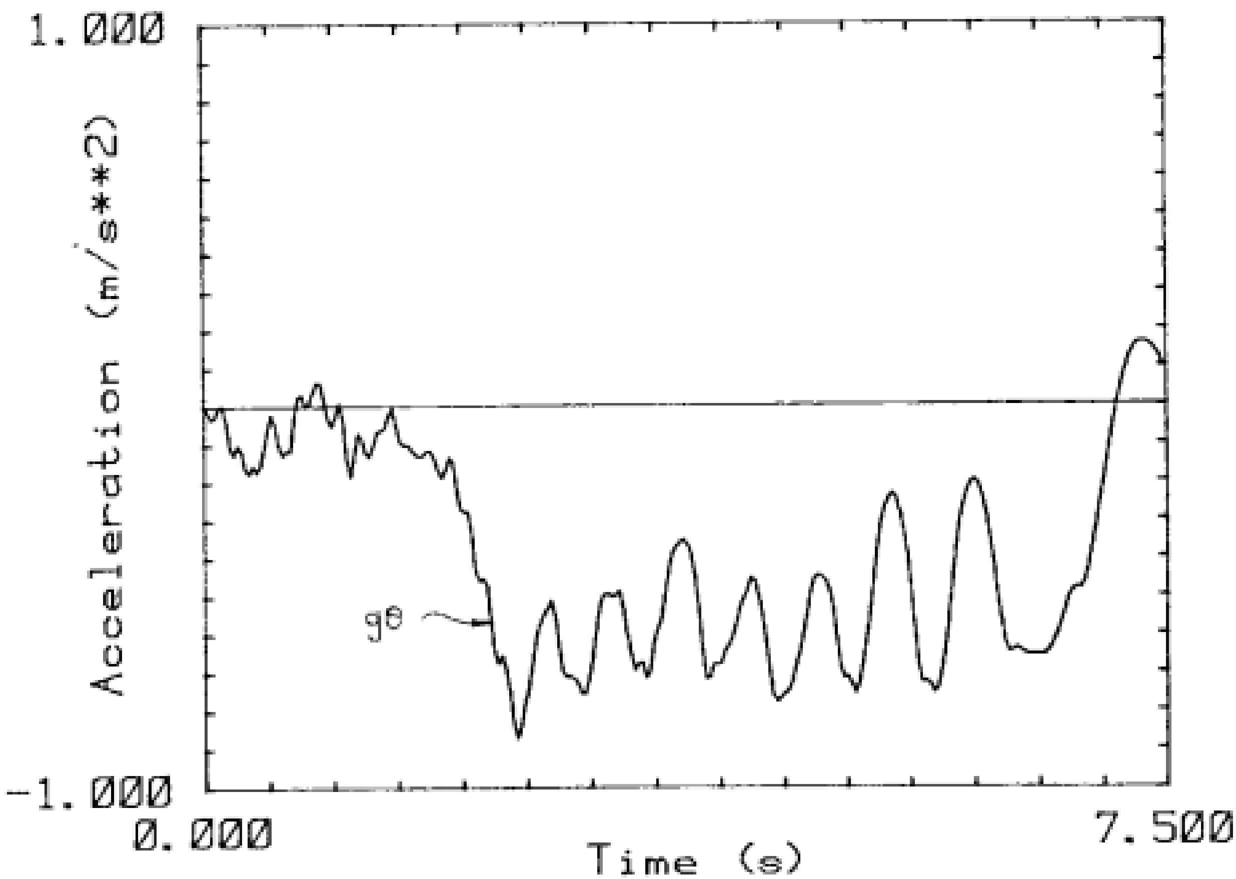

(b)

Figure A.15 Front brake displacement modulation test with 400 ml motorcycle.

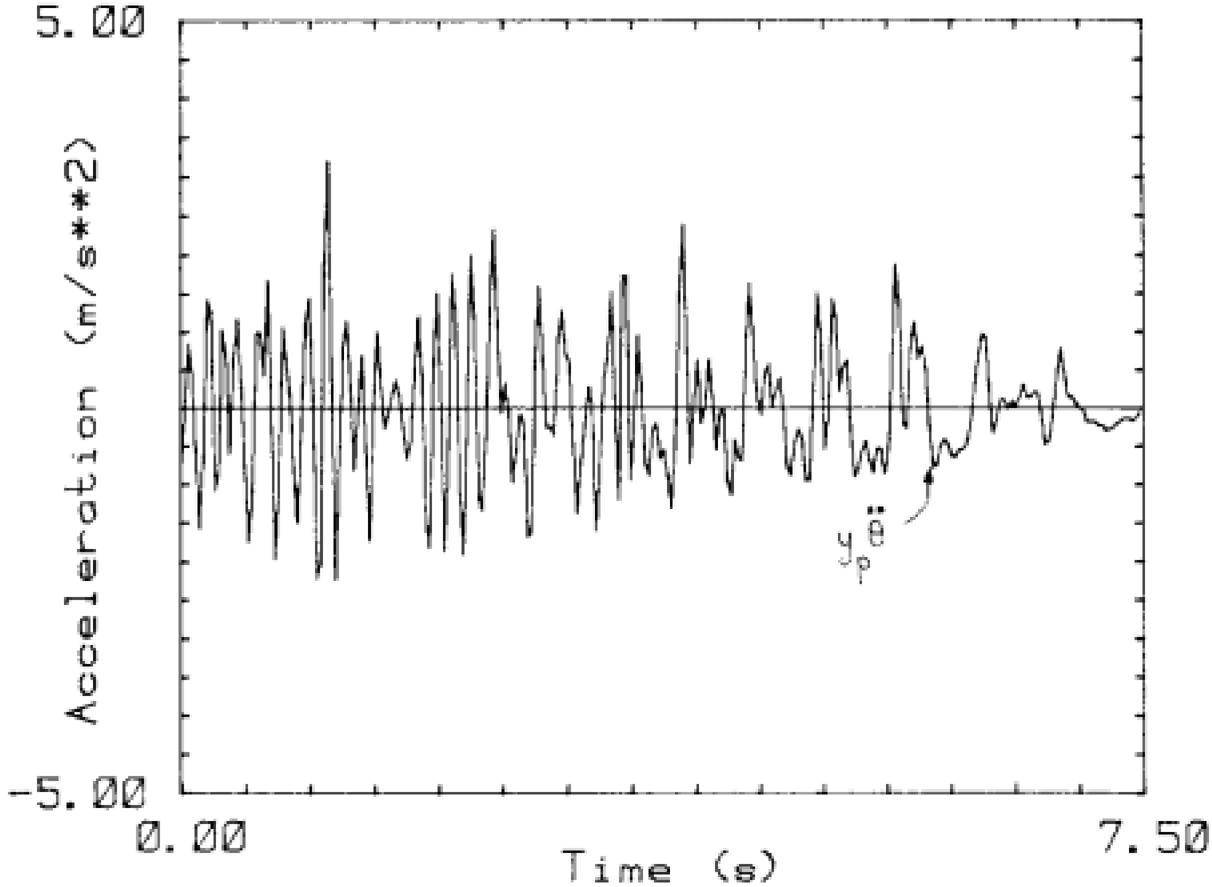

(c)

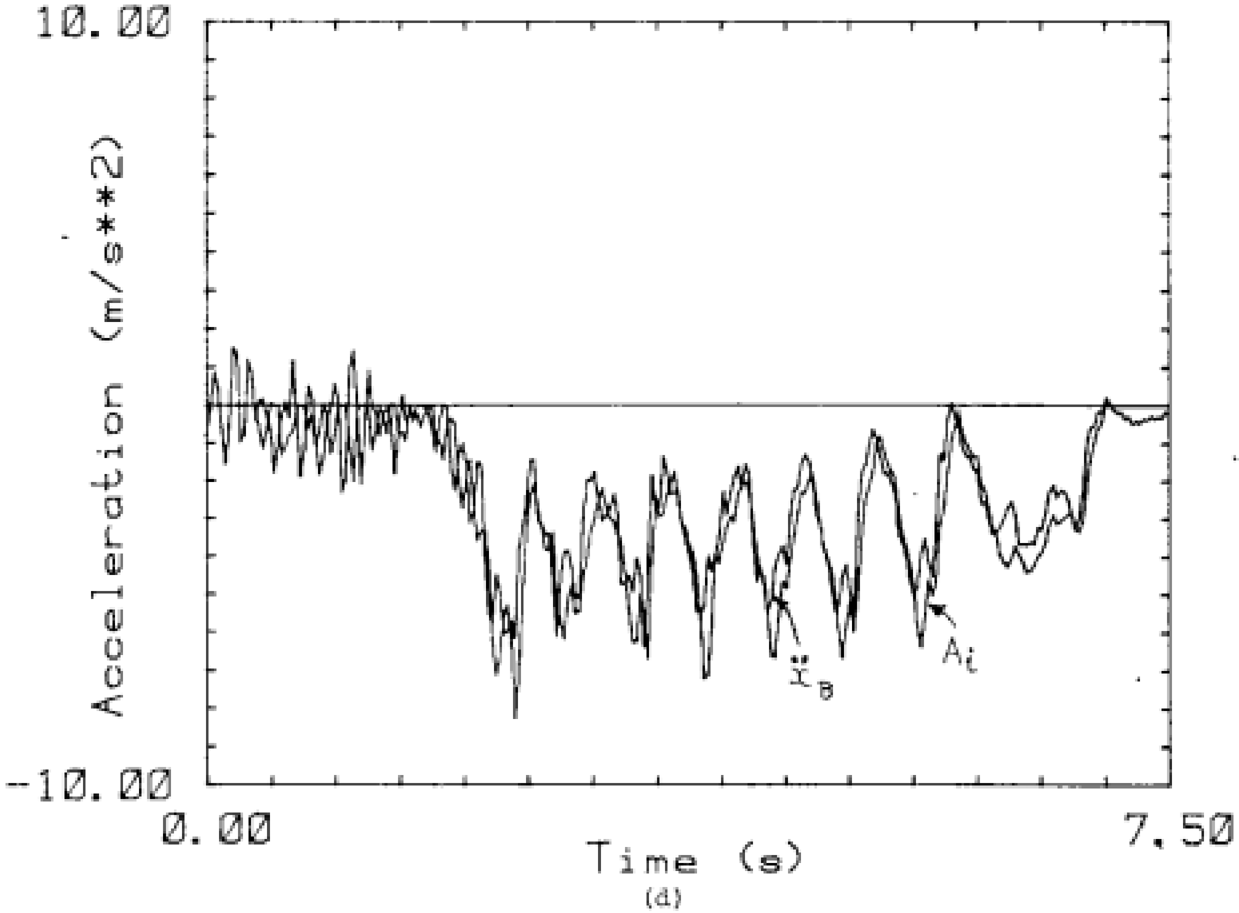

(d)

Figure A.15 (continued.)

APPENDIX B

RECOVERY RATE GRADIENT

Zellner and Klaber (1981) analyzed data on the performance of a variety of brake pad friction materials, under both wet and dry operating conditions. They found that the dry pad friction coefficient tends to increase during a braking stop due to the combined effects of reduced speed and increased temperature. Under wet braking conditions, they concluded that the initial brake torque obtained is usually less than that obtained with the same clamping force with dry pads, and that the brake torque then generally increases or 'recovers' towards the dry value. This behaviour is illustrated schematically in Figure B.1, taken from Zellner and Klaber's paper. It may be noted from this figure that some dry pads also experience substantial recovery rates.

For the purposes of brake characterization, Zellner and Klaber took the increase of deceleration to occur linearly with time and defined the 'recovery rate' RR as the rate of increase of deceleration normalized by the final deceleration:

$$RR = (a_2 - a_1)/a_2\Delta t \ , \qquad (B.1)$$

where a_1 and a_2 are the initial and final deceleration and Δt is the time taken to stop. They found that the recovery rate increased in proportion to the clamping force and so defined the 'recovery rate gradient' RRG as the recovery rate per unit of applied lever force F:

$$RRG = RR/F \ . \qquad (B.2)$$

In the present study brakes have been characterized by control gradients, or by their inverse, control gains. In this appendix it is shown that Zellner and Klaber's RRG can be interpreted as the rate of decrease with speed of the force control gain,

$G_F = a/F$.

That is,

$$G_F' = dG_F/dv \approx -RRG . \qquad (B.3)$$

To show this, assume that the disk/pad friction coefficient decreases linearly (say) with rubbing speed. Then we may write

$$\mu = \mu_2 - \mu' v ,$$

where μ_2 is the static coefficient of friction and $\mu' = -d\mu/dv$ is the (constant) rate of decrease of μ with motorcycle forward speed v.

The motorcycle deceleration can be taken to be proportional to the brake torque, which in turn will be proportional to the friction coefficient and the brake lever force:

$$a = k_a \mu F , \qquad (B.4)$$

where k_a is a constant of proportionality. That is, the force gain G_F is given by

$$G_F = a/F = k_a \mu . \qquad (B.5)$$

Thus, given the assumed friction-speed characteristic, the force gain will decrease linearly with speed:

$$G_F' = dG_F/dv = -k_a \mu' = \text{const}. \qquad (B.6)$$

The time rate of change of deceleration will be

$$da/dt = da/dv.dv/dt = (FG_F')(-a) . \qquad (B.7)$$

Integrating equation B.7 shows that the deceleration will vary (slowly), but exponentially rather than linearly with time:

$$a = a_1 \exp(-FG_F' t) \quad . \qquad (B.8)$$

(Actually, this exponential variation of deceleration is a better representation of the wet brake deceleration trace shown in Figure 14 of Zellner and Klaber's paper than is their linear assumption).

The proportional increase in deceleration over the stop will be

$$(a_2 - a_1)/a_2 = 1 - \exp(FG_F' \Delta t) \simeq -FG_F' \Delta t \quad , \qquad (B.9)$$

the approximation being reasonable provided that the recovery rate is not too large. Hence,

$$RRG = (a_2 - a_1)/a_2 \Delta t F = -G_F' \quad . \qquad (B.10)$$

That is, Zellner and Klaber's recovery rate gradient can be interpreted as the rate of decrease of the force gain with speed, as has been done in Chapter 2.

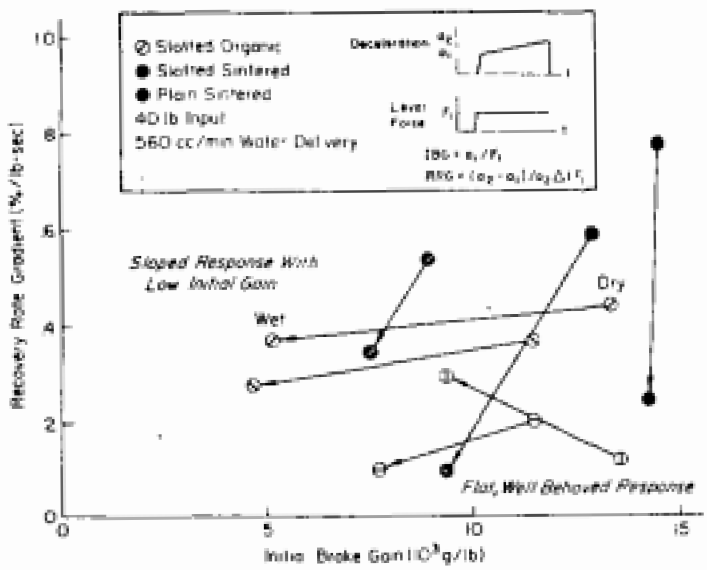

Figure B.1 Effect of water on brake gain, and recovery rate for several pads (from Zellner and Klaber, 1981)

APPENDIX C

MATHEMATICAL MODEL OF AN HYDRAULIC BRAKE SYSTEM

C.1 Simplified Model

In this Appendix a mathematical model is developed to account for the main response characteristics of a motorcycle hydraulic brake system.

Figure C.1 shows schematically the physical arrangement of a typical brake system. A simplified model for this system is illustrated in Figure C.2, in which the lumped representations of the main sources of elasticity, dry friction, viscous resistance and lost-motion are identified. The low-frequency relationship between brake lever force and displacement for this model was shown in the main text (Figure 2.14) to compare favourably in form with that measured for a production motorcycle (Figure 2.15).

The main concern in this Appendix is to account for the response characteristics observed in the step displacement and swept-sine displacement tests described in Chapter 2. For this purpose the model may be further simplified: The coulomb forces F_{C1}, F_{C2} and F_{C3} are ignored, and the displacement steps d_1, d_2, d_3 and d_4 are assumed to be 'taken up'. The resulting model, shown in Figure C.3 appears to provide the simplest representation which will exhibit the major response characteristics observed in dynamic testing of actual brake systems.

In Figure C.3 the spring of stiffness k_1 represents the master cylinder return spring. The other springs are lumped representations of the compressibility of the fluid in the master cylinder (k_2), that of the fluid in the brake line and the elasticity of the brake line walls (k_3) and the elasticity of the disc pad (k_4). The viscous resistance associated with the

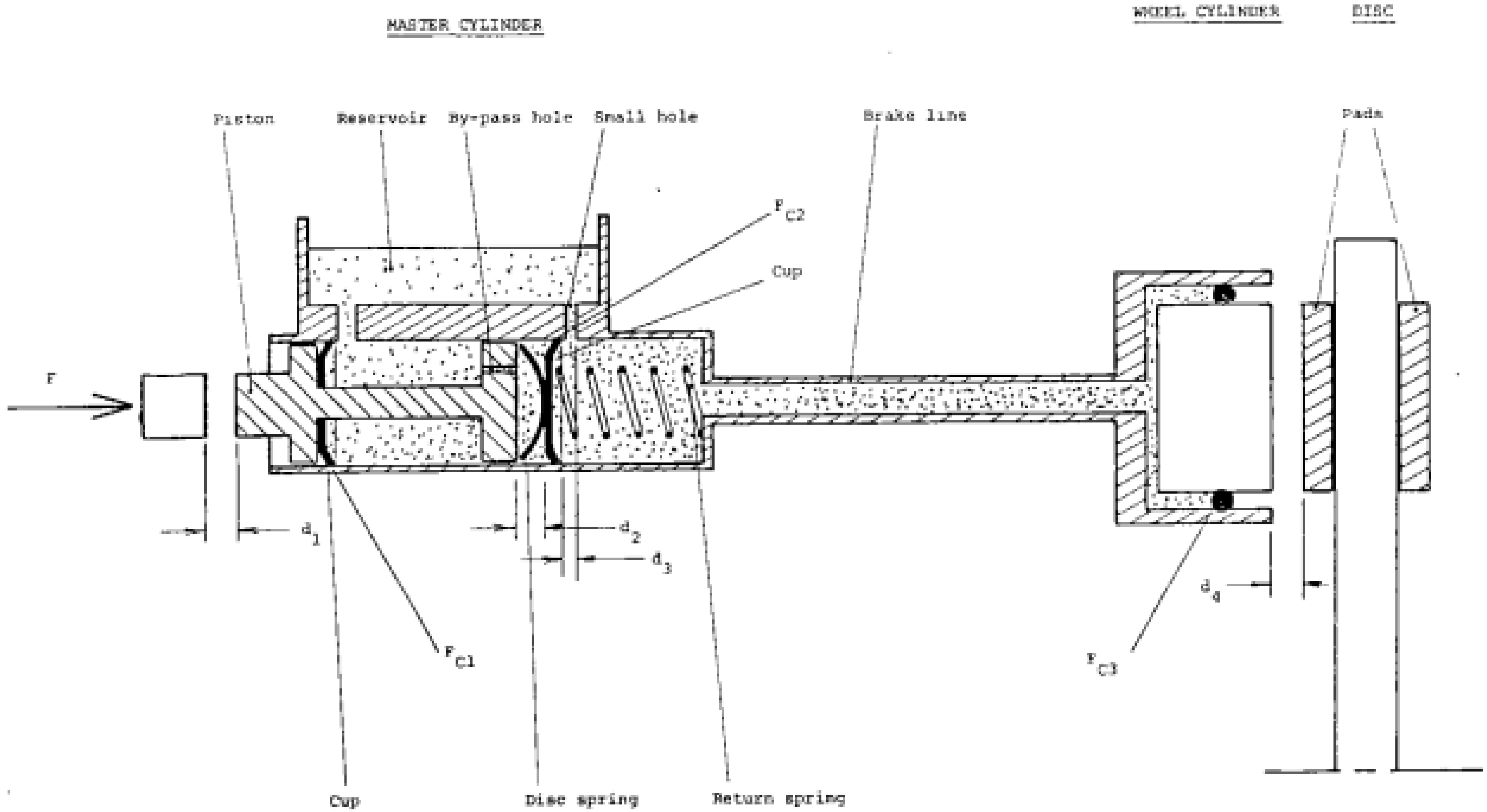

Figure C.1 Schematic physical arrangement of a motorcycle hydraulic brake system.

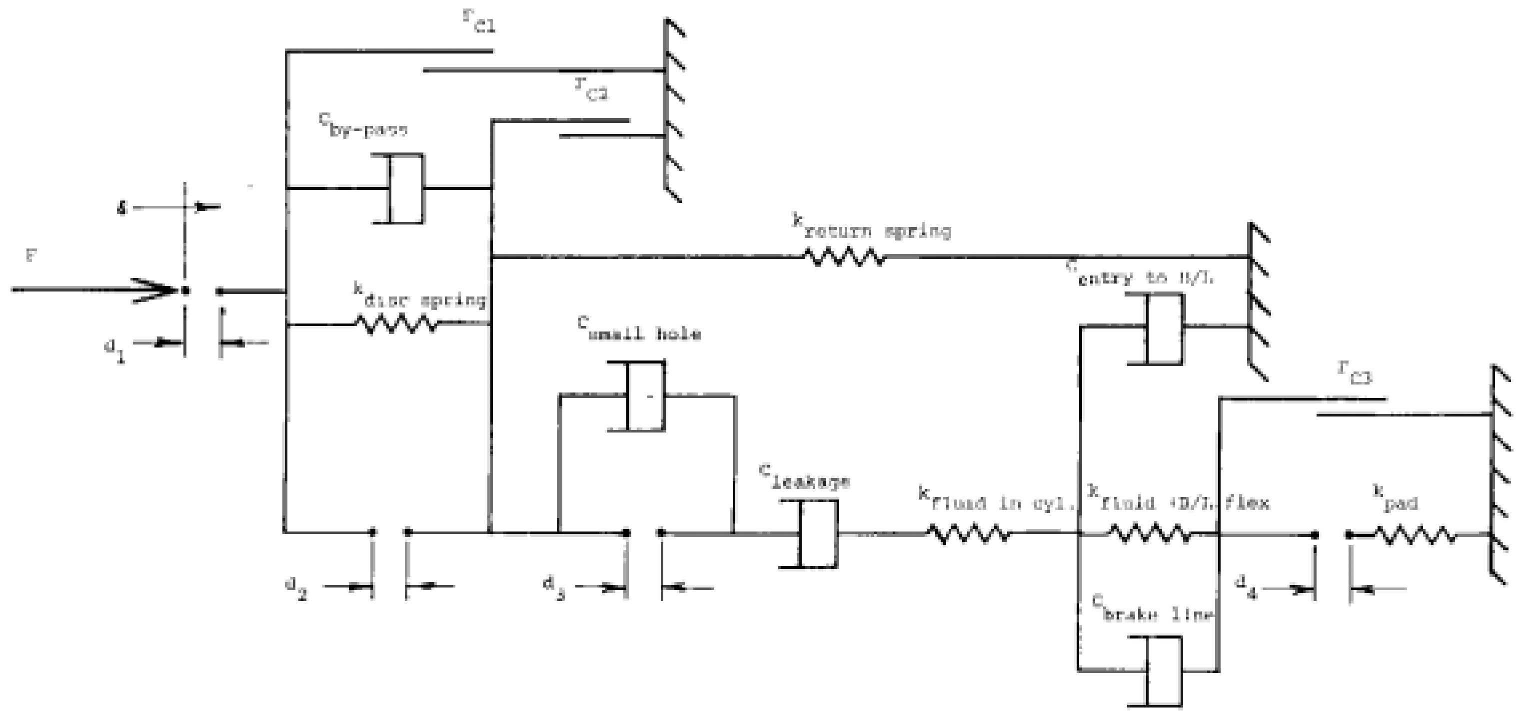

Figure C.2 Symbolic representation of motorcycle hydraulic brake system.

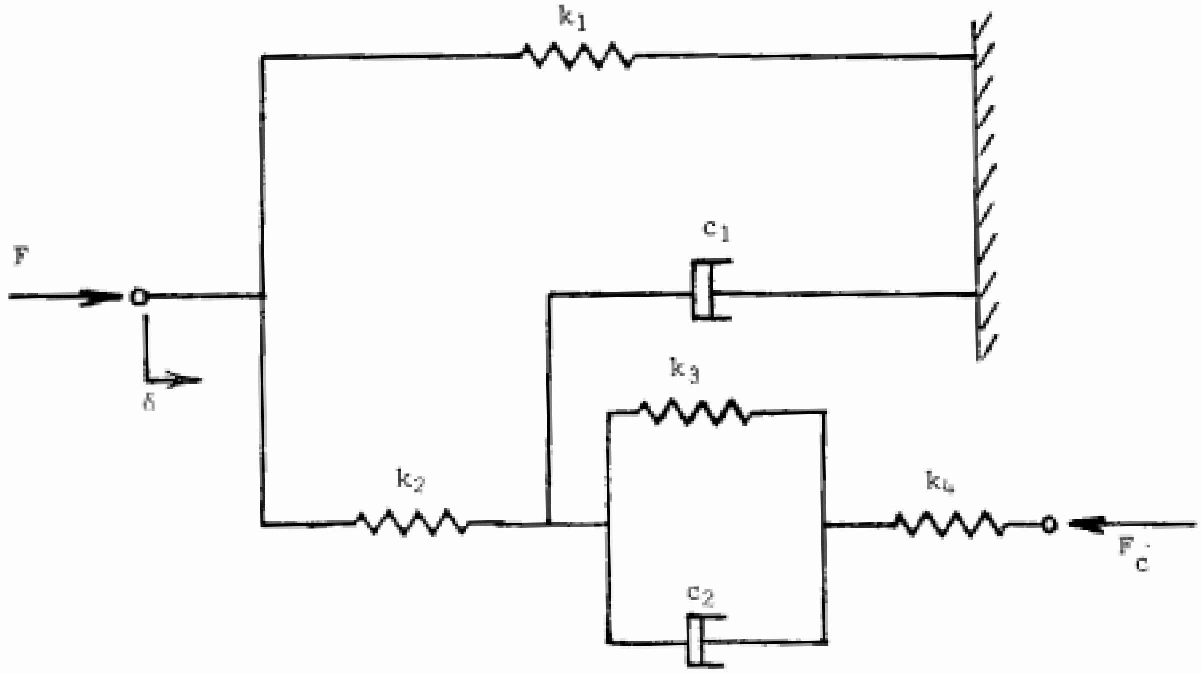

Figure C.3 Simplified linearised brake model.

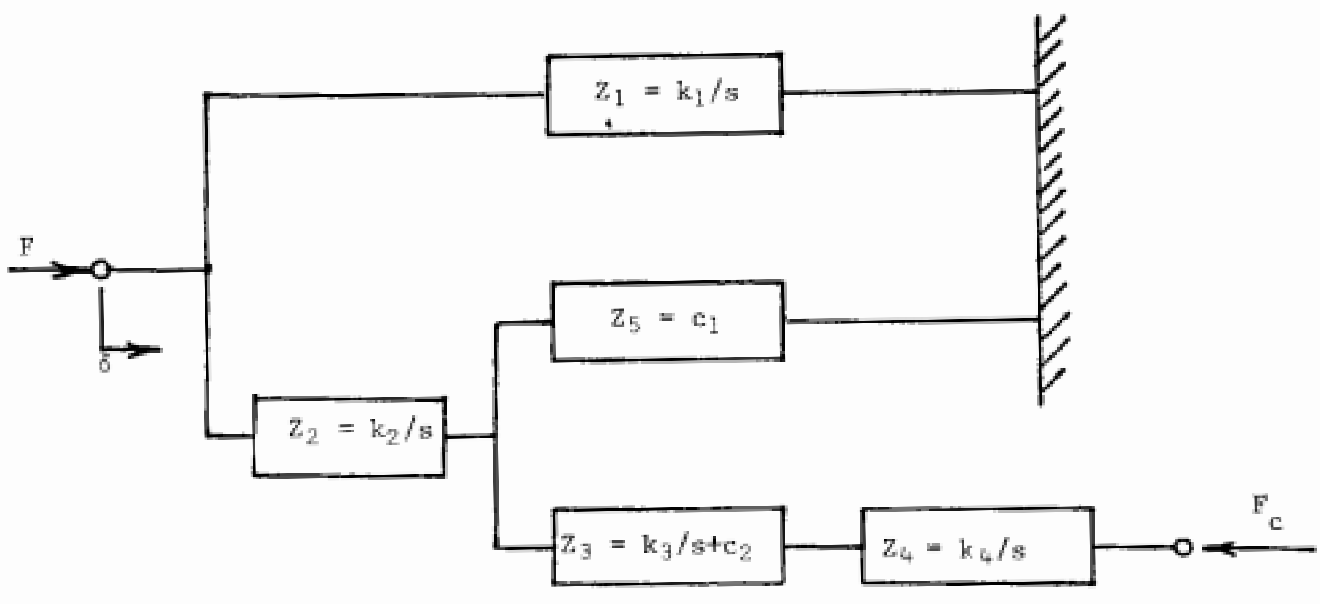

Figure C.4 Mechanical impedance representation of the simplified brake model.

contraction from the master cylinder to the brake line is represented by the damper c_1, while rate-dependence in the brake line flexing is accounted for by the damper c_2. The brake lever force and displacement are F and δ, respectively, and the disc clamping force is F_c.

C.2 TRANSFER FUNCTIONS

The 'mechanical impedance' approach may be usefully employed in this analysis: A harmonically varying quantity $f(t) = F_o.\cos(\omega t+\phi)$ is represented by the complex number $F.e^{st}$, where the amplitude F_o and phase ϕ are given by the complex 'phasor' $F = F_o.e^{i\phi}$, and the frequency ω by the complex variable $s = i\omega$. The 'impedance' of a spring of stiffness k is then written as $F/V = k/s$, where F and V are, respectively, phasors for the force transmitted by the spring and the rate of deformation of the spring. Similarly, the impedance of a damper of coefficient c is simply $F/V = c$ (Cannon, 1976).

The impedances of the brake system components are shown in Figure C.4. The 'series' combination of impedances $Z_3 = k_3/s + c_2$ and $Z_4 = k_4/s$ has an impedance of

$$Z_{34} = \frac{Z_3.Z_4}{Z_3 + Z_4} = \frac{k_4(k_3 + c_2 s)}{s(k_3 + k_4 + c_2 s)}.$$

The 'parallel' combination of Z_{34} and $Z_5 = c_1$ has an impedance of

$$\begin{aligned} Z_{345} &= Z_{34} + Z_5 \\ &= \frac{k_3 k_4 + (k_3 c_1 + k_4 c_1 + k_4 c_2)s + c_1 c_2 s^2}{s(k_3 + k_4 + c_2 s)}. \end{aligned}$$

By similar processes of combination the impedances Z_{2345} and Z_{12345} may be found. From the latter impedance the 'dynamic stiffness' of the brake system is obtained as

$$\begin{aligned} F/\delta &= s.Z_{12345} \\ &= \frac{A_1 + B_1 s + C_1 s^2}{A_2 + B_2 s + C_2 s^2}, \end{aligned} \qquad (C.1)$$

where

$$A_1 = k_1k_2(k_3 + k_4) + k_3k_4(k_1 + k_2)$$
$$B_1 = (k_1 + k_2)(k_3 + k_4)c_1 + [k_1k_2 + k_4(k_1 + k_2)]c_2 \qquad (C.2)$$
$$C_1 = (k_1 + k_2)c_1c_2$$

and

$$A_2 = k_2(k_3 + k_4) + k_3k_4$$
$$B_2 = (k_3 + k_4)c_1 + (k_2 + k_4)c_2 \qquad (C.3)$$
$$C_2 = c_1c_2.$$

If the component stiffness and damping coefficients were known, the polynomials in equation (C.1) could be factorized to yield a dynamic stiffness transfer function of the form

$$\frac{F}{\delta} = \left[k_1 + \frac{1}{1/k_2 + 1/k_3 + 1/k_4} \right] \frac{(1 + s/a_1)(1 + s/a_2)}{(1 + s/b_1)(1 + s/b_2)}. \qquad (C.4)$$

The static stiffness (the expression in square brackets in equation (C.4)) can be recognised as resulting from the parallel combination of k_1 with the series combination of k_2, k_3 and k_4.

The brake lever force F is resisted by the return spring force and the pressure force from the master-cylinder fluid:

$$F_2 = (Z_{2345}/Z_{12345})F. \qquad (C.5)$$

This force in turn is resisted by the viscous force at the brake line entry and the pressure force in the brake line. The latter force is equal to the disc clamping force F_c, and is given by

$$F_c = (Z_{34}/Z_{345})F_2. \qquad (C.6)$$

Hence the clamping force F_c in response to a dynamic lever displacement δ is given by

$$F_c = (F_c/F_2)(F_2/F)(F/\delta)\delta. \qquad (C.7)$$

Using equations (C.4) to (C.7), the lever-displacement to clamping-force transfer function is thus obtained as

$$F_c/\delta = (Z_{34}/Z_{345})Z_{2345}$$

$$= \frac{A_3 + B_3 s}{A_2 + B_2 s + C_2 s^2} \qquad (C.8)$$

where

$$A_3 = k_2 k_3 k_4$$

$$B_3 = k_2 k_4 C_2 \qquad (C.9)$$

and A_2, B_2 and C_2 were given previously in equation (C.3). Factorizing in equation (C.8) would yield the transfer function

$$\frac{F_c}{\delta} = \left[\frac{1}{1/k_2 + 1/k_3 + 1/k_4}\right] \frac{(1 + s/a_3)}{(1 + s/b_1)(1 + s/b_2)}, \qquad (C.10)$$

The lever-force to clamping-force gain is then easily obtained as

$$F_c/F = (F_c/\delta)(\delta/F)$$

which, from equations (C.4) and (C.10), may be written as

$$\frac{F_c}{F} = \left[\frac{1}{1 + k_1/k_2 + k_1/k_3 + k_1/k_4}\right] \frac{(1 + s/a_3)}{(1 + s/a_1)(1 + s/a_2)}. \qquad (C.11)$$

If it is assumed that the motorcycle deceleration is proportional to the disc clamping force, equations (C.10) and (C.11) can be used to predict the dynamic deceleration/displacement and deceleration/force gains, respectively.

C.3 TRANSFER FUNCTION PARAMETERS

By suitable selection of the parameters a_1, a_2, a_3, b_1 & b_2 in the transfer functions (C.4), (C.10) and (C.11) a variety of frequency response functions could be simulated. To assess the adequacy of the proposed model in representing an example of real brake behaviour, an attempt may be made to 'identify' these parameters from measured frequency response functions. Figures 2.7, 2.8 and 2.9, in the main text, show deceleration/displacement, deceleration/force and force/displacement frequency response functions measured for the front brake of the 400 ml motorcycle.

Comparison of the F_c/F transfer function in equation (C.11) with the data in Figure 2.8 suggests that frequencies a_1 and a_3 are approximately equal and that a_2 is high and close to the frequency bandwidth of the experimental data. The phase curve indicates that $a_2/2\pi$ = 6 Hz is not an unreasonable estimate and that a_3 is slightly smaller than a_1.

The increase in the deceleration/displacement gain in Figure 2.7 at around 0.8 Hz suggests that $a_3/2\pi$ in equation (C.10) should be approximately 0.8 Hz so that $a_1/2\pi$ = 0.6 Hz, say. The mid-frequency amplitude plateau and high-frequency phase roll-off suggest $b_1/2\pi$ = 1.8 Hz and $b_2/2\pi$ = 8 Hz. The estimates already made for a_1, a_2, b_1 and b_2 in equation (C.4) are quite consistent with the measured force/displacement frequency response function in Figure 2.9. Comparison of the phase curves in Figures 2.7 and 2.9 provides confirming evidence of a high-frequency lead at $a_2/2\pi$ = 6 Hz in the force/displacement transfer function.

The normalized Bode plots shown in Figures 2.17 to 2.19, obtained by evaluating equations (C.4), (C.10) and (C.11) with the suggested parameter values, show that the proposed model does indeed simulate the experimental frequency responses quite well.

The lever force and clamping force (or deceleration) responses to a step input of lever displacement, computed from the identified transfer functions, are shown in Figures 2.20 and 2.21. They display the characteristic 'dynamic magnification' effects observed in the corresponding experimental traces (eg. Figures 2.3, 2.10).

APPENDIX D

VBCG MOTORCYCLE HARDWARE DESIGN DETAILS

D.1 INTRODUCTION

The Variable Brake Control Gradient (VBCG) motorcycle was built to allow investigation of the effect of brake feel properties on rider deceleration performance, particularly in an emergency stopping manoeuvre. The general physical arrangement of the system is described in Chapter 3, and shown in Figure 3.1, which is reproduced here as Figure D.1 for convenience. This appendix contains the design details of the individual components of the system.

D.2 COMPONENT DETAILS

D.2.1 Pressure Controller

The pressure controller selected was a Clippard Minimatic MAR-1C, which is a normally-closed, three-way, piston-type valve with variable pressure output. The output pressure is increased proportionally as the plunger is depressed. When the plunger is released, the output port is exhausted to atmosphere and the input port is closed. It has a stem travel of 6.4mm and a working range from zero to 690 kPa. It was considered to be ideally suited to this application on account of its small size (approximately 60mm X 25mm). Figure D.2 shows the measured output pressure versus stem displacement characteristic for one of these devices, in which aproximately 0.4 mm displacement hysteresis is noted. Figure D.3 shows the magnitude and phase angle of the pressure/displacement transfer function for this controller. These two figures were obtained using an LVDT displacement transducer (Trans-Tek 246-000 J6) to measure stem displacement, and a pressure transducer to monitor output pressure. The pressure transducer was constructed by bonding

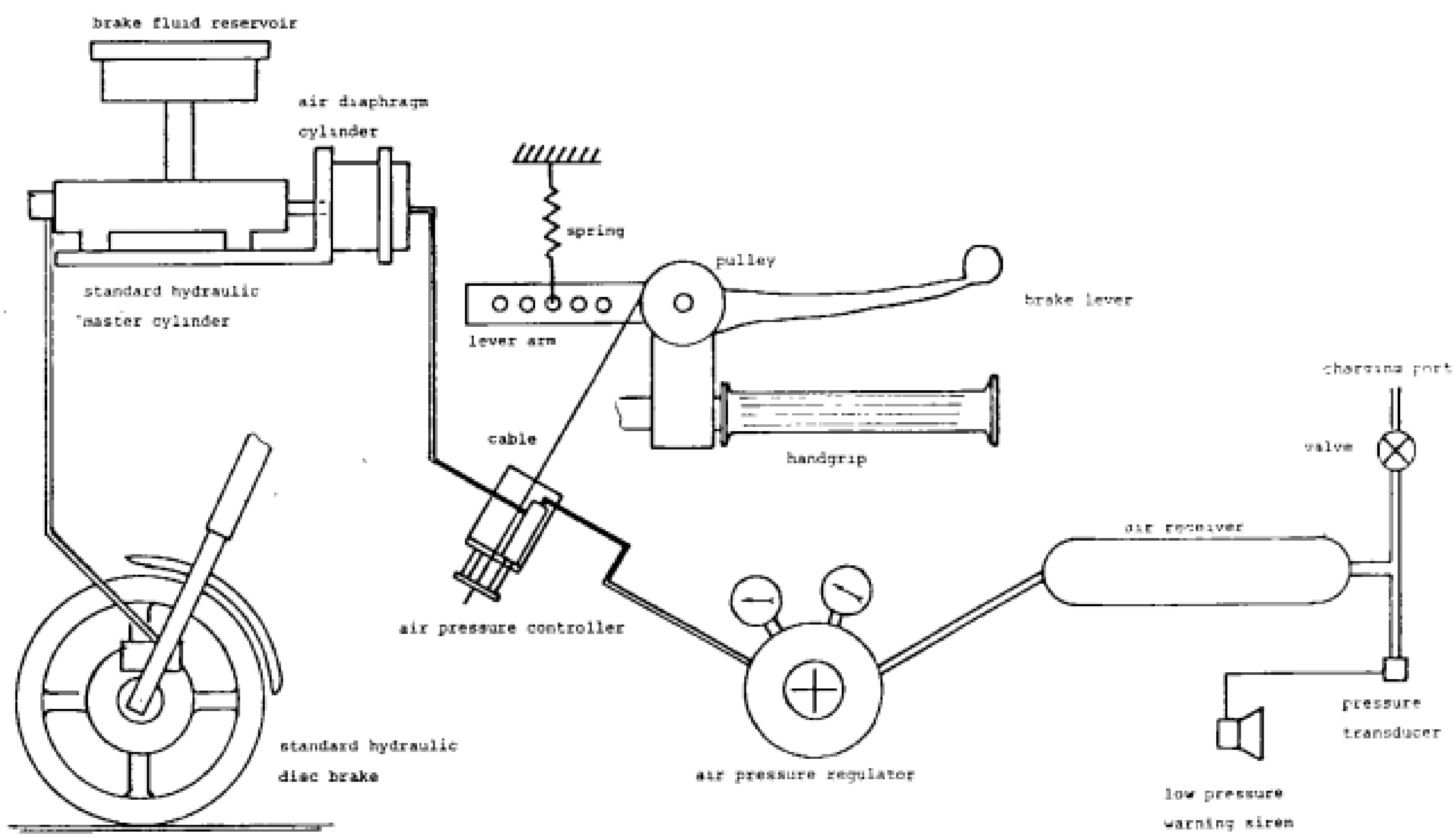

Figure D.1 Schematic layout of VBGC system.

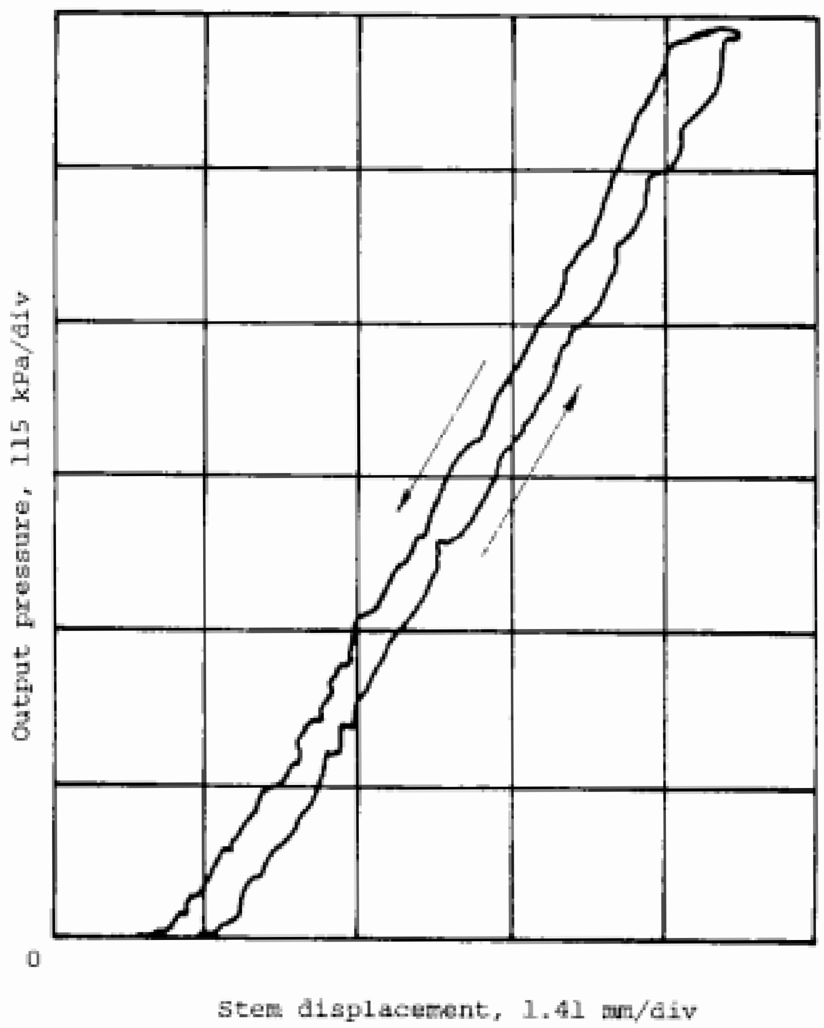

Figure D.2 Pressure-displacement characteristics of the pressure controller.

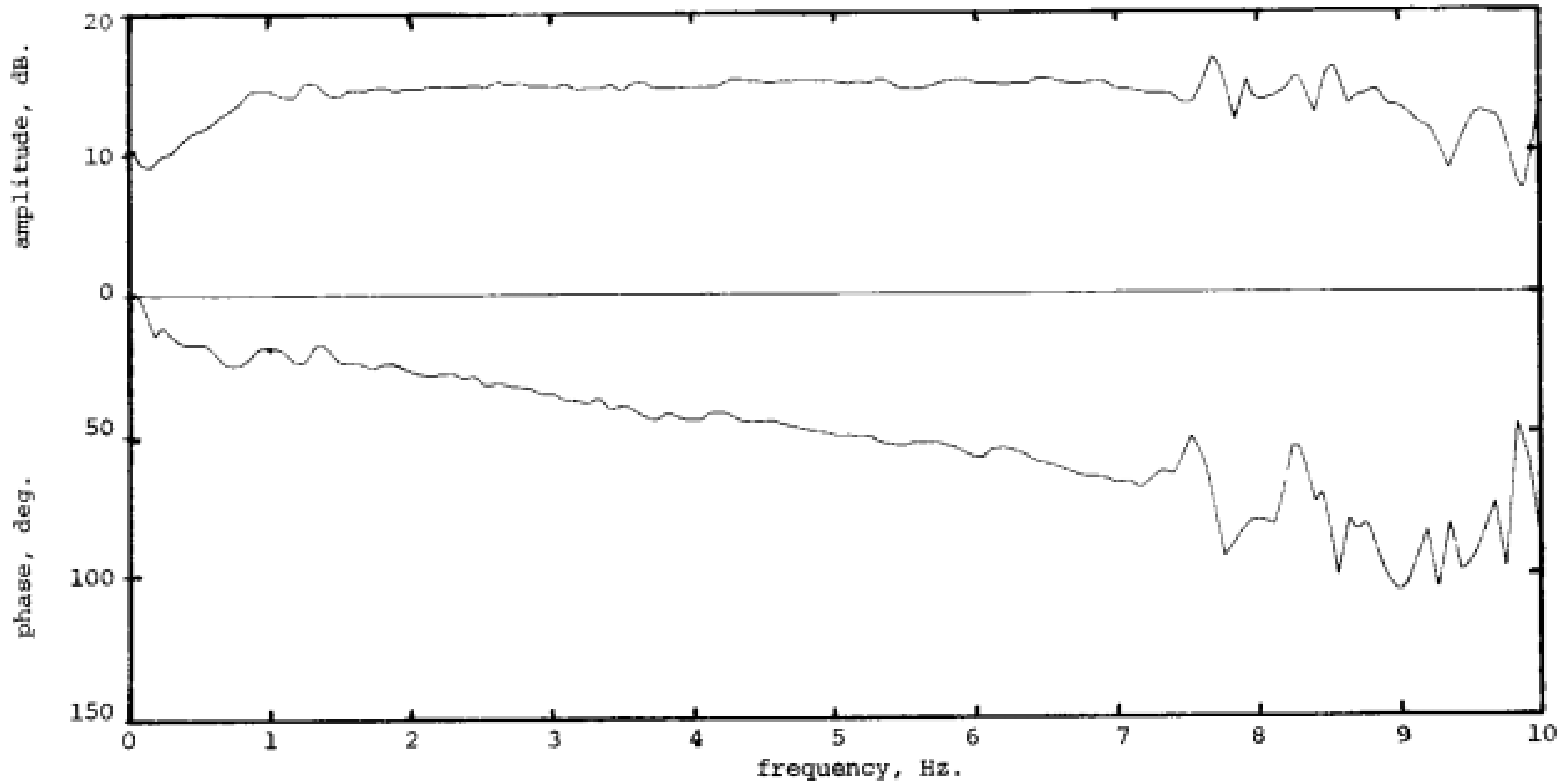

Figure D.3 Pressure/displacement transfer function for the pressure controller.

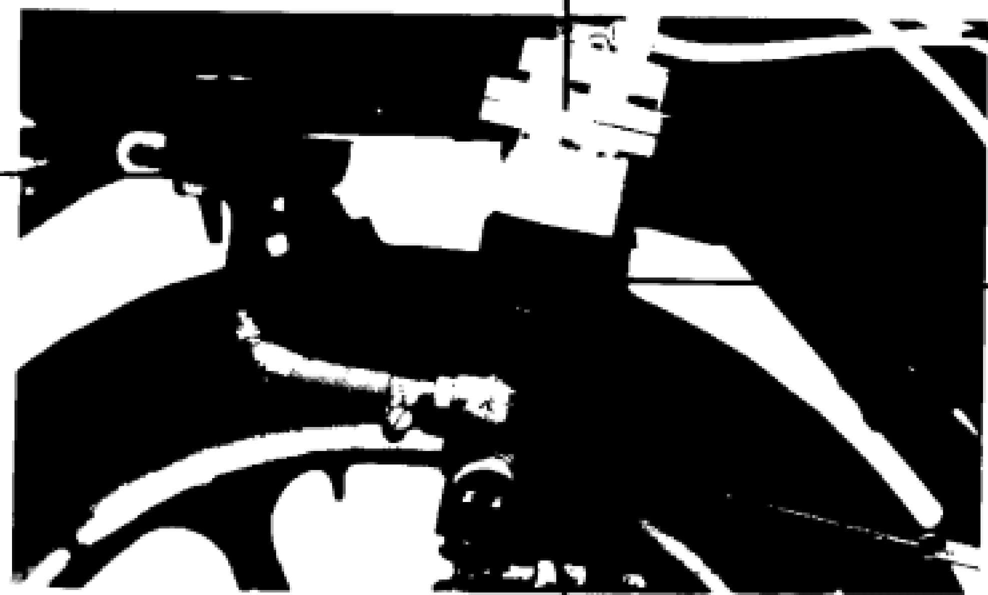

Figure D.4   Diaphragm air cylinder interfaced to hydraulic master cylinder.

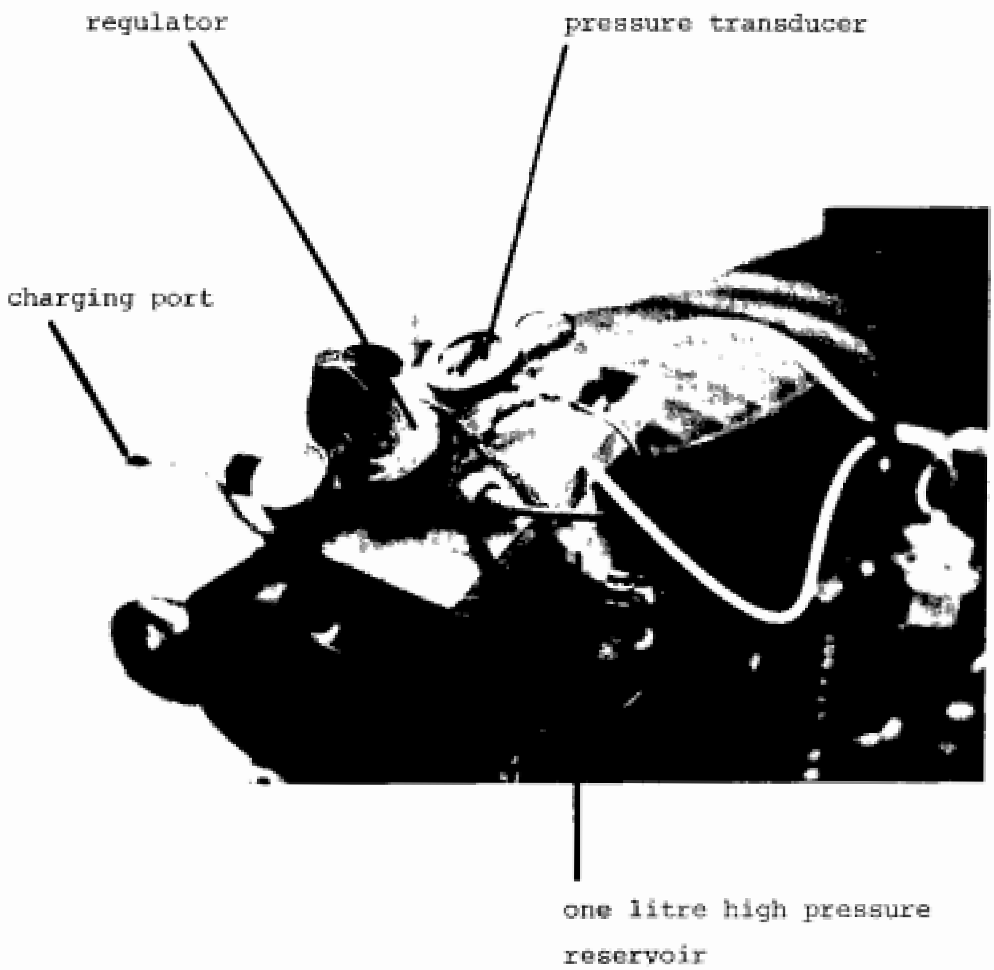

Figure D.5 High pressure air reservoir and regulator mounted on rear of VBCG motorcycle.

strain gauges in full bridge configuration to a bourdon tube pressure gauge. The bridge output was amplified to a suitable level with a d.c. amplifier. The outputs from the two transducers were connected to a Hewlett Packard 3582A spectrum analyzer and a swept-sine technique used to obtain the transfer function information. It is noted with reference to Figure D.3 that the phase lag increases approximately linearly with frequency to a value of 50^{o} at 5 Hz. This corresponds to a time delay of 28ms between stem motion and pressure reponse, which is not large in human control terms.

D.2.2 Actuating Cylinder

Several designs were considered for the actuating cylinder. After some experimentation, it became evident that for the variable brake system to behave similarly to production designs, force hysteresis in the actuating cylinder should be as small as possible. To this end, the diaphragm cylinder shown in Figure D.4 was designed and constructed. This design required only 4 kPa to cause the piston to move, representing only 0.6% of the maximum operating pressure (690 kPa).

D.2.3 Provision Of Air Supply

The air for the modified servo brake system controls was stored in a stainless steel vessel of one litre capacity. This reservoir was initially charged to 14 MPa. The pressure was reduced to the control system working value of 690 kPa with a modified oxygen welding regulator. This arrangement is shown in Figure D.5. The reservoir was recharged from a cylinder of industrial dry air connected to the one litre vessel charging port The control system was found to consume very little air, and more than 1000 brake applications would be required to exhaust a fully charged reservoir. This proved to be sufficient for a full day of testing without need for recharging the reservoir. As a safety measure a pressure transducer/low

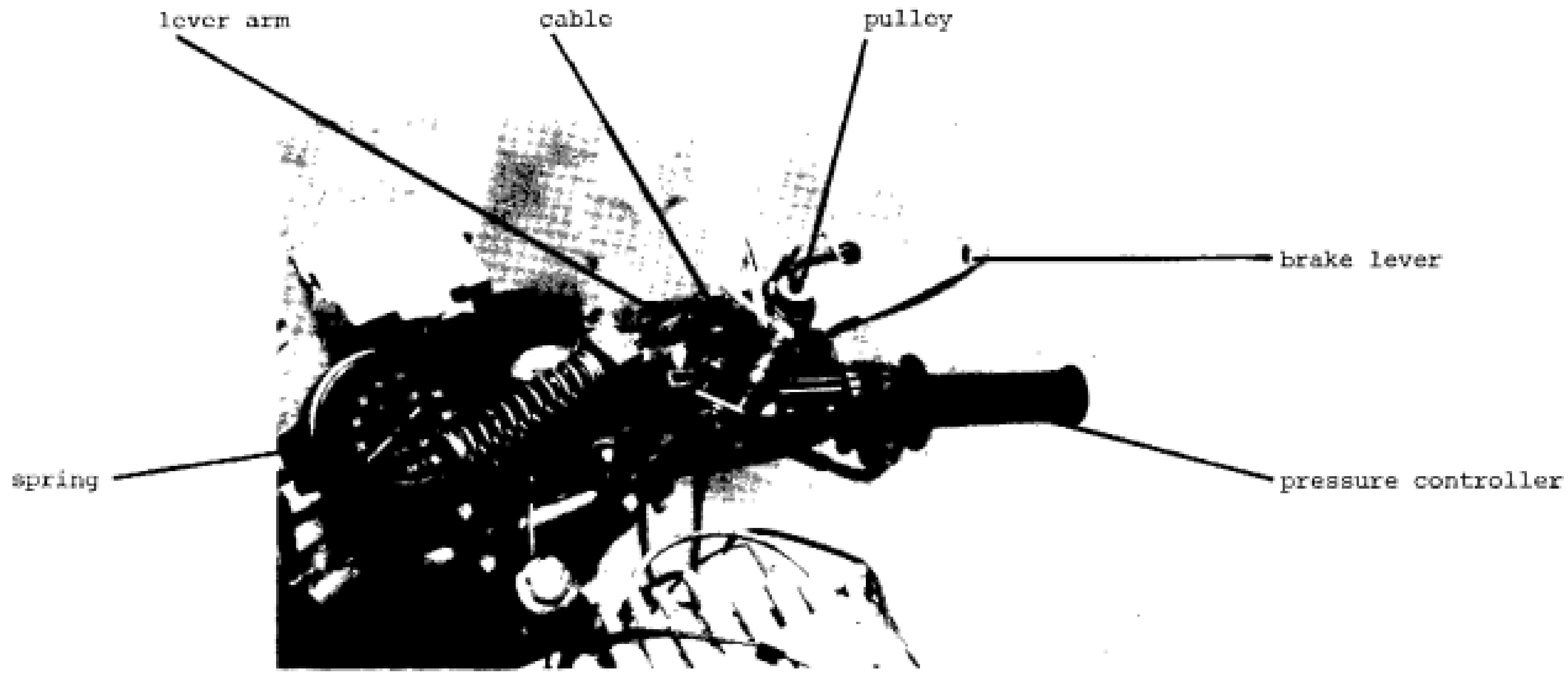

Figure D.6 VBCG front brake lever assembly pressure warning system was designed and fitted. A loud siren was triggered when 50 brake applications were left in the reservoir. To stop the siren, either the ignition had to be switched off, or the reservoir recharged. A meter to monitor reservoir pressure was mounted on the motorcycle instrument panel, thus enabling the rider to observe the quantity of air left in the receiver.

3.2.4 Realization Of Displacement Gradients

As was indicated in Figure D.1, the plunger of the pressure controller was to be actuated by the brake control lever. In order to provide a linear relationship between the control lever movement and the displacement of the plunger, a cable and pulley scheme was employed, as shown in Figure D.6. To obtain a particular displacement gradient, proper selection of the pulley diameter is required. This can really only be established by experiment. However, it was found that a plunger displacement of 3.65mm for the front and 2.8mm for the rear brake caused the respective wheels to lock. On this basis approximate displacement gradients may be readily established. Relative displacement gradients can be simply determined; e.g. doubling the pulley diameter will exactly halve the displacement gradient.

D.2.5 Realization Of Force Gradients

The force required to depress the pressure controller plunger sufficient to cause wheel lock is quite small, being approximately 50N for the rear wheel controller and 75N for the front. These values correspond to extremely small force/deceleration control gradients, and the motorcycle was found to be unmanageable when decelerating with these settings.

In order to increase the force requirements, a system of springs and levers was designed. Figure D.6 shows the arrangement employed for the front brake. By addition of

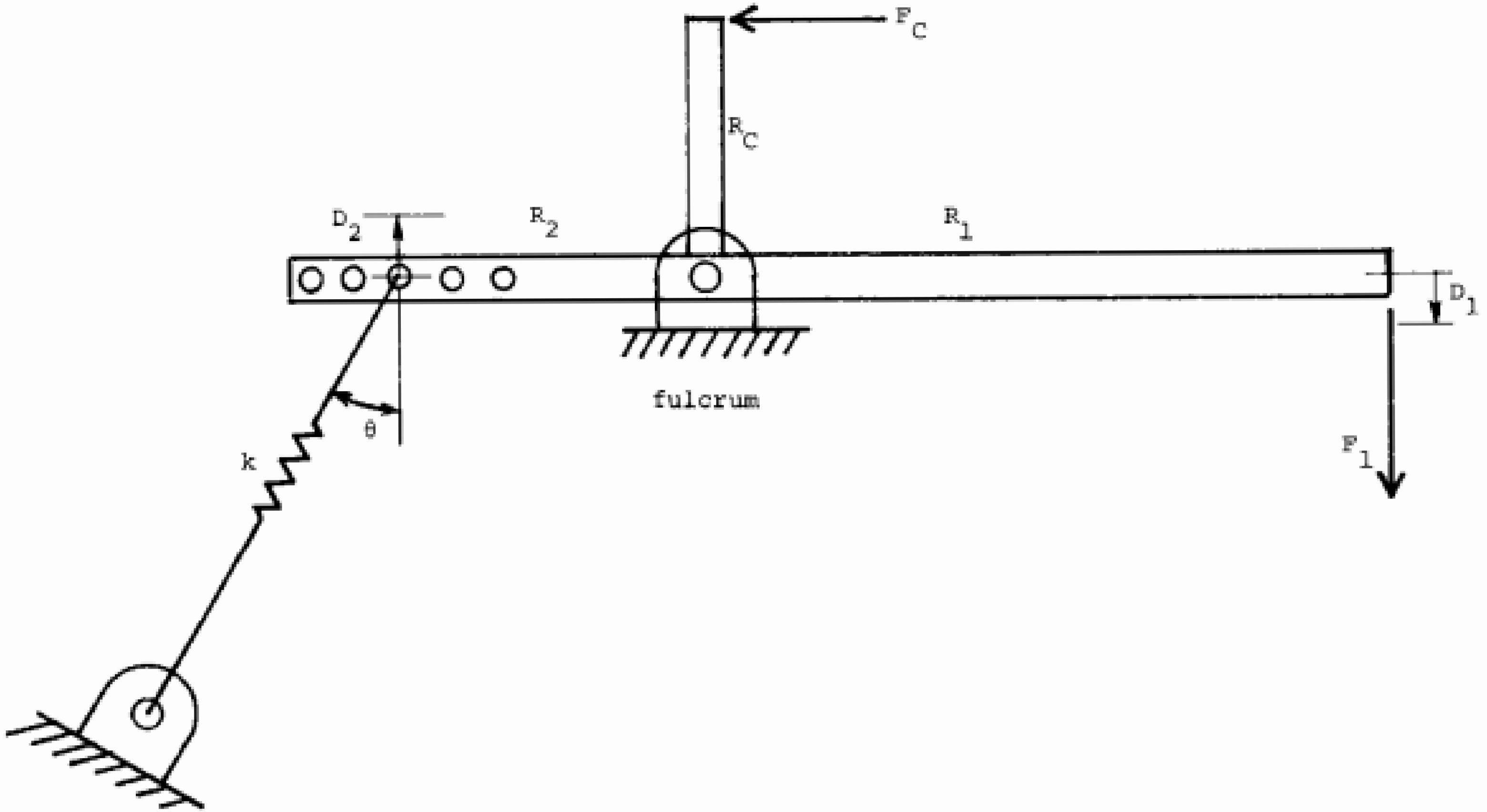

Figure D.7 Symbolic representation of variable force mechanism.

Figure D.8 VBCG rear brake lever assembly.

suitably designed springs, any desired force/deceleration gradient could be obtained. With reference to Figure D.7, two variables are available to obtain the desired control gradient setting: the spring stiffness, , and the radius from the fulcrum at which the spring control rod clevis is attached, . The following relationship exists:

$$F = k \cos^2\theta \; D_1 (R_2/R_1)^2 + F_C \; R_C/R_1 \qquad (D.1)$$

where: F = force at (rider input force)

k = spring constant

D_1 = displacement of control lever, at

R_1 = radius at which rider applies brake force

R_2 = radius at which spring clevis is attached

F_C = pressure controller force to lock wheel

= 75N front

= 50N rear

R_C = radius of pressure controller actuating pulley

θ = inclination angle of spring

Equation D.1 may be used to design for any desired force gradient, having first selected a displacement gradient. The latter will determine D_1, and R_C. Any relative force gradient may then be determined, but the actual value will require field calibration for verification (as mentioned in Section D.2.4 for the displacement gradients).

A similar configuration was employed on the rear brake. A photograph of the arrangement is given in Figure D.8.

D.2.6 Control Lever Fulcrum Considerations

The standard front brake lever and its mount incorporates an integral master cylinder. In order to accommodate the pressure controller, its actuating cable and pulley, and the spring lever system for obtaining force gradient, it was necessary to completely redesign the front hand control assembly. The redesigned lever employed a low friction ball bearing fulcrum, which minimized force hysteresis. The rear brake lever was used in its standard form, with a plain bearing of 19mm diameter as its fulcrum. It is thought that this bearing is the main cause of the high level of force hysteresis in the rear brake. For any future system, it would be desirable to use low friction ball bearing fulcrum pins in order to minimize force hysteresis.

APPENDIX E

VBCG RSM EXPERIMENTAL RESULTS

The tables in this appendix include the data for the two subjects obtained from the experiments with the VBCG motorcycle, followed by the results of SPSS multiple regression analysis of the data.

TABLE E.1
DATA FROM VBCG EXPERIMENTS
SUBJECT: RDH

	MEASURE (1)												
CONFIGURATION	AVAC1 m/s^2	AVAC2 m/s^2	F m/s^2	R m/s^2	OS m	TR ms	FBFR	FBDR	RBFR	RBDR	NSR	QSR	OMCR
1.1	-	-	-	-	2.2	394	32	32	57	56	56	28	8
1.2	6.20	6.27	3.67	3.93	2.4	425	67	75	67	63	71	56	49
1.3	4.61	4.83	2.74	1.78	1.8	-	43	38	50	64	56	46	20
1.4	6.83	6.83	4.73	2.02	1.1	363	32	29	63	67	50	42	15
1.5	6.38	6.26	4.01	1.43	2.1	394	67	82	60	61	89	77	58
1.6	7.07	6.70	5.92	1.91	0	331	82	32	71	53	75	73	42
1.7	6.81	6.96	6.02	1.44	-0.2	456	31	33	44	38	50	41	20
1.8	6.31	6.78	3.69	2.50	2.2	425	63	31	42	35	52	25	7
1.9	6.61	6.56	4.18	1.51	0.8	-	72	43	64	64	75	60	51
1.10	5.04	6.75	4.37	2.26	0.1	-	57	32	60	64	55	54	29
2.1	6.48	6.60	3.71	2.40	2.0	425	32	31	39	40	56	39	10
2.2	6.81	6.65	5.01	1.36	1.5	456	68	47	44	33	60	56	34
2.3	6.70	6.75	5.73	2.37	1.1	456	31	32	63	46	51	36	8
2.4	5.27	5.82	3.67	2.25	0.4	394	75	72	58	46	73	56	47
2.5	4.72	4.54	2.71	0.48	-0.4	394	31	35	63	56	49	32	7
2.6	6.23	6.09	3.58	1.04	-0.3	456	56	50	33	31	49	49	20
2.7	5.96	5.41	4.97	1.53	1.0	394	39	42	63	63	61	61	31
2.8	6.73	6.87	3.94	1.23	0	425	54	39	35	31	69	61	37
2.9	6.26	6.53	4.43	1.34	-0.4	394	65	65	65	65	75	63	61
2.10	5.64	5.82	3.79	2.54	1.8	425	71	32	63	42	51	34	15
3.1	5.66	5.72	4.27	1.98	2.8	425	42	38	63	42	75	72	27
3.2	6.90	7.04	6.54	1.09	1.7	362	31	36	58	39	55	42	19
3.3	5.69	5.69	3.16	1.95	1.7	362	31	38	61	51	52	32	24
3.4	7.06	7.22	5.50	1.33	-0.8	425	32	56	63	64	61	60	32
3.5	6.50	6.57	4.17	1.68	-0.2	394	78	74	65	43	80	71	56
3.6	6.52	6.56	3.99	2.29	1.0	394	69	53	79	74	75	75	56
3.7	5.49	6.53	3.88	0.80	1.0	-	39	40	60	46	60	37	20
3.8	5.39	5.71	3.36	3.68	2.0	-	38	32	39	42	50	42	14
3.9	6.63	6.67	4.18	2.56	2.3	425	63	74	68	69	62	64	47
3.10	6.63	6.83	4.44	2.86	1.4	-	35	32	38	42	56	41	10

TABLE E.2
DATA FROM VBCG EXPERIMENTS
SUBJECT: BG

	MEASURE (1)												
CONFIGURATION	AVAC1 m/s^2	AVAC2 m/s^2	F m/s^2	R m/s^2	OS m	TR ms	FBFR	FBDR	RBFR	RBDR	NSR	QSR	OMCR
1.1	5.71	5.64	2.30	3.01	3.6	331	12	21	40	21	30	5	0
1.2	6.06	6.05	3.10	1.62	0.6	394	74	73	29	40	74	50	41
1.3	6.59	6.48	4.36	1.71	1.6	488	66	66	52	63	75	68	49
1.4	5.43	5.41	2.28	1.39	0.1	363	92	86	62	75	93	93	86
1.5	6.57	6.61	3.32	1.95	1.3	363	62	41	30	41	46	34	24
1.6	4.70	4.52	2.25	1.59	-0.4	300	73	55	62	41	24	73	83
1.7	5.75	5.88	3.31	1.08	-0.2	456	64	60	75	75	68	75	61
1.8	6.29	6.30	2.50	2.04	0	456	90	90	40	55	94	90	92
1.9	6.72	6.82	3.92	1.94	0.8	363	58	77	63	78	75	76	73
1.10	6.73	6.89	3.48	2.35	-0.2	394	55	67	55	63	89	60	64
2.1	6.90	7.01	3.57	2.84	1.1	331	56	78	47	78	75	25	51
2.2	6.04	6.04	3.19	2.12	1.2	269	53	62	23	30	40	25	25
2.3	5.39	5.38	2.86	1.28	-0.4	331	90	90	88	88	98	94	92
2.4	6.47	6.34	3.58	1.98	-0.2	363	82	78	52	68	79	80	76
2.5	6.91	6.95	4.94	1.60	0.4	300	79	90	62	62	93	85	83
2.6	7.00	7.06	4.08	2.79	0.8	456	26	25	30	29	47	26	15
2.7	5.92	5.84	4.24	1.42	0	456	70	79	62	67	71	77	47
2.8	6.10	6.09	2.22	1.36	0.8	425	62	36	74	36	84	81	85
2.9	5.98	5.70	3.48	1.33	-0.3	425	77	60	40	49	93	79	78
2.10	5.73	5.69	3.67	2.19	0.8	394	52	75	30	32	84	18	32
3.1	6.43	6.39	3.68	1.90	1.1	394	90	90	78	62	93	75	59
3.2	5.04	5.33	1.95	1.48	1.3	331	45	56	23	55	22	17	
3.3	5.76	5.63	2.62	0.81	0.4	331	47	41	47	62	93	72	66
3.4	5.29	5.41	3.47	0	1.9	394	38	62	40	42	55	18	29
3.5	6.68	6.67	3.71	2.04	1.2	363	37	40	45	41	63	52	39
3.6	4.74	4.70	1.40	2.28	0	394	62	37	25	23	28	23	27
3.7	6.40	6.39	3.59	1.64	0.1	456	41	41	63	63	75	55	25
3.8	5.00	4.63	2.42	2.81	4.0	269	40	55	7	23	24	3	0
3.9	6.17	6.42	2.92	2.30	1.1	331	74	90	38	62	91	56	64
3.10	6.34	6.34	3.02	2.45	0.2	394	90	81	74	71	86	87	78

NOTES: (1) Explanation of abbreviations used for MEASURE

AVAC1 = average deceleration in quick stop, from accelerometer, m/s^2

AVAC2 = average deceleration in quick stop, calculated from speed record, m/s^2

F = average deceleration in quick stop from front brake, m/s^2

R = average deceleration in quick stop from rear brake, m/s^2

OS = overshoot of motorcycle beyond stopping line in quick stop, m

TR = reaction time to apply brakes in quick stop, ms

FBFR = front brake force rating

FBDR = front brake displacement rating

RBFR = rear brake force rating

RBDR = rear brake displacement rating

NSR = normal stop rating

QSR = quick stop rating

OMCR = own motorcycle comparison rating

The tables which follow show the results from SPSS multiple regression analysis of the data presented in Tables E.1 and E.2. The complete second order RSM model has been analyzed, which is as below:

$$
\begin{aligned}
Y = b_o &+ b_1\,FBD + b_2\,FBF + b_3\,RBD + b_4\,RBF \\
&+ b_{11}(FBD)^2 + b_{22}(FBF)^2 + b_{33}(RBD)^2 + b_{44}(RBF)^2 \\
&+ b_{12}\,FBD.FBF + b_{13}\,FBD.RBD + b_{14}\,FBD.RBF \\
&+ b_{23}\,FBF.RBD + b_{24}\,FBF.RBF \\
&+ b_{34}\,RBD.RBF
\end{aligned}
$$

where: Y = dependent variable (or MEASURE)

FBD = normalized front brake displacement gradient

FBF = normalized front brake force gradient

FBD = normalized rear brake displacement gradient

RBF = normalized rear brake force gradient

The value of each coefficient (b_{ij}) is tabulated, and their 'significances' are included. This is the probability of the null hypothesis $H_o : b_{ij} = 0$. The order in which each independent variable was stepwise entered into the regression equation (on the basis of the significance of an F ratio test) is also given, together with the resulting r^2 change when that particular variable was entered. The overall r^2 value is given, which indicates, the amount of variation in Y explained by the variation of all the independent variables in the equation. The overall significance of the regression is also given, which is the probability of the null hypothesis $Ho : b_1 = b_2 = . . . = b_{44} = 0$

TABLE E.3

RESULTS OF SPSS MULTIPLE REGRESSION ANALYSIS

MEASURE: AVERAGE DECELERATION IN QUICK STOP FROM SPEED TRACE (AVAC2, m/s^2)

SUBJECT: RDH SIGNIFICANCE OF REGRESSION: 0.183 r SQUARE: 0.621

Coefficient	Independent Variable	Value of Coefficient	Significance	Entered On Step Number	r Square Change
b_0	Constant	6.68			
b_1	FBD	-0.41	.007	1	.122
b_2	FBF	0.11	.369	8	.029
b_3	RBD	0.04	.785	13	.002
b_4	RBF	0.08	.536	12	.009
b_{11}	$(FBD)^2$	-0.11	.366	6	.037
b_{22}	$(FBF)^2$	-0.11	.144	4	.065
b_{33}	$(RBD)^2$	0.08	.542	11	.008
b_{44}	$(RBF)^2$	-0.14	.225	3	.067
b_{12}	FBD.FBF	-0.02	.916	14	.000
b_{13}	FBD.RBD	-0.34	.090	2	.149
b_{14}	FBD.RBF	0.11	.499	10	.014
b_{23}	FBF.RBD	0.20	.308	7	.031
b_{24}	FBF.RBF	0.22	.201	5	.073
b_{34}	RBD.RBF	0.21	.298	9	.017

TABLE E.4

RESULTS OF SPSS MULTIPLE REGRESSION ANALYSIS

MEASURE: FRONT BRAKE DECELERATION IN QUICK STOP (F, m/s^2)

SUBJECT: RDH SIGNIFICANCE OF REGRESSION: 0.121 r SQUARE: 0.62

Coefficient	Independent Variable	Value of Coefficient	Significance	Entered On Step Number	r Square Change
b_0	Constant	4.48			
b_1	FBD	-0.48	.019	1	.303
b_2	FBF	-0.18	.302	5	.038
b_3	RBD	0.22	.319	8	.014
b_4	RBF	0.15	.423	9	.016
b_{11}	$(FBD)^2$	0.18	.264	2	.078
b_{22}	$(FBF)^2$	-0.69	.510	7	.021
b_{33}	$(RBD)^2$	0.03	.870	13	.001
b_{44}	$(RBF)^2$	-0.19	.188	4	.049
b_{12}	FBD.FBF	-0.17	.485	10	.014
b_{13}	FBD.RBD	0.11	.674	11	.005
b_{14}	FBD.RBF	0.25	.292	3	.056
b_{23}	FBF.RBD	-0.38	.170	6	.025
b_{24}	FBF.RBF	-0.04	0.850	12	.001
b_{34}	RBD.RBF	-			

TABLE E.5

RESULTS OF SPSS MULTIPLE REGRESSION ANALYSIS

MEASURE: REAR BRAKE DECELERATION IN QUICK STOP (R, m/s^2)

SUBJECT: RDH SIGNIFICANCE OF REGRESSION: 0.115 r SQUARE: 0.659

Coefficient	Independent Variable	Value of Coefficient	Significance	Entered On Step Number	r Square Change
b_0	Constant	2.04	-		
b_1	FBD	0.16	.303	2	.091
b_2	FBF	0.20	.167	5	.032
b_3	RBD	-0.13	.459	4	.040
b_4	RBF	-0.46	.010	1	.334
b_{11}	$(FBD)^2$	-0.11	.409	8	.019
b_{22}	$(FBF)^2$	-0.09	.303	7	.020
b_{33}	$(RBD)^2$	-0.02	.885	14	.001
b_{44}	$(RBF)^2$	0.02	.856	13	.001
b_{12}	FBD.FBF	0.18	.359	6	.029
b_{13}	FBD.RBD	-0.17	.430	9	.010
b_{14}	FBD.RBF	-0.13	.515	10	.013
b_{23}	FBF.RBD	-0.12	.606	11	.004
b_{24}	FBF.RBF	-0.07	.710	12	.003
b_{34}	RBD.RBF	0.16	.487	3	.062

TABLE E.6

RESULTS OF SPSS MULTIPLE REGRESSION ANALYSIS

MEASURE: OVERSHOOT IN QUICK STOP (OS, m)

SUBJECT: RDH SIGNIFICANCE OF REGRESSION: 0.255 r SQUARE: 0.552

Coefficient	Independent Variable	Value of Coefficient	Significance	Entered On Step Number	r Square Change
b_0	Constant	0.59	-		
b_1	FBD	0.37	.102	2	.112
b_2	FBF	0.16	.439	4	.041
b_3	RBD	-0.26	.302	6	.033
b_4	RBF	-0.36	.120	5	.037
b_{11}	$(FBD)^2$	0.41	.046	3	.107
b_{22}	$(FBF)^2$	-0.06	.635	10	.006
b_{33}	$(RBD)^2$	-			
b_{44}	$(RBF)^2$	0.18	.324	8	.027
b_{12}	FBD.FBF	-0.15	.587	9	.010
b_{13}	FBD.RBD	0.05	.864	13	.001
b_{14}	FBD.RBF	0.25	.380	7	.032
b_{23}	FBF.RBD	0.11	.736	11	.002
b_{24}	FBF.RBF	0.08	.770	12	.003
b_{34}	RBD.RBF	0.43	.130	1	.140

TABLE E.7

RESULTS OF SPSS MULTIPLE REGRESSION ANALYSIS

MEASURE: REACTION TIME IN QUICK STOP (TR, ms)

SUBJECT: RDH SIGNIFICANCE OF REGRESSION: 0.551 r SQUARE: 0.596

Coefficient	Independent Variable	Value of Coefficient	Significance	Entered On Step Number	r Square Change
b_0	Constant	416.6	-		
b_1	FBD	2.79	.762	13	.004
b_2	FBF	-6.88	.451	6	.017
b_3	RBD	3.09	.724	10	.004
b_4	RBF	4.49	.676	9	.007
b_{11}	$(FBD)^2$	-3.47	.657	7	.018
b_{22}	$(FBF)^2$	-4.63	.347	4	.096
b_{33}	$(RBD)^2$	2.51	.764	11	.003
b_{44}	$(RBF)^2$	-5.04	.791	8	.007
b_{12}	FBD.FBF	19.50	.096	1	.150
b_{13}	FBD.RBD	-10.22	.385	2	.141
b_{14}	FBD.RBF	7.22	.517	5	.042
b_{23}	FBF.RBD	-1.40	.903	14	.001
b_{24}	FBF.RBF	3.17	.785	12	.003
b_{34}	RBD.RBF	11.40	.519	3	.106

TABLE E.8

RESULTS OF SPSS MULTIPLE REGRESSION ANALYSIS

MEASURE: FRONT BRAKE FORCE RATING (FBFR)

SUBJECT: RDH SIGNIFICANCE OF REGRESSION: 0.095 r SQUARE: 0.673

Coefficient	Independent Variable	Value of Coefficient	Significance	Entered On Step Number	r Square Change
b_0	Constant	58.07	-		
b_1	FBD	1.48	.658	11	.003
b_2	FBF	8.27	.018	2	.124
b_3	RBD	-1.91	.617	8	.024
b_4	RBF	2.05	.551	10	.005
b_{11}	$(FBD)^2$	-4.95	.110	4	.049
b_{22}	$(FBF)^2$	-6.08	.005	3	.185
b_{33}	$(RBD)^2$	3.10	.341	1	.160
b_{44}	$(RBF)^2$	-4.64	.111	6	.023
b_{12}	FBD.FBF	3.39	.433	9	.027
b_{13}	FBD.RBD	4.50	.354	5	.024
b_{14}	FBD.RBF	-1.04	.806	12	.003
b_{23}	FBF.RBD	-2.57	.606	13	.003
b_{24}	FBF.RBF	-1.83	.659	14	.005
b_{34}	RBD.RBF	-6.22	.221	7	.040

TABLE E.9

RESULTS OF SPSS MULTIPLE REGRESSION ANALYSIS

MEASURE: FRONT BRAKE DISPLACEMENT RATING (FBDR)

SUBJECT: RDH SIGNIFICANCE OF REGRESSION: 0.712 r SQUARE: 0.424

Coefficient	Independent Variable	Value of Coefficient	Significance	Entered On Step Number	r Square Change
b_0	Constant	45.36	-		
b_1	FBD	5.02	.233	2	.109
b_2	FBF	2.43	.531	11	.012
b_3	RBD	-0.44	.925	8	.011
b_4	RBF	1.11	.792	14	.003
b_{11}	$(FBD)^2$	-2.36	.519	7	.016
b_{22}	$(FBF)^2$	-0.97	.673	12	.007
b_{33}	$(RBD)^2$	2.59	.514	1	.145
b_{44}	$(RBF)^2$	-2.60	.453	6	.016
b_{12}	FBD.FBF	-2.47	.641	9	.009
b_{13}	FBD.RBD	-2.87	.627	10	.009
b_{14}	FBD.RBF	2.12	.685	4	.021
b_{23}	FBF.RBD	-2.17	.723	13	.004
b_{24}	FBF.RBF	-7.36	.161	3	.047
b_{34}	RBD.RBF	-6.57	.289	5	.015

TABLE E.10

RESULTS OF SPSS MULTIPLE REGRESSION ANALYSIS

MEASURE: REAR BRAKE FORCE RATING (RBFR)

SUBJECT: RDH SIGNIFICANCE OF REGRESSION: 0.733 r SQUARE: 0.273

Coefficient	Independent Variable	Value of Coefficient	Significance	Entered On Step Number	r Square Change
b_0	Constant	57.22	-		
b_1	FBD	0.57	.850	8	.002
b_2	FBF	0.33	.903	11	.001
b_3	RBD	-1.60	.609	3	.032
b_4	RBF	-			
b_{11}	$(FBD)^2$	-0.86	.742	7	.007
b_{22}	$(FBF)^2$	-			
b_{33}	$(RBD)^2$	-			
b_{44}	$(RBF)^2$	-3.39	.175	2	.077
b_{12}	FBD.FBF	-0.79	.829	9	.002
b_{13}	FBD.RBD	3.27	.457	5	.031
b_{14}	FBD.RBF	0.48	.903	10	.001
b_{23}	FBF.RBD	-4.97	.274	4	.018
b_{24}	FBF.RBF	-2.73	.454	6	.021
b_{34}	RBD.RBF	-8.03	.048	1	.082

TABLE E.11

RESULTS OF SPSS MULTIPLE REGRESSION ANALYSIS

MEASURE: REAR BRAKE DISPLACEMENT RATING (RBDR)

SUBJECT: RDH SIGNIFICANCE OF REGRESSION: 0.344 r SQUARE: 0.479

Coefficient	Independent Variable	Value of Coefficient	Significance	Entered On Step Number	r Square Change
b_0	Constant	58.83	-		
b_1	FBD	2.93	.309	9	.026
b_2	FBF	-2.25	.379	10	.024
b_3	RBD	-1.71	.602	3	.027
b_4	RBF	-0.97	.742	11	.003
b_{11}	$(FBD)^2$	-5.32	.046	1	.109
b_{22}	$(FBF)^2$	-			
b_{33}	$(RBD)^2$	-2.99	.278	8	.040
b_{44}	$(RBF)^2$	-3.84	.117	4	.030
b_{12}	FBD.FBF	-5.44	.131	2	.042
b_{13}	FBD.RBD	1.01	.791	12	.002
b_{14}	FBD.RBF	-			
b_{23}	FBF.RBD	-7.12	.110	6	.031
b_{24}	FBF.RBF	-5.16	.145	7	.084
b_{34}	RBD.RBF	-9.14	.042	5	.060

TABLE E.12

RESULTS OF SPSS MULTIPLE REGRESSION ANALYSIS

MEASURE: NORMAL STOP RATING (NSR)

SUBJECT: RDH SIGNIFICANCE OF REGRESSION: 0.475 r SQUARE: 0.471

Coefficient	Independent Variable	Value of Coefficient	Significance	Entered On Step Number	r Square Change
b_0	Constant	61.17	-		
b_1	FBD	3.61	.180	2	.082
b_2	FBF	2.17	.381	7	.021
b_3	RBD	-			
b_4	RBF	2.60	.290	4	.033
b_{11}	$(FBD)^2$	0.36	.875	12	.001
b_{22}	$(FBF)^2$	-1.63	.275	6	.019
b_{33}	$(RBD)^2$	2.55	.319	1	.155
b_{44}	$(RBF)^2$	-2.02	.362	8	.015
b_{12}	FBD.FBF	-3.43	.307	3	.059
b_{13}	FBD.RBD	-2.44	.516	10	.015
b_{14}	FBD.RBF	-1.56	.639	11	.009
b_{23}	FBF.RBD	-1.35	.713	12	.005
b_{24}	FBF.RBF	-3.23	.311	5	.033
b_{34}	RBD.RBF	-3.91	.322	9	.026

TABLE E.13

RESULTS OF SPSS MULTIPLE REGRESSION ANALYSIS

MEASURE: QUICK STOP RATING (QSR)

SUBJECT: RDH SIGNIFICANCE OF REGRESSION: 0.122 r SQUARE: 0.583

Coefficient	Independent Variable	Value of Coefficient	Significance	Entered On Step Number	r Square Change
b_0	Constant	52.86	-		
b_1	FBD	4.22	.156	6	.040
b_2	FBF	1.17	.671	11	.004
b_3	RBD	-0.01	.998	4	.044
b_4	RBF	3.11	.308	10	.026
b_{11}	$(FBD)^2$	-			
b_{22}	$(FBF)^2$	-2.83	.091	2	.104
b_{33}	$(RBD)^2$	3.25	.248	1	.144
b_{44}	$(RBF)^2$	-3.91	.116	3	.043
b_{12}	FBD.FBF	-6.09	.118	7	.032
b_{13}	FBD.RBD	-1.31	.734	12	.003
b_{14}	FBD.RBF	-			
b_{23}	FBF.RBD	-8.01	.080	8	.031
b_{24}	FBF.RBF	-6.72	.068	9	.075
b_{34}	RBD.RBF	-7.24	.106	5	.038

TABLE E.14

RESULTS OF SPSS MULTIPLE REGRESSION ANALYSIS

MEASURE: OWN MOTORCYCLE COMPARISON RATING (OMCR)

SUBJECT: RDH SIGNIFICANCE OF REGRESSION: 0.477 r SQUARE: 0.508

Coefficient	Independent Variable	Value of Coefficient	Significance	Entered On Step Number	r Square Change
b_0	Constant	33.26	-		
b_1	FBD	2.64	.512	11	.019
b_2	FBF	4.89	.205	2	.050
b_3	RBD	0.87	.848	14	.001
b_4	RBF	3.76	.365	7	.037
b_{11}	$(FBD)^2$	-3.68	.307	5	.036
b_{22}	$(FBF)^2$	-2.51	.271	3	.038
b_{33}	$(RBD)^2$	3.52	.365	1	.144
b_{44}	$(RBF)^2$	-4.80	.164	4	.040
b_{12}	FBD.FBF	-5.54	.289	10	.031
b_{13}	FBD.RBD	-2.29	.690	12	.004
b_{14}	FBD.RBF	-1.26	.804	13	.002
b_{23}	FBF.RBD	-7.70	.209	8	.032
b_{24}	FBF.RBF	-8.01	.120	6	.032
b_{34}	RBD.RBF	-7.10	.241	9	.041

TABLE E.15

RESULTS OF SPSS MULTIPLE REGRESSION ANALYSIS

MEASURE: AVERAGE DECELERATION IN QUICK STOP FROM SPEED TRACE (AVAC2, m/s^2)

SUBJECT: BG SIGNIFICANCE OF REGRESSION: 0.456 r SQUARE: 0.461

Coefficient	Independent Variable	Value of Coefficient	Significance	Entered On Step Number	r Square Change
b_0	Constant	6.19	-		
b_1	FBD	0.28	.075	1	.167
b_2	FBF	-			
b_3	RBD	0.08	.642	6	.014
b_4	RBF	0.19	.239	3	.061
b_{11}	$(FBD)^2$	-0.02	.872	13	.001
b_{22}	$(FBF)^2$	-0.05	.575	9	.007
b_{33}	$(RBD)^2$	-0.08	.591	11	.004
b_{44}	$(RBF)^2$	-0.12	.364	5	.014
b_{12}	FBD.FBF	0.13	.471	7	.010
b_{13}	FBD.RBD	-0.22	.323	4	.035
b_{14}	FBD.RBF	-0.07	.723	12	.004
b_{23}	FBF.RBD	0.41	.053	2	.125
b_{24}	FBF.RBF	0.11	.529	8	.010
b_{34}	RBD.RBF	-0.13	.562	10	.004

TABLE E.16

RESULTS OF SPSS MULTIPLE REGRESSION ANALYSIS

MEASURE: FRONT BRAKE DECELERATION IN QUICK STOP (F, m/s^2)

SUBJECT: BG SIGNIFICANCE OF REGRESSION: 0.152 r SQUARE: 0.547

Coefficient	Independent Variable	Value of Coefficient	Significance	Entered On Step Number	r Square Change
b_0	Constant	3.41	-		
b_1	FBD	0.48	.006	1	.170
b_2	FBF	-0.29	.040	2	.141
b_3	RBD	0.14	.383	8	.011
b_4	RBF	0.14	.387	9	.021
b_{11}	$(FBD)^2$	-0.10	.498	7	.012
b_{22}	$(FBF)^2$	-			
b_{33}	$(RBD)^2$	-0.20	.183	4	.042
b_{44}	$(RBF)^2$	-0.55	.681	12	.005
b_{12}	FBD.FBF	0.88	.612	10	.007
b_{13}	FBD.RBD	0.19	.356	5	.043
b_{14}	FBD.RBF	-0.87	.662	11	.005
b_{23}	FBF.RBD	-			
b_{24}	FBF.RBF	-0.10	.557	6	.015
b_{34}	RBD.RBF	-0.34	.142	3	.076

TABLE E.17

RESULTS OF SPSS MULTIPLE REGRESSION ANALYSIS

MEASURE: REAR BRAKE DECELERATION IN QUICK STOP (R, m/s^2)

SUBJECT: BG SIGNIFICANCE OF REGRESSION: 0.205 r SQUARE: 0.591

Coefficient	Independent Variable	Value of Coefficient	Significance	Entered On Step Number	r Square Change
b_0	Constant	1.79	-		
b_1	FBD	0.08	.546	9	.012
b_2	FBF	0.19	.122	4	.056
b_3	RBD	-0.34	.025	2	.094
b_4	RBF	-0.20	.143	3	.077
b_{11}	$(FBD)^2$	-0.02	.839	14	.001
b_{22}	$(FBF)^2$	-0.18	.029	1	.120
b_{33}	$(RBD)^2$	0.11	.383	8	.012
b_{44}	$(RBF)^2$	0.09	.448	10	.008
b_{12}	FBD.FBF	0.22	.172	5	.076
b_{13}	FBD.RBD	0.04	.823	13	.001
b_{14}	FBD.RBF	0.06	.7144	12	.003
b_{23}	FBF.RBD	0.24	.169	6	.074
b_{24}	FBF.RBF	0.14	.336	7	.042
b_{34}	RBD.RBF	0.13	.487	11	.015

TABLE E.18

RESULTS OF SPSS MULTIPLE REGRESSION ANALYSIS

MEASURE: OVERSHOOT IN QUICK STOP (OS, m)

SUBJECT: MG SIGNIFICANCE OF REGRESSION: 0.227 r SQUARE: 0.546

Coefficient	Independent Variable	Value of Coefficient	Significance	Entered On Step Number	r Square Change
b_0	Constant	0.40	-		
b_1	FBD	0.09	.668	11	.004
b_2	FBF	-0.12	.537	9	.010
b_3	RBD	-0.39	.099	3	.136
b_4	RBF	-0.51	.029	1	.142
b_{11}	$(FBD)^2$	0.12	.544	10	.007
b_{22}	$(FBF)^2$	0.12	.342	8	.012
b_{33}	$(RBD)^2$	0.08	.698	12	.004
b_{44}	$(RBF)^2$	0.34	.078	4	.035
b_{12}	FBD.FBF	-0.28	.299	6	.014
b_{13}	FBD.RBD	0.04	.887	13	.001
b_{14}	FBD.RBF	0.15	.534	7	.012
b_{23}	FBF.RBD	0.50	.072	2	.097
b_{24}	FBF.RBF	-			
b_{34}	RBD.RBF	0.47	.138	5	.072

TABLE E.19

RESULTS OF SPSS MULTIPLE REGRESSION ANALYSIS

MEASURE: REACTION TIME IN QUICK STOP (TR, ms)

SUBJECT: BG SIGNIFICANCE OF REGRESSION: 0.027 r SQUARE: 0.726

Coefficient	Independent Variable	Value of Coefficient	Significance	Entered On Step Number	r Square Change
b_0	Constant	394.7	-		
b_1	FBD	27.44	.012	1	.174
b_2	FBF	-11.62	.206	5	.048
b_3	RBD	38.23	.002	2	.109
b_4	RBF	32.03	.008	3	.198
b_{11}	$(FBD)^2$	-4.41	.617	12	.005
b_{22}	$(FBF)^2$	-5.18	.353	8	.013
b_{33}	$(RBD)^2$	3.41	.717	9	.007
b_{44}	$(RBF)^2$	-4.82	.563	11	.004
b_{12}	FBD.FBF	2.79	.812	14	.001
b_{13}	FBD.RBD	-3.96	.771	13	.002
b_{14}	FBD.RBF	-6.86	.577	10	.004
b_{23}	FBF.RBD	-19.96	.125	4	.108
b_{24}	FBF.RBF	15.64	.166	6	.031
b_{34}	RBD.RBF	11.22	.418	7	.022

TABLE E.20

RESULTS OF SPSS MULTIPLE REGRESSION ANALYSIS

MEASURE: FRONT BRAKE FORCE RATING (FBFR)

SUBJECT: BG SIGNIFICANCE OF REGRESSION: 0.604 r SQUARE: 0.411

Coefficient	Independent Variable	Value of Coefficient	Significance	Entered On Step Number	r Square Change
b_0	Constant	72.37	-		
b_1	FBD	2.49	.610	9	.011
b_2	FBF	0.84	.851	12	.001
b_3	RBD	5.47	.253	2	.062
b_4	RBF	-			
b_{11}	$(FBD)^2$	1.67	.703	10	.005
b_{22}	$(FBF)^2$	-4.04	.152	3	.045
b_{33}	$(RBD)^2$	-7.95	.095	1	.047
b_{44}	$(RBF)^2$	-5.74	.175	5	.037
b_{12}	FBD.FBF	7.14	.231	4	.042
b_{13}	FBD.RBD	-0.75	.912	12	.001
b_{14}	FBD.RBF	-2.01	.742	11	.004
b_{23}	FBF.RBD	-5.74	.361	8	.051
b_{24}	FBF.RBF	-5.41	.322	7	.033
b_{34}	RBD.RBF	-9.30	.165	6	.072

TABLE E.21

RESULTS OF SPSS MULTIPLE REGRESSION ANALYSIS

MEASURE: FRONT BRAKE DISPLACEMENT RATING (FBDR)

SUBJECT: BG SIGNIFICANCE OF REGRESSION: 0.334 r SQUARE: 0.503

Coefficient	Independent Variable	Value of Coefficient	Significance	Entered On Step Number	r Square Change
b_0	Constant	79.89	-		
b_1	FBD	4.50	.319	9	.022
b_2	FBF	-1.65	.689	11	.004
b_3	RBD	4.13	.384	3	.070
b_4	RBF	-4.03	.377	8	.025
b_{11}	$(FBD)^2$	-			
b_{22}	$(FBF)^2$	-3.66	.155	5	.055
b_{33}	$(RBD)^2$	-11.64	.013	1	.126
b_{44}	$(RBF)^2$	-6.22	.111	4	.044
b_{12}	FBD.FBF	6.04	.274	6	.044
b_{13}	FBD.RBD	2.80	.657	10	.007
b_{14}	FBD.RBF	-1.17	.837	13	.001
b_{23}	FBF.RBD	-1.44	.803	12	.003
b_{24}	FBF.RBF	-4.88	.340	2	.074
b_{34}	RBD.RBF	-7.34	.254	7	.028

TABLE E.22

RESULTS OF SPSS MULTIPLE REGRESSION ANALYSIS

MEASURE: REAR BRAKE FORCE RATING (RBFR)

SUBJECT: BG SIGNIFICANCE OF REGRESSION: 0.113 r SQUARE: 0.607

Coefficient	Independent Variable	Value of Coefficient	Significance	Entered On Step Number	r Square Change
b_0	Constant	53.83	-		
b_1	FBD	-0.54	.886	13	.001
b_2	FBF	-5.41	.122	4	.066
b_3	RBD	11.27	.009	1	.157
b_4	RBF	5.44	.163	2	.107
b_{11}	$(FBD)^2$	1.04	.760	11	.003
b_{22}	$(FBF)^2$	-0.34	.874	12	.001
b_{33}	$(RBD)^2$	-4.88	.182	5	.053
b_{44}	$(RBF)^2$	-3.17	.329	9	.011
b_{12}	FBD.FBF	7.47	.114	3	.085
b_{13}	FBD.RBD	-5.41	.265	8	.032
b_{14}	FBD.RBF	-6.77	.162	7	.033
b_{23}	FBF.RBD	-			
b_{24}	FBF.RBF	6.10	.143	6	.031
b_{34}	RBD.RBF	-5.23	.331	10	.026

TABLE E.23

RESULTS OF SPSS MULTIPLE REGRESSION ANALYSIS

MEASURE: REAR BRAKE DISPLACEMENT RATING (RBDR)

SUBJECT: BG   SIGNIFICANCE OF REGRESSION: 0.303   r SQUARE: 0.478

Coefficient	Independent Variable	Value of Coefficient	Significance	Entered On Step Number	r Square Change
b_0	Constant	61.63	-		
b_1	FBD	3.94	.352	7	.026
b_2	FBF	-5.19	.177	6	.023
b_3	RBD	9.20	.033	1	.142
b_4	RBF				
b_{11}	$(FBD)^2$	-2.35	.536	9	.017
b_{22}	$(FBF)^2$	1.13	.635	12	.007
b_{33}	$(RBD)^2$	-8.30	.044	2	.125
b_{44}	$(RBF)^2$	-2.76	.442	8	.019
b_{12}	FBD.FBF	3.12	.539	3	.036
b_{13}	FBD.RBD	-5.20	.333	4	.033
b_{14}	FBD.RBF	-4.05	.441	10	.011
b_{23}	FBF.RBD				
b_{24}	FBF.RBF	2.62	.557	11	.012
b_{34}	RBD.RBF	-6.72	.240	5	.029

TABLE E.24

RESULTS OF SPSS MULTIPLE REGRESSION ANALYSIS

MEASURE: NORMAL STOP RATING (NSR)

SUBJECT: BG SIGNIFICANCE OF REGRESSION: 0.056 r SQUARE: 0.654

Coefficient	Independent Variable	Value of Coefficient	Significance	Entered On Step Number	r Square Change
b_0	Constant	84.39	-		
b_1	FBD	2.13	.610	10	.006
b_2	FBF	3.00	.418	8	.027
b_3	RBD	12.57	.010	1	.183
b_4	RBF	2.74	.521	9	.012
b_{11}	$(FBD)^2$	-1.03	.782	13	.002
b_{22}	$(FBF)^2$				
b_{33}	$(RBD)^2$	-12.10	.007	2	.176
b_{44}	$(RBF)^2$	-7.87	.037	3	.056
b_{12}	FBD.FBF	7.63	.113	4	.058
b_{13}	FBD.RBD	-9.52	.121	6	.037
b_{14}	FBD.RBF	-3.95	.461	11	.006
b_{23}	FBF.RBD	7.40	.184	7	.024
b_{24}	FBF.RBF	3.05	.522	12	.009
b_{34}	RBD.RBF	-7.23	.233	5	.057

TABLE E.25

RESULTS OF SPSS MULTIPLE REGRESSION ANALYSIS

MEASURE: QUICK STOP RATING (QSR)

SUBJECT: BG — SIGNIFICANCE OF REGRESSION: 0.081 — r SQUARE: 0.559

Coefficient	Independent Variable	Value of Coefficient	Significance	Entered On Step Number	r Square Change
b_0	Constant	66.46	-		
b_1	FBD	-			
b_2	FBF	1.71	.719	10	.003
b_3	RBD	19.02	.003	1	.238
b_4	RBF	7.32	.194	2	.089
b_{11}	$(FBD)^2$				
b_{22}	$(FBF)^2$	-1.73	.566	9	.006
b_{33}	$(RBD)^2$	-9.84	.071	4	.057
b_{44}	$(RBF)^2$	-6.23	.185	6	.044
b_{12}	FBD.FBF	11.86	.084	3	.062
b_{13}	FBD.RBD				
b_{14}	FBD.RBF	-5.55	.391	7	.020
b_{23}	FBF.RBD	-4.56	.477	8	.015
b_{24}	FBF.RBF	-0.64	.916	11	.000
b_{34}	RBD.RBF	-12.22	.125	5	.025

TABLE E.26

RESULTS OF SPSS MULTIPLE REGRESSION ANALYSIS

MEASURE: OWN MOTORCYCLE COMPARISON RATING (OMCR)

SUBJECT: BG SIGNIFICANCE OF REGRESSION: 0.352 r SQUARE: 0.533

Coefficient	Independent Variable	Value of Coefficient	Significance	Entered On Step Number	r Square Change
b_0	Constant	72.21	-		
b_1	FBD	-4.09	.504	11	.010
b_2	FBF	2.79	.617	12	.008
b_3	RBD	12.25	0.67	1	.130
b_4	RBF	3.98	.515	7	.015
b_{11}	$(FBD)^2$	-4.17	.450	9	.010
b_{22}	$(FBF)^2$	-2.85	.410	10	.014
b_{33}	$(RBD)^2$	-12.16	.051	2	.063
b_{44}	$(RBF)^2$	-11.13	.044	5	.043
b_{12}	FBD.FBF	11.34	.134	4	.052
b_{13}	FBD.RBD	-6.39	.455	8	.013
b_{14}	FBD.RBF	-11.13	.158	3	.051
b_{23}	FBF.RBD	2.42	.756	14	.003
b_{24}	FBF.RBF	2.40	.725	13	.002
b_{34}	RBD.RBF	-14.63	.102	6	.118

APPENDIX F

OPTIMUM PROPORTIONING OF BRAKING EFFORT

In Juniper and Good (1983) it was determined for a decelerating motorcycle that the normal force at the front and rear wheels was given by:

$$N_f = m/\ell.(gb + Dh) \tag{F.1}$$

$$N_r = m/\ell.(ga - Dh) \tag{F.2}$$

where: N_f = front wheel normal force

N_r = rear wheel normal force

m = motorcycle mass

D = deceleration

g = gravitational acceleration

a,b,ℓ,h - see Figure F.1

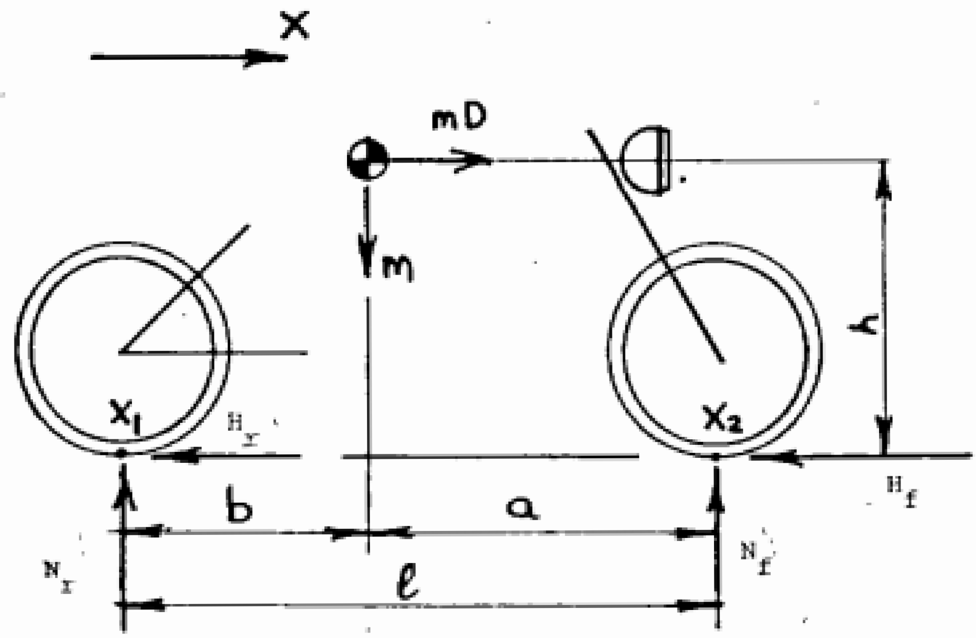

Figure F.1 Basic dimensions of motorcycle, front and rear brakes applied.

The friction force which is 'available' at each wheel with these normal loads is H_f and H_r. Optimum utilization of the available friction force at each wheel is made when they are in the same proportion, α of the respective normal loads.

i.e. $$H_f = \alpha \mu N_f \qquad (F.3)$$

$$H_r = \alpha \mu N_r \qquad (F.4)$$

Let $H_f = m F$

and $H_r = m R$

where F = optimum deceleration contribution at the front wheel

R = optimum deceleration contribution at the rear wheel

then $$H_f + H_r = m(F + R) = m D \qquad (F.5)$$

so $$F = \alpha \mu g(b + Dh/g)/\ell \qquad (F.6)$$

$$R = \alpha \mu g(a - Dh/g)/\ell \qquad (F.7)$$

therefore: $$F + R = \alpha \mu g = D \qquad (F.8)$$

from which: $$F = D(b + Dh/g)/\ell \qquad (F.9)$$

$$R = D(a - Dh/g)/\ell \qquad (F.10)$$

The optimum rear wheel deceleration contribution, R has been plotted against the optimum front wheel deceleration contribution, F with the total deceleration D as a parameter in Figure 4.18.